FINAL PROJECT REPORT # 00047948

GRANT: DTRT13-G-UTC45
Project Period: 8/1/2014 – 12/31/19

Volume I: Strengthening and Repair of Structural Concrete with a Fabric-Reinforced-Cementitious-Matrix (FRCM): Laboratory Studies

Participating Consortium Member:
Missouri University of Science and Technology

Authors:
Dr. John J. Myers, Ph.D., P.E., (PI)
Dr. Zena Aljazaaeri, Ph.D.
Missouri University of Science and Technology

RE-CAST:
REsearch on Concrete Applications for Sustainable Transportation
Tier 1 University Transportation Center

DISCLAIMER

The contents of this report reflect the views of the authors, who are responsible for the facts and the accuracy of the information presented herein. This document is disseminated under the sponsorship of the U.S. Department of Transportation's University Transportation Centers Program, in the interest of information exchange. The U.S. Government assumes no liability for the contents or use thereof.

TECHNICAL REPORT DOCUMENTATION PAGE

1. Report No. RECAST UTC # 00047948	**2. Government Accession No.**	**3. Recipient's Catalog No.**
4. Title and Subtitle Volume I: Strengthening and Repair of Structural Concrete with a Fabric-Reinforced-Cementitious-Matrix (FRCM): Laboratory Studies		**5. Report Date** January 2020 **6. Performing Organization Code:**
7. Author(s) Dr. John J. Myers and Dr. Zena Aljazaaeri		**8. Performing Organization Report No.** Project # 00047948
9. Performing Organization Name and Address RE-CAST – Missouri University of Science and Technology 500 W. 16th St., 223 ERL Rolla, MO 65409-0710		**10. Work Unit No.** **11. Contract or Grant No.** USDOT: DTRT13-G-UTC45
12. Sponsoring Agency Name and Address Office of the Assistant Secretary for Research and Technology U.S. Department of Transportation 1200 New Jersey Avenue, SE Washington, DC 20590		**13. Type of Report and Period Covered:** Final Report Period: 8/1/2014 – 12/31/19 **14. Sponsoring Agency Code:**
15. Supplementary Notes The investigation was conducted in cooperation with the U. S. Department of Transportation.		
16. Abstract Externally bonded fiber reinforced cementitious matrix (FRCM) for structural members was tested and evaluated as a new class of composite material for repairing and strengthening infrastructures. In comparison with fiber reinforced polymer (FRP) composites, FRCM composite has a superior high temperature resistance and great compatibility with concrete substrates. Experimental investigation is ongoing in the United States to evaluate the structural and durability performance of FRCM composite to be implemented in field applications. This experimental program consisted of testing 12 strengthened reinforced concrete (RC) beams to study the fatigue and flexure performance under environmental exposure and sustained stress, 10 strengthened RC beams to study the influence of FRCM composite in shear performance, 13 one-way RC slabs strengthened with three different composite types to evaluate their flexural performance, 30 FRCM concrete prisms to address the durability and bond performance of the FRCM composite, and 7 RC anchored-strengthened RC beams to delay the premature debonding failure of the FRCM composite under flexural loading. Experimental works demonstrated the effectiveness of FRCM composite on enhancing the fatigue, flexure, bond, and shear capacities of RC structural members. The durability performance of the FRCM composite in terms of resisting different exposure conditions such as freezing and thawing, high temperature and humidity cycles, alkaline solution, and salt solution were determined within reason. The conclusions and summary from this study open the door to use the FRCM composite for repairing and strengthening RC slab decks or RC beams for bridges.		
17. Key Words Strengthening and Repair; Structural Concrete; Fabric-Reinforced-Cementitious-Matrix	**18. Distribution Statement** No restrictions. This document is available to the public.	
19. Security Classification (of this report) Unclassified	**20. Security Classification (of this page)** Unclassified	**21. No of Pages** 199

Form DOT F 1700.7 (8-72) Reproduction of form and completed page is authorized.

Report for

RE-CAST-Research on Concrete Applications for Sustainable Transportation
Tier 1 University Transportation Center (UTC)

Grant: DTRT13-G-UTC45

Strengthening and Repair of Structural Concrete with a Fabric-Reinforced-Cementitious-Matrix (FRCM): Laboratory Studies

by

Dr. John J. Myers, Ph.D., P.E., (PI)
Dr. Zena Aljazaaeri, Ph.D.

Missouri University of Science and Technology
Department of Civil, Architectural & Environmental Engineering

January 2020

PUBLICATION REPORT OPTION

This report has been prepared in the style of the major project tasks that align with manuscripts submitted for publication.

Paper I (pages 38-59) is a manuscript entitled "Fatigue and Flexural Behavior of Reinforced-Concrete Beams Strengthened with Fiber-Reinforced Cementitious Matrix" This manuscript was published in the ASCE Journal of Composites for Construction.

Paper II (pages 60-94) is a manuscript entitled "Strengthening of Reinforced Concrete Beams in Shear with a Fabric-Reinforced Cementitious Matrix" This manuscript was published in the ASCE Journal of Composites for Construction.

Paper III (pages 95-127) is a manuscript entitled "Mechanical and Durability Performance of Reinforced Concrete One-Way Slabs Strengthening in Flexural: Evaluation of Different Composite Materials" was published in the ASCE Journal of Materials in Civil Engineering.

Paper IV (pages 128-146) is a manuscript entitled "Durability Performance of FRCM Composite Bonded to Concrete under Different Environmental Aging Conditions'' was published in the 8th International Conference on Fibre-Reinforced Polymer (FRP), Composites in Civil Engineering (CICE 2016).

Paper V (pages 147-169) is a manuscript entitled "A Novel and Effective Anchorage System for Enhancing the Flexural Capacity of RC Beams Strengthened with FRCM Composites" was published in the Composite Structures Journal published by ELSEVIER.

EXECUTIVE SUMMARY

Externally bonded fiber reinforced cementitious matrix (FRCM) for structural members was tested and evaluated as a new class of composite material for repairing and strengthening infrastructures. In comparison with fiber reinforced polymer (FRP) composites, FRCM composite has a superior high temperature resistance and great compatibility with concrete substrates. Experimental investigation is ongoing in the United States to evaluate the structural and durability performance of FRCM composite to be implemented in field applications. This experimental program consisted of testing 12 strengthened reinforced concrete (RC) beams to study the fatigue and flexure performance under environmental exposure and sustained stress, 10 strengthened RC beams to study the influence of FRCM composite in shear performance, 13 one-way RC slabs strengthened with three different composite types to evaluate their flexural performance, 30 FRCM concrete prisms to address the durability and bond performance of the FRCM composite, and 7 RC anchored-strengthened RC beams to delay the premature debonding failure of the FRCM composite under flexural loading. Experimental works demonstrated the effectiveness of FRCM composite on enhancing the fatigue, flexure, bond, and shear capacities of RC structural members. The durability performance of the FRCM composite in terms of resisting different exposure conditions such as freezing and thawing, high temperature and humidity cycles, alkaline solution, and salt solution were determined within reason. The conclusions and summary from this study open the door to use the FRCM composite for repairing and strengthening RC slab decks or RC beams for bridges.

ACKNOWLEDGMENTS

The authors are grateful to the RE-CAST-Research on Concrete Applications for Sustainable Transportation Tier 1 University Transportation Center (UTC) that allowed this research work to be undertaken as well as the Ruredil Company for material donations.

Several other individuals provided technical support to this endeavor. In particular, the authors thank the wonderful technician support of Jason Cox, Garry Abbot, Jason Cox, Brain Swift, John Bullock, Greg Leckrone, and Mike Lusher at Missouri S&T.

The authors would also like to thank our fellow colleagues that contributed time and/or support including Dr. Zuhair Aljaberi, Dr. Hayder Alghazali, Mr. Saipavan Rallabhandhi, Dr. Wei Wang, Dr. Meyyada Alabdulhady, Dr. Eli Hernandez, and Ms. Noor Yasob as well as undergraduate research assistants, Mr. Reed Norphy and Mr. Michael Janke.

TABLE OF CONTENTS

LIST OF ILLUSTRATIONS

Page

SECTION

PAPER I

PAPER II

PAPER III

LIST OF TABLES

Page

SECTION

1. INTRODUCTION

1.1. BACKGROUND

Advanced composite materials have been developed for the retrofitting and strengthening of the existing infrastructure. Existing RC structures may require strengthening or repairing for several reasons. For example, it is often desirable to increase the loading to which a structure is subjected, as when a bridge needs to carry heavier traffic or when a building needs to be used for a purpose other than what it was originally designed for. It may also be necessary to strengthen old RC structures as a result of recent code requirements or due to damage to the RC structure after being exposed to harsh environmental conditioning.

During the last few decades, fiber reinforced polymer (FRP) composites have been successfully used for repairing and upgrading deficient structural members. Externally-bonded FRP bars, plates, sheets, and wraps are a common FRP application used for repairing or strengthening RC, steel, or prestressed structural members as well as masonry structural members. The primary advantages of FRP composites are related to their light weight, ease of application, resistance to corrosion, and minimal effects on structural aesthetics. Generally, FRP composites have been bonded to existing RC structures with epoxy adhesives to improve the structural behavior for both serviceability and the ultimate state conditions.

Although the use of epoxy resin has proven to provide excellent bond performance to the concrete surface, exposing the epoxy resin to temperature levels at or beyond its glass transition temperature degrades its bond characteristics.

The bond degradation leads to loss of connection between the externally bonded FRP composites and concrete surfaces, which is an undesired phenomena. As a consequence, a new generation of composite material that was previously known as textile-reinforced mortar (TRM) and has very recently been denoted as a fabric reinforced cementitious matrix (FRCM) is presented to address some of epoxy adhesive limitations.

The TRM composite or FRCM composite consists of two components. The first component is the reinforcement mesh made of different types of fabric such as polyparaphenylene-benzobisoxazole (PBO), carbon, Aramid, or glass. The second component is the bonding agent made of a cement-based mortar. The FRCM composite has superior physical-durability properties such as high temperature resistance, elimination of toxic fumes in case epoxy resin is subjected to fire, and application on wet concrete surface as the cementitious matrix is compatible with concrete.

The focus of the present work is on applicability of the FRCM composites in improving and extending the life span of RC structural members from different structural aspects. The experimental-based testing was selected to validate the use of FRCM composite in addressing its serviceability and ultimate loading state in order to be launched in field applications as it is a new innovative composite. In addition, the experimental evidence was assessed to define and determine the effectiveness of material parameters to be used for design perspectives.

The PBO fabric was the proposed type of FRCM composite in this study. The PBO fabric was made of 5 mm (0.2-in.) and 3 mm (0.125-in.) wide yarns in the longitudinal and transverse directions, respectively, as shown in Fig.1.1.

The free space between the yarns was roughly 5 mm (0.2-in.) and 22 mm (0.9-in.) in the longitudinal and transverse directions, respectively, and the nominal thickness of the yarns in each direction was 0.2 mm (0.008-in.) and 0.12 mm (0.045-in.) in the longitudinal and transverse directions, respectively. The cement-based mortar was made of a combination of portland cement, silica fume, and fly ash as a binder. It had less than 5 percent polymer. The cement-based mortar also contained glass fibers to improve the bond between the PBO mesh and the cement mortar and to provide better tensile properties. The other type of cement mortar was used as a base mortar to level the concrete surface, close the crack opening, and improve the bond performance between the FRCM composite and the concrete substrate. The base mortar was made of fine cement particles and silica fume. The base mortar contained polypropylene fibers to bridge concrete cracks and to improve the bond performance of the FRCM composite-concrete surfaces. All FRCM composite materials are presented in Fig. 1.1.

(a) (b) (c) (d)

Fig. 1. 1. FRCM composite materials: a) Polyparaphenylene benzobisoxazole (PBO) mesh, b) Inorganic Matrix, c) Glass fiber, and d) Polypropylene fiber

1.2. OBJECTIVE AND SCOPE OF WORK

The objective of this report is to give FRCM composite a framework from which experimental testing and findings could be better targeted to understand its durability and mechanical performance based on five interrelated experimental studies. The main objective and focus of each experimental work is illustrated herein.

The first experimental study undertaken was the first major study that initialed to investigate the applicability of using FRCM composite in strengthening RC beams under the effect of fatigue loading. As one of the most important aspects for a structural element in bridge application is its ability to resist oscillatory loads through its entire life, the aim of this pilot study was to:

1- Develop and propose the fatigue performance of FRCM composite intended to be used for strengthening or retrofitting RC beams in bridge applications,

2- Develop evidence that this material will perform satisfactorily when exposed to natural environments; specifically, freeze-thaw, high temperature, high-relative humidity conditions, and sustained service stresses,

3- Address the stiffness degradation of strengthened RC beams after 2 million cycles of applied fatigue loading,

4- Address the post fatigue-monotonic performance of strengthened RC beams in terms of flexural strength enhancement, energy absorption, effect of using multiple strengthening layers, and the failure mode,

5- Evaluate the ACI 549 (2013) building code in terms of anticipating the ultimate design loads in comparison with the experimental ultimate loads.

The second experimental study was conducted to investigate the behavior of RC beams strengthened in shear using an externally applied FRCM composite. The intention to increase the load carrying capacity of the RC beam correspondingly led to an increase in its shear load. If the RC beam is loaded to the level beyond its shear capacity, a shear failure will be the control. A sudden shear crack failure can influence the continuity of transforming the loads between the connected RC beams and cause of concentrated local damages. For that, the aim of the second study was to:

1- Determine the performance of U-wrapping FRCM composite in strengthening RC beams to resist additional shear loads in the availability or the absence of internal transverse shear reinforcements,
2- Specify the most effective strengthening configuration that can be used to improve the shear strength in RC beam applications,
3- Address the shear failure mode of the strengthened RC beams with and without internal shear reinforcement,
4- Evaluate the effect of the FRCM composite's reinforcement ratio,
5- Compare the experimental ultimate loads with the theoretical ultimate loads based on the ACI 549 (2013) building code and validate the efficiency of the ACI 549 (2013) approach in anticipating the ultimate shear loads,
6- Associate the current experimental test results with the pervious test results related to the use of FRP and FRCM composites for shear strength enhancement.

The third experimental study addressed investigating the mechanical and durability performance of strengthened RC one-way slab systems with different composite types.

Specifically, this study was to evaluate the flexure performance of FRCM composite, as it is a new innovative composite material, in comparison with the conventional FRP composites. Accordingly, the intention of the third study was to:

1- Evaluate and compare the flexural performance of FRCM composite in strengthening RC one-way slab systems with two traditional FRP composites: carbon fiber reinforced polymer grid (CFRP-grid) and steel reinforced polymer (SRP),
2- Evaluate the effect of environmental exposure on the flexural performance of three composite materials,
3- Associate the experimental ultimate loads of tested slabs with their theoretical ultimate loads based on ACI 440 (2008) and ACI 549 (2013),
4- Provide appropriate information on the reduction safety factor for environmental conditions.

The fourth experimental study addressed the durability performance of FRCM composite through externally bonded samples to concrete prisms. Because an aggressive environment may cause damage to the cementitious materials, curing agents of FRCM composite may allow chemical agents to attack the PBO fabrics. Where the accelerated interfacial fiber/matrix debonding can interfere and reduce the FRCM composite mechanical performance. So, the aim of the fourth study was to:

1- Evaluate the long-term durability performance of FRCM composite that was externally bonded to concrete prisms and exposed to various environmental aging conditions,

2- Address the effect of aging time, exposure condition, concrete surface roughness, and the number of strengthening layers on bond performance of FRCM composite,
3- Determine the failure mode of FRCM composite.

The fifth experimental study was a state-of-the-art investigation on using a novel anchorage system for enhancing the FRCM mechanical performance in retrofitting RC structural members. As a matter of fact, the interfacial fiber/matrix debonding failure lowered the effectiveness of using multi-layers of strengthening; the aim of this study was to:

1- Specify the influence of anchorage systems on the efficiency of FRCM composite in terms of load carrying capacity and ductility performance of RC beams,
2- Determine the required FRCM composite layers to achieve the desired flexure enhancement,
3- Determine the failure mode of FRCM composite and the anchorage systems.

1.3. RESEARCH SIGNIFICANCE

The work presented herein was a part of a larger research program that progressed in collaboration with research at University of Miami, Coral Gables, Florida, to develop an experimental base for FRCM composites targeted specifically for structural repairing and strengthening applications. With this intention, this work was to underline the specifics of the behavior of the reinforcing mesh within the cementitious matrix class of materials, and the relevance and importance of the parameters that need to be undertaken in design building codes and field implementations.

The larger research program on FRCM technology was conducted through the Research on Concrete Applications for Sustainable Transportation (RECAST) Tier 1 University Transportation Center housed at Missouri University of Science and Technology (Missouri S&T).

1.4. REPORT ORGANIZATION

The research study outcomes are presented via a manuscript publication style. All findings and conclusions of this intensive research study have been submitted and accepted to technical journals and conference proceedings reviewed by experts in the field for technical review and vetting. The report is divided into three sections: introduction, papers, and conclusions & recommendations.

INTRODUCTION: this section presents a brief introduction to the research topics and explains the need for this research study and the objective of each experimental work. Then, the literature review is presented for the previous experimental work with FRCM composite toward the pilot features of the proposed research topics.

PAPERS: this section is the main body of the report. It consists of five technical papers that relate to the use of FRCM composite in strengthening or repairing RC structural members to resist fatigue, flexure, and shear loadings. An investigation on the durability performance of FRCM composite is presented in three papers wherein the strengthened RC structural members were subjected to different environmental conditioning. In addition, the fifth paper was associated to the anchorage systems for enhancing the use of multilayers FRCM strengthening.

SUMMARY, CONCLUSIONS AND RECOMMENDATIONS: this section summarizes the relevant key findings of all experimental works in comparison with the theoretical analyses, which were executed during each research study, as well as a recommendation for future research.

2. LITERATURE REVIEW

There is an increasing need and a great challenge to repair and upgrade transportation infrastructures. A recent report published by the Federal Highway Administration (FHWA) indicated that there are more than 63,000 bridges throughout the United States defined as “structurally deficient” and in need of serious repair. The Missouri Department of Transportation (MoDOT) stated in 2015 that approximately 1,400 bridges in the state have posted weight limits and many of those bridges are in critical condition. Composite materials and techniques for structural repair and strengthening are under development. The FRP composites have become a common repair and/or strengthening material for structural applications in the last two decades. Advanced composite materials made of a cement-based matrix reinforced by different types of fabric material are advocated as a replacement material to FRP composites where the organic resin is substituted by an inorganic mortar. These composites are proposed under different names including textile-reinforced concrete (TRC), textile-reinforced mortar (TRM), fiber-reinforced concrete (FRC), mineral-based composites (MBC), and fiber-reinforced cementitious mortar (FRCM) (Aljazaeri and Myers 2016).

Toutanji et al. (2006; 2007) studied the flexure performance of RC beams strengthened with carbon fiber sheets bonded with inorganic (low viscosity resin) and organic (epoxy resin) matrixes. The experimental results showed that the inorganic matrix had a positive response of bonding different types of fabrics to structural members and enhancing the strength as the organic resin. Several valuable experimental studies in Europe and the United States have been implemented to determine the structural performance of FRCM composites in civil applications (Nanni 2012).

Many experimental investigations have been conducted recently in the literature that were focused on the mechanical characterization properties, flexural strengthening, shear strengthening, and confinement applications of FRCM composites (Tommaso et al. 2008; Ombres, 2011, 2012, and 2015; D'Ambrisi and Focacci 2011; Babaeidarabad et al. 2013 and 2014; Arboleda et al. 2014; Loreto et al. 2014; Baggio et al. 2014; Trapko et al. 2015). The results revealed the efficiency of FRCM composites in enhancing the mechanical performance of RC and masonry structural elements. In addition, the experimental and analytical studies carried out by D'Ambrisi et al. 2013; Carloni et al. 2013; D'Antino et al. 2014; Arboleda et al. 2012 and 2015; Sneed et al. 2015; and Olivito et al. 2016 related to the structural bond performance and failure mechanisms of FRCM composites. Although the use of cementitious composite materials for strengthening or repairing RC structures are available for some structural applications, there remains a lack of knowledge on the long-term behavior of FRCM strengthened RC structural members that can be subjected to fatigue cyclic loadings as well as the durability performance of FRCM composite in terms of bonding efficiency and maintaining a considerable amount of carrying load during its service life.

2.1. CHARACTERIZATION OF THE PBO-FABRIC

The mechanical characterization of the materials is the key factor to deliberate PBO-fabric as a functional structural material. Fig. 2.1 shows the stress-strain curves of the high strength zylon (PBO) fabric in comparison with other structural fibers. The figure demonstrates that the PBO fabric has the highest tensile strength and tensile modulus among all the widely used fibers and comparable stiffness to carbon fibers.

The other outstanding character of PBO fabric is its resistance to thermal conditioning. Even though, the experimental testing showed that the relative strength of PBO fabric decreased as the temperature increased to 500°C (932°F) from room temperature, the PBO fabric retained 40% of its strength after exposure to 500°C (932°F) and 75% of its modulus after exposure to 400°C (752°F), Toyobo (2005).

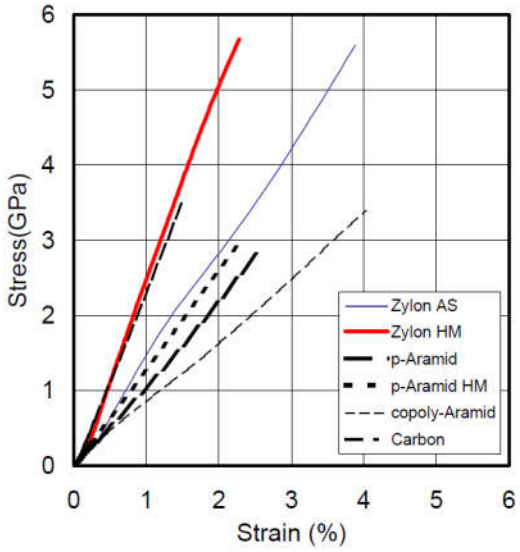

Conversion units: 1-in. = 25.4 mm; 1 kip = 4.45 kN

Fig. 2. 1. Tensile strength vs. elongation relationships of zylon (PBO), aramid and carbon fibers, (Adapted from Toyobo, 2005)

2.2. TENSILE AND BOND PERFORMANCE OF FRCM COMPOSITE

In a performance based specification, the values of the tensile and bond properties of any composite material should be specified as a design parameter to determine their influence on increasing the ultimate loads in repairing or strengthening applications.

The tensile properties of the FRCM composite were determined following the testing methods of defining the TRC composites' tensile properties. As mentioned previously, the TRC composite is a composite construction material consisting of high-performance filament yarns of glass, polymeric, or carbon fiber and a matrix of fine-grained concrete (Butler et al., 2010). Different gripping methods and failure mechanisms are presented through the literature review regarding the tensile properties of the TRC composite.

Orlowsky and Raupach (2008) used the clamped grips method for determining the mechanical tensile properties of the TRC composite. Butler et al. (2010) also used clamped grips in characterizing the mechanical properties of the TRC composite. The typical stress–strain curve was subdivided into three characteristic zones. Zone I represented the behavior of the TRC composite in the uncracked state where the stiffness of both matrix and fibers contributed in elastic loading stage, while the stress level of initial cracking mainly depended on the tensile strength of the matrix. In zone II, multiple cracking occurred that exceeded the quasi-ductile behavior of the composite. In this zone, the stress–strain curve was exhibited numerous jumps that indicated a brief partial unloading of the coupon specimen due to formation of new cracks. The authors stated that the slope and the length of zone II essentially depended on the quality of the bond between the textile and matrix as well as on the volume content of fibers in the coupon specimen. In zone III, the load continuously increased until the tensile strength and the strain capacity of textile were reached due to failure of the TRC composite.

Contamine et al. (2011) developed clamps that allowed hinging conditions to minimize or eliminate the effect of bending moments and applied a direct tensile load on the TRC composite coupon specimens. For this type of gripping, the stress-strain curve of TRC composite had a bilinear behavior and the failure of the coupon specimens occurred randomly along the specimens' height.

Hartig et al. (2012) used two types of load application. Type A, rigid load application, was done by gluing steel plates with epoxy resin to the specimen or by placing a steel sheet inside the coupon specimens. Then, the gripping plates were hung into the pin connections that were fixed to the testing machine jaws. Hartig et al. (2012) stated that "the main transfer mechanism between the coupon specimen and the clamping grips is transferred through adhesive tension and shear, and no slip occurred between the steel plates and the coupon specimens.'' Type B, soft clamping was done by gluing the rubber interlayer between the steel plates and the coupon specimens. Then, the load was transferred between coupon specimens and clamping grips based on coulomb friction when the gripping sides were directly fixed between the testing machine's jaws. In such gripping types, concrete cracks were facilitated in the supported parts of the coupon specimens and slips occurred between the coupon specimens and clamping grips if static frictions were exceeded. The results revealed a strong dependency of the load application type on the measured ultimate loads and failure positions in the coupon specimens. Coupon specimen testing with rigid load application (type A) showed lower ultimate loads and frequent failures. In contrast, the soft load application by means of friction (type B) led to higher ultimate loads and less frequent failures in the coupon specimens.

Arboleda et al. (2012) demonstrated an experimental work to determine the PBO-FRCM composite's tensile properties. The PBO-FRCM coupons were performed from cutting off large casted panels or molds. Arboleda et al. (2012) stated that during tensile testing, the load is transferred to the coupon specimen ends through a pin action mechanism. The pin grips type was simulated to prevent applying torsion or bending forces on the coupon specimens. The idealized tensile stress-strain curve of the PBO-FRCM coupon specimens had the same bilinear behavior that was observed in the TRC composite. The initial linear segment of the curve corresponded to the PBO-FRCM uncracked linear elastic behavior and was characterized by the uncracked tensile modulus of elasticity, E_f^*. The second linear segment was corresponded to the PBO-FRCM cracked linear inelastic behavior and was characterized by the cracked tensile modulus of elasticity, E_f, as shown in Fig. 2.2. (Arboleda et al. 2012).

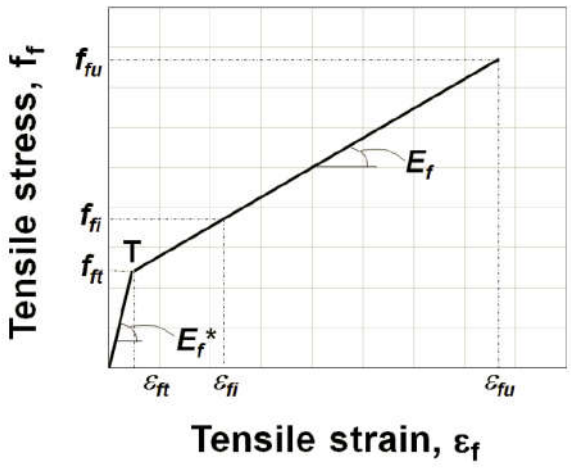

Fig. 2. 2. Idealized tensile stress versus strain curve of an FRCM coupon specimen, (Adapted from AC 434, 2013)

However, the failure mechanism of the PBO-FRCM coupon specimens was determined in the gripping areas due to the result of concentrated shear forces that exceeded the shear capacity of the FRCM bonding agent (cementitious matrix). Even though, using pin grips did not actually specify the full tensile capacity of FRCM coupon specimens, this testing procedure was considered the test methodology in AC 434 (2013).

De Santis and de Felice (2015) used five different gripping types for clamping mortar-based composites: direct clamping of reinforcement textile (free of mortar), aluminum tabs glued to the specimen ends (free of mortar), aluminum tabs glued to the specimen ends (free of mortar and reinforced with FRP), spherical articulation and aluminum tabs glued to the mortar matrix, and direct clamping on the mortar matrix reinforced with FRP. The coupon test results showed that the direct clamping on the mortar allowed an appropriate load application to the whole coupon specimen and full characterization of the strengthening composite under tension. The authors recommended reinforcing the ends of the coupon specimen to prevent mortar crushing and applying an adequate transverse load to avoid pull-out effects or sliding in the gripping areas.

Arboleda et al. (2015) stated that “the apparent uniaxial tensile behavior of FRCM composite was influenced by several factors, including the load transfer mechanism (grip method), specimen geometry and fabrication, and strain measurement technique.”

Arboleda et al. (2015) determined that the difference in the selected gripping types specified different failure mechanisms in FRCM composite coupons. Specifically, the pin grips specified the stress-strain curve of the FRCM composite by a bilinear behavior, while the clamping grips specified the trilinear behavior of the FRCM composite.

In the clamped grips method, the third phase represented the influence of the reinforcing fibers' tensile properties only after cracking of the cementitious matrix and slippage of the reinforcing fibers out of the cementitious matrix. The failure mode of the FRCM coupon specimens with pin grips was a slippage of the reinforcing fibers out of the cementitious matrix, while a rupture failure in some reinforcing fibers was observed when tensile testing with clamping grips. Even though the clamped grips method assisted to fully characterize the tensile properties of the FRCM composite, the recommended test method for design perspective was based on the pin grips method, because the third phase in the clamped grips method only represented the reinforcing fibers' tensile properties with no contribution from the cementitious matrix, as shown in Fig. 2. 3. Thus, from previous experimental investigations on characterizing the mechanical properties of FRCM composite, the pin grips method was used in this study.

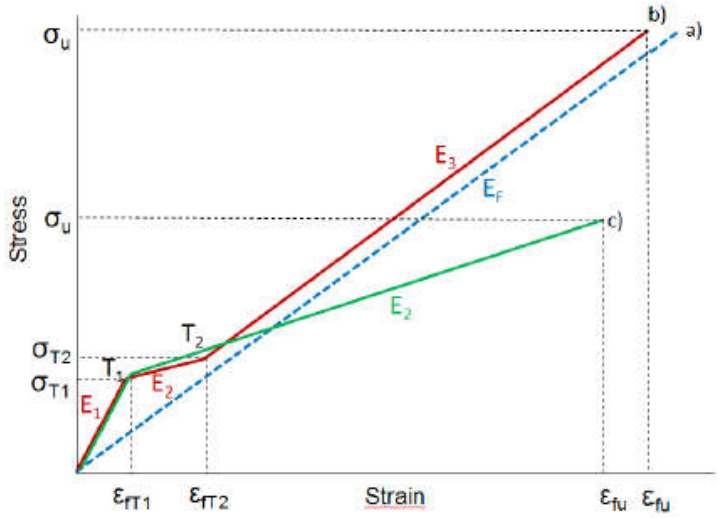

Fig. 2. 3. Idealized stress-strain curves a) stand-alone fabric, b) clamped FRCM, c) pinned FRCM, (Adapted from Arboleda et al., 2015)

The other characterization property of the FRCM composite is the interfacial bond performance of the FRCM composite attached to concrete substrates. A study on the bond strength-slip relations for the PBO-FRCM composite externally bonded to concrete blocks was reported by D'Ambrisi et al. (2012). Carloni et al. (2013) conducted an experimental study on the applicability of the fracture mechanic approach to understand the stress transfer mechanism of FRCM composite externally bonded to concrete substrates. Both test results analyzed the effective bond length and established the load-carrying capacity of the FRCM interface for design purposes. Moreover, the test results determined the interfacial fiber/ cementitious matrix debonding failure and highlighted the role of the cementitious matrix in the stress transfer mechanism.

D'Ambrisi et al. (2013) determined the bond performance of FRCM composite that was made out of PBO fabric embedded in the cement-based matrix and attached to the concrete. The test results allowed estimating for the effective anchorage length of the PBO fabric and evidenced the debonding failure mode at the fibers/matrix interface after a significant slippage of fibers inside the cementitious matrix. The results also confirmed the effectiveness of the FRCM composites as external reinforcements for structural members and used to calibrate the local bond-slip relations of the FRCM composite for design considerations.

Another study by D'Ambrisi et al. (2013) investigated the experimental and analytical bond performance of carbon-FRCM composite attached to masonry blocks under double shear testing. The study involved different bond lengths that were intended to calibrate local bond-slip relations of carbon-FRCM composite attached to masonry elements.

D'Antino et al. (2014) directed a single-lap shear test to determine the FRCM composite performance bonded to concrete blocks. Test parameters included different FRCM composite attachment areas and reinforcement ratios. The stress-transfer mechanism of the FRCM composite was determined. The durability performance of FRCM composite in terms of different environmental exposure was carried out by Arboleda et al. (2014) using the pull-off test method. Two types of FRCM composite were investigated (carbon fabric and PBO fabric with cement-based matrix). The FRCM composite bond strength results revealed no significant degradation after environmental exposure.

Sneed et al. (2015) conducted a comparison study on the bond performance of the FRCM composite-concrete substrate using a double-lap test and single-lap shear test. The experimental program included the effect of bonded FRCM composites' widths and lengths. The test results showed that the same peak load was reached for the two testing types if the debonding failure occurred simultaneously in both of the composite strips in double shear test. However, if only one composite strip failed, then the other attached composite strip would continue to carry loads by means of interlocking between the fibers or between the fibers and the matrix.

Ombres (2015) shaded light on a comparison between experimental results and theoretical predictions on the bond-slip law of the PBO-FRCM composite attached to concrete substrates. The comparison results concluded that the nonlinear proposed model of the bond-slip law was associated with the experimental results.

In addition, the experimental work examined the long-term durability performance of bonded FRCM composite to concrete substrates for many aspects such as bond testing methods, environmental aging conditions, concrete surface preparation, multilayers of FRCM composite, and failure mode of FRCM composite.

The influence of the concrete substrate preparation on the bond behavior of PBO FRCM-concrete joints was studied by D'Antino et al. (2015). The experimental test results by Ombres (2015) and D'Antino et al. (2015) proved that there was no significant variation in the failure mode or ultimate bond strength for untreated or treated concrete surfaces due to the variety in compressive strength of concrete substrate. However, the authors recommended to surface preparation of the concrete substrates for better bond performance.

Another study to D'Antino et al. (2016) investigated the behavior of FRCM composite concrete joints. The FRCM composites were comprised of a glass or carbon fiber net embedded into a cementitious matrix under a single-lap shear test. It was found that the carbon-FRCM composite failed due to fibers debonding at the matrix-fiber interface, while the glass-FRCM composite failed due to fibers debonding at the matrix-fiber interface with rupture of one or more fiber bundles in some specimens. Thus, the ultimate loads of glass-FRCM composite were compromised with glass fiber strength and higher than carbon-FRCM composite for the same bonded length. The higher ultimate loads in glass-FRCM composite indicated the remarkable bond performance of the glass fibers-matrix interface than the carbon fibers.

Olivito et al. (2016) carried out an experimental investigation on the bond adhesion between sustainable composite materials and masonry support.

The work included an experimental testing and a theoretical approach. Double-lap shear bond tests were performed on masonry clay bricks that were externally strengthened with two different FRCM composite materials (natural fiber: Flax-FRCM and PBO-FRCM). The flax-FRCM composite had revealed more remarkable bond behavior than PBO-FRCM composite as a result of a complete use of Flax-FRCM composite's mechanical properties. In this work, two testing methods were conducted to determine the bond performance of PBO-FRCM composite attached to concrete substrate with the potential of age-related environmental conditions. FRCM composite was exposed to different environmental conditions based on the application to be used. It is valuable to know its bond performance in such environments in order to assess its applicability.

The experimental work through Paper II was based on two bond test set-ups: the pull-off test and the bending test. The bond durability performance of FRCM composite attached to concrete substrates determined the bond strength of PBO-FRCM composite under different environmental exposures. The environmental conditions included freezing and thawing cycles, high relative humidity and high temperature cycles, immersion into alkaline solution, and immersion into salt solution.

2.3. FLEXURE PERFORMANCE OF FRCM COMPOSITE

In cooperation with FRCM composite material characterization research studies, a parallel line of experimental studies was conducted to explore the effectiveness of the FRCM composite for flexural enhancement in repairing real-scale structural concrete members.

Tommaso et al. (2008) presented experimental testing on RC beams strengthened with PBO-FRCM and carbon-FRCM composites. All tests showed that failure of the strengthened beams was produced by the drop of composite action at ultimate load stage; nevertheless, the failure mode was determined to happen in different modalities depending on the number of engaged layers. In addition, the results evidenced the effectiveness of both FRCM composites in terms of increasing the ultimate strength and displacement ductility of strengthened beams.

Ombres (2011) conducted another experimental study to inspect more about the performance of PBO-FRCM composite in flexural strengthening of RC beams. The author stated that "the ultimate capacity of strengthened beams increased from 10% to 44% with respect to the capacity of un-strengthened beams." D'Ambrisi and Focacci (2011) conducted an experimental study on strengthening RC beams in flexure using different FRCM composite materials (carbon fabric and PBO fabric). Different strengthening figures, cementitious matrices, and the number of strengthening layers were considered. The test results illustrated that various debonding failure modes were observed depending on the fibers type and the matrix. In most cases, fiber debonding was exhibited at the fibers/matrix interface without concrete detachment.

Ombres (2012) conducted a study on analyzing the debonding failure modes that were captured in previous experimental works with FRCM composite using a nonlinear bond-slip law and a bilinear bond slip law. The predicted results of the bilinear bond slip law were more conservative than those of the nonlinear bond slip law.

Pellegrino and D'Antino (2013) conducted a study on the behavior of FRCM strengthened full-scale precast prestressed double-T beams through experimental testing. The test results stated that the use of FRCM composites to strengthen RC structures increased their ultimate load capacity. Pellegrino and D'Antino (2013) observed an increase of 20% for the strengthened beam with carbon-FRCM and 24% for the strengthened beam with steel-FRCM with respect to the unstrengthen control beam.

However, there were various failure modes for strengthened beams with respect to the fiber type (carbon and steel). The strengthened beam with carbon-FRCM exhibited a sliding of the fibers into the cementitious matrix near mid-span followed by rupture of some carbon fibers, while the strengthened beam with steel-FRCM composite exhibited a debonding failure between the steel fiber and the cementitious matrix.

Loreto et al. (2013) discussed the performance and analysis of RC slabs strengthened with FRCM composite. The failure mode, ultimate load, and ultimate displacement ductility were evaluated. The results showed a 40% and 100% increase in the ultimate load for one ply and four plies, respectively.

Babaeidarabad et al. (2014) demonstrated an experimental program on testing 18 RC beams strengthened in flexure with different PBO-FRCM composite's reinforcement ratios. The experimental results indicated that the PBO-FRCM composite improved the flexural strength of RC beams. For low-strength concrete, the flexural capacity increased by 32% and 92% for one ply and four plies, respectively. For high-strength concrete, the flexural capacity increased between 13% and 73% for one ply and four plies, respectively.

Jung et al. (2015) presented an experimental and analytical study on the flexural enhancement of RC beams strengthened with FRCM composite.

Jung et al. (2015) stated that “the slippage between the PBO fabric and cementitious matrix occurred at a high strain level and all of the FRCM-strengthened beams failed by debonding at ultimate loads.’’ In addition, the proposed bond strength model for fiber/matrix slippage agreed well with the experimental ultimate loads at debonding. From the above literature review, the increase in the load carrying capacity of the RC structures and the failure mode of the FRCM composites were determined.

However, a very limited data set of experimental results is available in terms of an evaluation study on the flexure performance of PBO-FRCM composite in comparison with other conversional FRP composites. In Paper III, a comparison study was conducted to evaluate the flexure performance of RC one-way slab systems strengthened using three composite materials: PBO-FRCM composite, CFRP composite, and steel reinforced polymer (SRP) composite. The full-scale RC slabs were included specimens under laboratory and environmental aging conditions. The exposed specimens determined if there was any degradation on the flexural properties (stiffness, ultimate loads, ductility, and failure mode) provided by the composite materials with respect to unexposed specimens. From this work, information about the environmental condition’s safety factor is determined as a knock-down factor for design consideration.

2.4. FATIGUE PERFORMANCE OF FRP COMPOSITE

There is no available literature relative to experimental testing conducted on the use of FRCM composite under fatigue loading conditions.

However, some of the pervious experimental works of using the FRP composites in resisting fatigue loading are presented herein.

Senthilnath et al. (2001) studied the performance of CFRP strengthened RC beams in the presence of delamination and lap splices under fatigue loading. The test results indicated that the fatigue performance of carbon-FRP strengthened RC beams was not influenced by the delamination size. However, it was influenced by the provided splice length. Masoud et al. (2001) carried out an experimental program to examine the flexural behavior of RC beams strengthened by carbon-FRP sheets under corrosive environment.

The experimental results proved that the fatigue life of strengthened-corroded RC beams was increased within a range of 2.5–6.0 times the unstrengthen-corroded RC beam. However, it was lower than that of the non-corroded RC beam.

Ekenel et al. (2006) investigated the flexure fatigue behavior of strengthened RC beams with carbon-FRP sheets and procured laminates. A glass fiber spike was used to anchor the carbon fabric to the RC beam substrate. The FRP precured laminate was bonded to RC beams with epoxy adhesive for one specimen and mechanical fasteners for the other specimen. The test results determined the efficiency of carbon-FRP strengthening systems in terms of resisting fatigue loading cycles up to 2 million. On the other hand, the results showed that anchor spikes increased the ultimate strength of strengthened RC beams and mechanical fasteners could be an alternative way to bond the precured laminate systems.

Wang et al. (2007) tested T-sectional girders strengthened with FRP composites under fatigue loading. Two types of FRP plates were used: carbon and glass FRP plates.

Unidirectional stitched carbon-FRP plates were used as longitudinal reinforcement for flexural strengthening, and unidirectional glass-FRP in u-strip forms were used for improving the bond condition of carbon-FRP plates and enhancing the shear strength of the retrofitted girders. The girders were subjected to more than 1 million cycles of fatigue loading. The fatigue loading represented the minimum and maximum stresses in the reinforcing steel that ranged between 40 MPa and 240 MPa. The test results disclosed that the behavior of strengthened beams with FRP composites observed significant stiffness degradation due to high range of fatigue loading.

Kim and Heffernan (2008) presented a review study on the recent accomplishment on the use of FRP composites in strengthening reinforced or prestressed concrete beams under the action of fatigue loads. The review by Kim and Heffernan (2008) specifically focused on the fatigue life, bond behavior of FRP composite, crack propagation and damage, size effects, residual strength, and failure modes. The review study concluded three important features. The first feature was that the externally bonded FRP composites significantly improved the fatigue life and the residual strength of strengthened structures by reducing the stress levels in the reinforcing steel. The second feature was that the level of the applied stress range with respect to the reinforcing steel service stresses was an important factor in the determined fatigue life of FRP-strengthened RC beams. In particular, no significant fatigue damage was observed in the case of the FRP-strengthened structures exposed to typical service load ranging between 30 to 60% of the steel yielding capacity. However, when the load range exceeded the service load levels, considerable fatigue damage occurred with a significant decrease in the fatigue life of the strengthened structures.

The third feature indicated that the fatigue limit state needs to be considered in the design stage of aged bridge components.

Ekenel and Myers (2009) conducted an experimental campaign to study the fatigue performance of carbon-FRP strengthened RC beams under the effect of environmental conditioning and sustained load. Ekenel and Myers (2009) specified that all beams survived 2 million fatigue cycles without showing significant bond degradation between the CFRP composites and beams 'substrate. However, the environmental conditioning produced significant flexural stiffness degradation in the strengthened RC beams.

The behavior of FRCM-concrete joints subjected to fatigue and post-fatigue monotonic loading was studied by D'Antino et al. (2015). The conducted test was a single-lap shear test. The fatigue loading protocol was designed to explore the different fatigue frequencies and loading ranges on the bond performance of the FRCM composite. The study parameters were the interfacial slip, the dissipated energy during cycles, the stiffness degradation of the interface, and the post-fatigue monotonic behavior. In general, it was observed that different combinations of amplitude and mean load range implied different damage in terms of slip, energy dissipation, and stiffness degradation. The fatigue failure of PBO FRCM-concrete joints was caused by rupture of the fibers within the bonded area. The test results inferred that an increase in the mean applied load led to an increase in the interfacial damage even in the case of a few fatigue cycles.

The experimental work in Paper I considered the important parameters for fatigue testing from previous experimental works of using FRP composites in order to determine the fatigue performance of the PBO-FRCM composite.

2.5. SHEAR PERFORMANCE OF FRCM COMPOSITE

The other interesting topic in terms of increasing the ultimate loads of existing deteriorated structural members is to hold higher shear loads. On the aspect of using strengthening composites to increase the ultimate flexural loads of the existing structures, the effect of that increase in load on its shear performance needs to be addressed as the shear failure mechanism is a catastrophic failure mode. Many experimental investigations were carried out on strengthening RC structural members with the FRP composites that effectively enhanced the shear strength of existing structures.

However, in this review, the focus is directed on the new family of composites (TRM or FRCM). Triantafillou and Papanicolaou (2006) used TRM composite to increase the shear resistance of RC members as an alternative solution for many of the problems associated with the FRP composite's durability performance. TRM jackets were used either as conventionally wrapped fabrics or helically applied strips. The experimental results of strengthened RC members concluded the substantial enhancement provided by the TRM jacketing and the percentage of enhancement was higher as the number of TRM layers increased.

Al-Salloum et al. (2012) used two different mortar types (cementitious and polymer-modified cementitious mortars) as a bonding agent for textile sheets. The study parameters included the effect of textile's reinforcement ratio and the orientation of the textile material. The experimental response of RC beams strengthened in shear concluded that the TRM composite provided a substantial gain in shear strength; that gain was higher as the textile's reinforcement ratio increased. A 45° orientated textile with polymer-modified cementitious mortar provided the highest shear strength enhancement.

A comparison study with FE modeling was carried out by the authors. A good correlation was determined between the experimental and numerical results in terms of the ultimate loads of TRM composites.

Azam and Soudki (2014) studied experimentally the effectiveness of different types of FRCM composites to strengthen shear critical RC beams. The test parameters included the strengthening composite (glass-FRCM and carbon-FRCM) and the strengthening scheme (side bonded and U-wrapped). The test results revealed that FRCM strengthening effectively enhanced the shear load of RC beams. The increase in ultimate shear load of strengthened beams ranged between 19% and 105%. Both strengthening schemes (side bonded and U-wrapped) provided similar behavior, and the experimental results were also compared with theoretical predictions according to FRP composite design guidelines in North America with some modifications.

Baggio et al. (2014) used U-wrapped FRCM strips to strengthen RC beams in shear. The test results showed that ultimate shear loads were enhanced by 30% using FRCM composite, and diagonal shear failures followed by debonding of FRCM composite were observed. An experimental study on the shear performance of the PBO-FRCM composite on strengthening RC beams under two loading schemes was implemented by Ombres (2015). The beams were strengthened with different PBO-FRCM's reinforcement ratio and two configurations (U-wrapped continuous and U-wrapped strips). The test results showed a 25% increase in shear loads for strengthened beams with continuous U-wrapped configurations while the U-wrapped strips did not permit a contribution to the shear loads.

Loreto et al. (2015) used the FRCM composite in a U-wrapped continuous to strengthen RC beams in shear. The shear capacity increased by 20% to 60% based on the FRCM composite's reinforcement ratio.

Trapko et al. (2015) demonstrated a study on strengthening RC beams in shear with a PBO-FRCM composite and anchoring system. The beams differed in terms of the inclination angle of the PBO-FRCM composite and the anchoring type. The experimental test results showed that the application of the PBO-FRCM composite functionally improved the shear strength of RC beams. The anchoring type and anchoring shape had a great impact on the effectiveness of the PBO-FRCM composite. However, the proposed method of anchoring external strips of FRCM composite did not ensure a complete utilization of the PBO mesh's tensile strength.

Tetta et al. (2015) presented an experimental work on strengthening rectangular RC beams in shear with advanced composite materials. The key study parameters included the strengthening system (TRM jacketing and FRP jacketing), the strengthening configuration (side-bonding, U-wrapping, and fully-wrapping), and the number of strengthening layers. The experimental comparison between TRM and FRP composites concluded that TRM composite was less effective than FRP composite in increasing the shear capacity of RC beams. However, the TRM composite's effectiveness depended on both the strengthening configuration and the number of TRM layers. The U-wrapped strengthening configuration was much more influential than side-bonding strengthening configuration in the case of TRM jackets, and the effectiveness of TRM jackets was noticeably amplified with the increasing in the number of TRM layers.

Based on the literature review of using PBO-FRCM composite in shear strengthening of RC members, the experimental work conducted in Paper II included using FRCM composite in shear strengthening RC beams in cases of the availability or absence of the internal shear reinforcements. The absence of internal shear reinforcement represented a unique study to determine if PBO-FRCM composite could be used for shear strengthening in case the steel rebar had a limited strength or corroded through aging.

2.6. ANCHORAGE RESPONSE WITH FRP AND FRCM COMPOSITES

On behalf of increasing the effectiveness of the different types of externally bonded strengthening composites in order to delay the premature debonding of composites, many types of anchorage systems have been developed to allow the composite materials to continuously carry a load in shear or flexure in which valuable advantage of high strength fabrics can be determined. On the other hand, proper anchorage systems allowed reducing either the required cross-sectional area of the expensive composite material or the number of strengthening layers.

Khalifa et al. (1999) conducted a study on a novel anchor system called u-anchor on the purpose of improving the surface-mounted FRP composites' performance for concrete and masonry structures. Laboratory testing confirmed the excellent performance of the u-anchor system in reducing the high stress concentration around the external FRP strengthening.

Piyong et al. (2003) conducted a study on the flexural performance of a concrete slab strengthened with prestressed CFRP sheets. Glass fiber anchor spikes used to prevent or delay the debonding of the prestressed CFRP sheets. The test results indicated that the prestressed CFRP sheets significantly increased the service and ultimate states of the strengthened slab and the presence of the glass-FRP anchor spikes prevented debonding of the carbon-FRP sheets.

Wu and Huang (2005) introduced a new hybrid bonding technique that combined an adhesive bonding agent with a new mechanical fastening. In the new technique, the mechanical fastening worked in a way that delayed the separation of the strengthening sheets from the concrete substrate. The bond strength of the new hybrid bonding technology was about 7.5 times that of the traditional method of bonding.

Orton et al. (2008) presented a review study related to the general anchor design consideration with carbon-FRP composite. The study included surface preparation, cross-sectional area of anchorage with respect to the longitudinal carbon-FRP sheet, type and property of carbon-FRP materials, and the spacing between anchors.

Kim et al. (2008) used a novel anchoring technique for strengthening RC beams with prestressed carbon-FRP sheets. The study was specifically for replacing the steel anchors with nonmetallic anchors after transferring the prestressing force, as the steel anchors are more likely to be susceptible to corrosion. Nine double RC beams were tested with various types of nonmetallic anchor systems such as non-anchored u-wraps, anchored u-wraps, and mechanically anchored u-wraps. Kim et al. (2008) concluded that the developed nonmetallic anchorages successfully transferred the sustained prestress force into carbon-FRP sheets with insignificant prestress losses.

Smith et al. (2011) reported on testing one-way simply-supported RC slabs strengthened with FRP-anchored composites in flexure. The main parameter of study was the effect of different arrangements of FRP anchors. The test results showed that the anchorage systems had a great influence on the flexural performance (ultimate loads and ductility). The ultimate load enhancement of anchored strengthened slabs was between 30% and 110%, respectively, over the unanchored FRP-strengthened slab. In addition, the different arrangement of FRP anchors concluded the optimal strength and deflection enhancement in FRP-strengthened RC slabs.

Bae and Belarbi (2012) investigated three different anchorage techniques through an experimental work on full-scale reinforced concrete T-beams. The anchorage systems were discontinuous mechanical anchorage (DMA system), sandwich panel mechanical anchorage (SDMA system), and additional horizontal FRP strips (HS system). Bae and Belarbi (2012) pointed out that the SDMA system performed best, followed by the DMA and HS systems. In addition, there was interaction between the external FRP strengthening and the internal stirrups, and the mechanical anchorages influenced the performance of the internal transverse shear reinforcements.

Another study on using a prestressed-CFRP system for strengthening RC beams was investigated by You et al. (2012). Eight small-scale and two large-scale concrete beams strengthened with different arrangements of prestressed CFRP strips were tested up to failure. The main study parameters were the level of prestressing force and the mechanical end anchorages. The test results indicated that the prestressed CFRP strips were able to produce higher first-cracking, steel-yielding, and experimental ultimate loads in the strengthened beams.

However, the increase in loads was based on the level of prestressing force, and the loads increased up to a limited value. The strengthened beam with prestressed CFRP strips and mechanical anchorage at the ends exhibited a higher ultimate load and very significant ductility enhancement with respect to the prestressed strengthened beam without anchorage.

Grelle and Sneed (2013) and Kalfat et al. (2013) presented a review study on the use of anchor systems in strengthening and retrofitting FRP composite applications. The intensive study included different mechanical anchorage systems that were discussed in terms of their purpose, performance, mechanism of work, and areas in need of future research.

In 2016, Tetta et al. conducted another experimental investigation on the use of TRM jacketing in shear strengthening for full-scale reinforced concrete T-beams. The study focused on the behavior of a novel end-anchorage system comprised of textile-based anchors. The study parameters, as stated by the authors, included the use of textile-based anchors as end-anchorage system of TRM u-jackets, the number of TRM layers, the textile properties (material, geometry), and the strengthening system. Tetta et al. (2016) proved the effectiveness of textile-based anchors on enhancing the shear performance of TRM jackets and the shear strength proportionally improved as the number of textile anchors increased. Thus, Tetta et al. (2016) concluded that TRM jackets could be as effective as FRP jackets in increasing the shear capacity of full-scale RC T-beams.

2.7. OTHER EXPERIMENTAL WORKS WITH FRCM COMPOSITE

Zhu et al. (2011) investigated the dynamic tensile testing of fabric cement composites. Three different fabrics were included: AR-glass weave bonded, PE knitted short weft, and carbon knitted weft insertion. The study was conducted to determine the extreme resistance of coupon composite specimens under service dynamic load. The responses of the coupons were determined based on the actual properties of the fabrics. Composite made out of carbon fabric confirmed its significant effectiveness in resisting the high speed tensile testing (strength and ductility) among other composites.

Abegaz (2013) and Trapko (2014) used FRCM composite for confinement of columns in square, rectangular, and circular-cross sections. The experimental results showed that the significant efficiency of FRCM composite was obtained in confining circular cross-section columns rather than rectangular cross-section columns.

Colajanni et al. (2014) used FRCM composites for confinement of concrete columns. The investigation included experimenting and modeling analysis. The experimental results showed that the FRCM confinement systems produced a noticeable increase in strength and ductility of RC columns.

Michels (2014) conducted a study on strengthening and testing RC slabs with carbon-FRCM composite at ambient and elevated temperature. Static testing of strengthened slabs with one or two layers of strengthening composite at ambient temperature proved the efficiency of carbon-FRCM composite in terms of increasing the yield and ultimate loads. In addition, the tested slab under fire showed that the FRCM composite was able to carry a significant static load for two hours without any sign of collapse.

In particular, exposing the slab to a 300°C (572°F) did not seem to affect the residual tensile strength, while an increase to 500°C (932°F) led to a strength drop of approximately 42%. Babaeidarabad et al. (2013, 2014) studied in-plane and out-of-plane behavior of unreinforced masonry walls strengthened with PBO-FRCM composite. Both experimental works concluded the increasing of the in-plane shear capacity for minimizing the damages due to earthquakes and increasing the out-of-plane flexural capacity of unreinforced masonry.

Bisby and Stratford (2016) conducted an experimental investigation on the fire performance of well-anchored TRM, FRCM, and FRP flexural strengthening systems. The results of the series of novel tests determined that the anchored strengthening systems were able to withstand exposure to temperatures up to 464°C (867°F) depending on the level of sustained stress/strain in the strengthening system. It was also found that the TRM and FRCM systems had better resistance to the fire exposure in terms of producing non-combustible and non-toxic fumes and provided additional concrete cover to the internal steel reinforcement, thus enhancing the fire performance of RC elements even in cases where the strengthening system was rendered ineffective during fire exposure. D'Agata et al. (2016) conducted a numerical simulation to evaluate the performance of RC slab strengthening by FRCM composite. Good correlation between FE results and experimental data were highlighted both in terms of the load–deformation behavior and the failure load.

Donnini et al. (2016) conducted experimental testing to determine the mechanical properties of FRCM composite using carbon fabrics with different coating treatments and a quartz sand layer.

Three different test methods were conducted to determine the influence of the coating treatments. These test methods involved the direct tensile, pull-off, and shear double lap tests. The experimental test matrix was based on different types of fabrics and mortars under different dosage of coating treatments during fabrication. Experimental evidence presented a better bond performance between the treated fabric and matrix composite verses the untreated fabric and matrix composite. The enhancement in bond performance between the treated fabric and matrix composite was found to be associated with the percentages of resin and the type of mortar used.

2.8. FRCM COMPOSITE IN FIELD APPLICATIONS

ACI 549 (2013) reported a few field applications related to the use of FRCM composite in repairing and strengthening deteriorated structures. FRCM composite was used to strengthen a railroad bridge along the Roma-Formia line in Italy (Berardi et al. 2011). FRCM composite was used to strengthen RC tunnel lining along the Egnatia Odos Motorway in Greece in order to correct its structural deficiency (Nanni 2012).

FRCM composite was selected for confinement of the Trestle bridge base in New York (Nanni 2012). The RC bridge piers of a structure located in Novosibirsk, Russia were strengthened with FRCM composite (Nanni 2012). Those piers were reconstructed in 1958 by increasing their dimensions. After the reconstruction, significant temperature and shrinkage cracks were formed along the construction joints and new corbels.

Although the cracks were epoxy-injected in 1991, they reappeared six years later. Thus, the owner elected to repair and strengthen the structure with FRCM composite.

PAPER

I. FATIGUE AND FLEXURAL BEHAVIOR OF REINFORCED CONCRETE BEAMS STRENGTHENED WITH A FIBER REINFORCED CEMENTITIOUS MATRIX

Zena R. Aljazaeri [1], John J. Myers [2*] F.ASCE
[1] Graduate Research Student, Missouri University of Science and Technology, 1304 Pine Street, 201 Pine Building, Rolla, MO 65409, USA. Email: zracnb@mst.edu
[2] Professor of Civil, Arch. and Envir. Engr, Missouri University of Science and Technology, 325 Butler-Carlton CE Hall, Rolla, MO 65409, USA.
Email: jmyers@mst.edu
*Corresponding author

ABSTRACT

The need for repair and rehabilitation is crucial issue in order to achieve sustainable concrete infrastructures with their efficient working and safe conditions. One of the most recent innovative composite materials that have been proposed to the market is a fabric reinforced cementitious matrix (FRCM) strengthening system. This system consists of two components: a structural reinforcement mesh and a cementitious matrix. The structural reinforcement mesh consists of a polyparaphenylene benzobisoxazole (or PBO) fiber composite, while the cementitious matrix is a nontoxic grout system based on portland cement with a low dosage of dry polymers. The first aim of this study was to evaluate the fatigue resistance of reinforced concrete (RC) beam strengthened with FRCM under fatigue loading and post-fatigue flexural strength. The second aim was to investigate the durability performance of the FRCM after exposure to environmental conditioning including temperature, moisture, and sustained stress.

All of the beam specimens examined in this study were subjected to fatigue loading for 2 million cycles before flexure testing. The stiffness reduction of both unstrengthened and strengthened RC beams was evaluated. The effects of environmental exposure were also examined. Results indicated that the FRCM strengthening system can enhanced the fatigue and flexure performances of RC beams. Higher stiffness degradation was observed in beam specimens that were exposed to environmental conditioning. The exposed beam specimens exhibited improved performance under the post-fatigue flexure test.

KEYWORDS

Fabric reinforced cementitious matrix (FRCM); environmental conditioning, fatigue behavior; flexural behavior; strengthening; beam stiffness.

INTRODUCTION

The use of fiber reinforced polymer composites specifically for strengthening and retrofitting reinforced concrete structures has become a common practice in structural rehabilitation applications in the last decade (Hojatkashani and Kabir 2012). The primary advantages of fiber reinforced polymer (FRP) composites are related to their light-weight, ease of application, resistance to corrosion, and minimal effects on structural aesthetics (Babaeidarabad et al. 2014; Ekenel et al. 2006). However, the resin's poor behavior at temperatures above its glass-transition temperature, poor fire resistance, low reversibility, and lack of vapor permeability, have been observed in many applications (ACI 549, 2013).

Different composites made of a cement-based matrix reinforced by continuous dry-fabric were proposed to address the disadvantages of the FRP composites.These composites include textile reinforced concrete (TRC), textile reinforced mortar (TRM), fiber reinforced concrete (FRC), mineral based composites (MBC) and fiber reinforced cementitious mortar (FRCM). The FRCM system was used in this study to strengthen RC beams. The FRCM system has several distinct properties that allow this composite material to exceed the performance of the conventional fiber reinforced polymers (FRP). These properties include an enhanced impact tolerance, compatibility with chemical, physical, and mechanical properties of the concrete substrate, ease of installation, good performance at elevated temperatures and fire resistance, and ease of reversibility (ACI 549, 2013).

The FRCM system's mechanical and durability properties have been investigated by Arboleda (2014). It was concluded that this system can address the resin's fire resistance problems, moisture resistance issues, and energy absorption flaws. Several studies were recently conducted to investigate the efficiency of the FRCM system in strengthening structural concrete members. Previous results showed that the use of the FRCM system enhanced the flexural and shear capacities of the strengthened RC members (Babaeidarabad et al. 2014; Ombres 2011; Loreto et al. 2014). However, the RC beams in bridge engineering applications are continuously subjected to oscillatory loads through their entire lives. These loads can create fatigue cracks that could significantly reduce the structure's life expectancy (Masoud et al. 2001). The fatigue performance of RC beams strengthened with an FRCM system under different environmental exposures was investigated in this study.

TEST SPECIMENS AND MATERIAL CHARACTERIZATIONS

Eight RC beam specimens were fabricated. Each specimen was 2.133 m (7-ft) long with a 305 mm (12-in.) depth and a 203 mm (8-in.) wide rectangular cross section. The bottom reinforcement consisted of three 10 mm (No. 3) diameter deformed rebar. The top reinforcement consisted of two 10 mm (No. 3) diameter deformed rebar. The transverse shear reinforcement consisted of 10 mm (No. 3) in diameter deformed rebar spaced at 127 mm (5-in.). The typical beam specimen' geometry and reinforcement is illustrated in Fig. 1.

Ready mixed concrete was used to cast the beam specimens. A series of standard cylindrical specimens 100 mm (4-in.) in diameter and 200 mm (8-in.) in height was used to specify concrete properties. The concrete's average compressive strength was about 38.4 MPa (5570 psi) in accordance with ASTM C39 (2014) at the date of beam specimens' testing. The concrete's modulus of elasticity was about 30 GPa (4400 ksi) in accordance with ASTM C469 (2014). Three coupons were tested to determine the tensile yield strength of both longitudinal and transverse reinforcement rebar. The coupons had an average yielding of 482 MPa (70 ksi) and an average ultimate rupture of 538 MPa (78 ksi) according to ASTM A370 (2012).

The PBO mesh tensile properties are presented in Table 1 as measured by the manufacturing company. The tensile strength of the PBO mesh in the main direction was about four times that in the secondary direction as thicker fibers preserved. The mechanical properties of the FRCM strengthening system were developed in this study based on the recommendations of the AC 434 (2013).

Five 50 mm (2-in.) cubes were tested to determine cementitious mortar's compressive strength. The average compressive strength of the cubes was 31 MPa (4500 psi) at 28 days in accordance with ASTM C109 (2013). Five FRCM coupons were prepared from the batching used to strengthen the RC beam specimens in order to characterize FRCM's mechanical properties. Laboratory preparing and testing of the FRCM coupon were conducted following the AC 434 protocol (2013) (see Table 1).

PBO-FRCM STRENGTHENING SCHEMES

Two RC beam specimens served as control beams. The other beam specimens were strengthened with one and four plies of the FRCM system at their tension face respectively. Before the FRCM strengthening system was installed, all beams were pre-cracked to 65% of their expected ultimate load capacity which represented an approximate service loading level except beam (B2-0). Beam (B2-0) was pre-cracked to 65% of the experimental ultimate load capacity. The beam specimens were then sandblasted to avoid or delay the FRCM system's debonding failure mode as recommended by the ACI 549 (2013).

The hand lay-out method proposed by Ruredil Company for construction chemicals and building technology and ACI 549 (2013) was followed for this installation. The strengthening PBO-fabric was applied in a 203 mm (8-in) width and a 1880 mm (74-in) length. The procedure consisted of applying the non- shrink mortar with polypropylene fibers (Exocem FP) that provides a better bond between the concrete substrate and the FRCM plies. The first layer of the cementitious mortar (X MORTAR 750) was applied with a nominal typical thickness of 3 mm (0.1-in.).

The PBO-fabric was placed and pressed gently into the cementitious mortar. Then, the second layer of the cementitious mortar was applied. This procedure was repeated successively for the specimens strengthened with four plies of FRCM.

All strengthened beam specimens were cured for 28 days under laboratory conditions before any testing was performed. The beams were identified using the following labels: the first letter (B) and the first number (1 to 8) indicate the number of the sequence, and the second number (0, 1, or 4) indicates the number of the FRCM's plies.

The test matrix was divided into two groups as presented in Table 2. In group one, the beams were maintained under laboratory conditions. In group two, beams were placed into the environmental chamber and exposed to varying cycles of freezing and thawing, elevated temperatures, and high relative humidity. Some of these beams were subjected to self-weight loading conditions only while the others were subjected to a sustain load up to 40% of their expected ultimate load capacities.

The environmental regime was developed and based on Missouri state weather conditions. The data collected was from the National Weather Service and Worldwide Weather Station during a time frame from 1980 to 2013 to determine a suitable weather conditioning regime.

Environmental cycles were set up for 100 freezing and thawing cycles from −18 to 4°C (0 to 40°F); 150 extreme temperature cycles between 27 and 49°C (80 to 120°F); and 150 relative humidity cycles between 60% and 100%. The environmental regime is presented in Fig. 2.

EXPERIMENTAL TEST SET-UP AND INSTRUMENTATION

A steel loading fixture was used to maintain the beam specimens under a sustained load inside the environmental chamber. The first beam specimen was set on a steel frame at both sides. The second beam specimen was inverted and placed over the first beam. Steel plates with two springs were used to separate the two beam specimens and apply the sustained load. The top ends of the inverted beam were restrained by the stiff steel plates and nuts. The nuts were tightened to the level that the two springs were equally compressed to provide the required sustained load. Fig. 3 shows the fixture set-up. The springs were loaded in a compression machining to obtain the load-deflection response in the elastic region. A 38 mm (1.5-in) displacement was enforced on each spring to produce a total sustained load of 27 kN (6 kip). The applied sustained load represented the average of the sustained load for the two beam specimens (B5-1 and B8-4). The displacement of the springs was checked occasionally during conditioning to verify that no relaxation in the load was occurring. A balanced level of the applied load on the beam specimens for their entire time inside the chamber was maintained.

Before testing, two types of strain gauges were used to record the strain data. The 20CBW type had a 50 mm (2-in.) gauge length for the FRCM system that was attached to its surface. The 250BG type had a 6.35 mm (0.25-in.) gauge length for the longitudinal rebar. A linear variable differential transducer (LVDT) was used to measure the mid-span displacements. During testing the beam specimens were each subjected to a constant amplitude fatigue loading over a simply supported span of 1888 mm (74-in.), as depicted in Fig. 4.

The applied fatigue load ranged between 35% and 65% of the expected ultimate load carrying capacity of the beam specimens listed in Table 3. The applied fatigue loadings were equivalent to the minimum and maximum expected loads that beam specimens can carry at a service stage in bridge engineering applications (AASHTO specifications 2012). Except, for beam specimen (B2-0) which was loaded based on the actual ultimate flexure capacity of the control beam specimen (B1-0). The beam specimen (B2-0) was under a high loading rate in order to determine the effectiveness of the strengthened beam under high loading rates. All of the beam specimens successfully lasted fatigue cycling for up to two million cycles under a fatigue frequency of 5Hz (5 cycles /second). The selected number of cycles was based on the estimation from the general information provided by AASHTO specifications (2012) and previously conducted studies (Ekenel et al. 2009, Hojatkashani et al. 2012).

The fatigue loading frequency was selected within the frequency limit specified by ACI 215 (1997) which stated that the frequency between 1 Hz to 15 Hz has little effect on the fatigue strength where the maximum applied stress is less than 75% of the ultimate capacity of the members. An objective of this work was to study the effect of increasing the number of fatigue cycles on the degradation in the beam specimens' stiffness. The first ten cycles were run under 0.2 Hz frequency to measure the initial stiffness of the beam specimens.

The stiffness measurements were calculated at the end of 250,000 cycle increments up to 2 million cycles. A frequency of 0.2 Hz was selected to be closer enough as if a monotonic loading was applied. A post fatigue monotonic test was accomplished at the end of the fatigue cycles.

FATIGUE RESULTS

The plots of the stiffness measurements versus the number of the fatigue cycles are presented in Fig. 5a and 6b. The stiffness measurements were based on the maximum mid-span displacement at the maximum fatigue loading. For the control beam specimen (B1-0), its stiffness degradation was 8% from the initial measured stiffness at the first 250,000 cycles followed by a stabilized stiffness degradation of 14% at the end of 2 million cycles. The strengthened beam specimens with one ply of the FRCM system (B3-1, B4-1, and B5-1)) exhibited stiffness degradations of 11%, 25%, and 26% at the first 250,000 cycles, respectively. After 2 million cycles, the degradations of the stiffness in these beams were 12%, 27%, and 35%, respectively. The beam specimen (B2-0) was under a high loading rate in order to evaluate the effectiveness of using multiple plies of the FRCM in the fatigue enhancement. The observed stiffness degradation in beam specimen (B2-0) was 22% at 250,000 cycles. Then, the test was terminated when the beam specimen lost 33% of its stiffness at 500,000 cycles as excessive cracks developed. The strengthened beam specimens with four plies (B6-4, B7-4, and B8-4) exhibited stiffness degradations less than those beam specimens strengthened with one ply. The stiffness degradations for beam specimens (B6-4, B7-4, and B8-4) were 8%, 21%, and 12% at the first 250,000 cycles, respectively. After 2 million cycles, the degradations of the stiffness in these beams were 11%, 22%, and 31%, respectively.

The environmental conditioning increased the beam specimens' initial stiffness while their final stiffness was significantly degraded after 2 million cycles of the fatigue loading. The initial stiffness was increased as these beam specimens went through recurring conditions due to many cycles of exposure to high temperature and humidity.

The exposed beam specimens under no sustained stress (B4-1 and B6-4) had a higher stiffness degradation compared to unexposed beam specimens (B3-1) and (B6-4). The exposed beam specimens under sustained stress had a significant impact on the beam specimens' stiffness around a 30% reduction as the control beam specimen (B2-0). However, the observed cracks in the control beam (B2-0) after 500,000 cycles had a width of 0.64 mm (0.025-in) at the mid-span, while only hair cracks developed in the strengthened beam specimens with the FRCM system as seen in Figs. 6a and 6b. The FRCM system provided restraint against propagation of wider fatigue cracks. None of the strengthened beam specimens observed cracks extending into the strengthening system, as seen in Fig. 6c.

The average strain readings in the longitudinal rebar were ranged between 0.0004 mm/mm (in/in) [in the beam specimens with a low load rating] and 0.0008 mm/mm (in/in) [in the beam specimens with a high load rating]. The average strain readings in the FRCM system were ranged between 0.0006 mm/mm (in/in) [in the beam specimens with a low load rating] and 0.001 mm/mm (in/in) [in the beam specimens with a high load rating].

POST-FATIGUE MONOTONIC LOADING

Each beam specimen was subjected to monotonic four point loading up to failure after 2 million successfully completing fatigue cycles. The loading rate was used displacement control of 1.3 mm/minute (0.05 in/min).

LVDT was used to measure the mid-span displacements and the same strain gauges that attached for fatigue loading were used to measure the strain gauge readings in the longitudinal rebar and the FRCM system. The load- displacement curves are shown in Fig. 7. The experimental results of the ultimate load capacity were compared with the ACI expected ultimate load capacity, as presented in Table 4. The results indicated that the beam specimens failed at approximately twice the estimated load using ACI 318 (2014) and ACI 549 (2013). The underestimate of the expected ultimate load by ACI 549 (2013) is due to the limit of the tensile stresses in the steel reinforcement rebar's to its yielded values as well as the limit of the effective maximum stresses in the FRCM system to prevent debonding failure mode.

The control beam's (B1-0) longitudinal rebar yielded and was followed by concrete crushing. The control beam (B2-0) failed under high fatigue loading after lasting for 500,000 cycles. The failure mode was yielding of the longitudinal rebar followed by concrete crushing, as seen in Fig. 8. All strengthened beam specimens with one ply observed yielding of their longitudinal rebar followed by FRCM slippage, as seen in Fig. 8. The FRCM slippage was defined as the PBO mesh slipping out of the cementitious matrix at the mid-span location where the maximum displacement occurred (Babaeidarabad et al. 2014). The strengthened beam specimens with four plies of the FRCM system observed a different failure mode. The longitudinal rebar yielded. Then the FRCM system debonded at the ultimate stage, as seen in Fig. 8.

The strain reading was between 0.006 mm/mm (in./in.) and 0.009 mm/mm (in./in.) in the longitudinal rebar. The strain reading was between 0.01 mm/mm (in/in) and 0.025 mm/mm (in/in) in the FRCM system.

The percentage increase in the strengthened beam specimens' ultimate load capacity compared to the control beam (B1-0) is presented in Table 4. The strengthened beam specimens with one ply of the FRCM system exhibited a 13%, 36%, and 15% increase in the ultimate load capacity. The strengthened beam specimens with four plies of the FRCM system exhibited a 23%, 62%, and 60% increase in the ultimate load capacity. The variation in the enhancement for one reinforcement ratio is due to variation of exposure and loading conditions. The beam specimens inside the environmental chamber observed higher ultimate load due to curing effect of high temperature and humidity cycles.

The percentage increase in the ultimate load of the strengthened beam specimens were agreed with the experimental results that found by Babaeidarabad et al. (2014). Those results indicated the stiffness degradations after 2 million cycles of the fatigue loading had little influence on the beam specimen's ultimate capacities.

The displacement ductility was also determined as the displacement at ultimate load divided by the displacement at yield load (δ_u/δ_y), as seen in Table 5. The results showed that strengthened beam specimens reached high ultimate loads with lower displacement ductility than the control beam. While the displacement ductility was lower compared to the control beam, the strengthened beams showed improved energy absorption, as shown in Table 5. The energy absorption was represented by the area under the load-displacement curves. The energy absorption index was calculated as the ratio of energy absorption of the strengthened beams over the energy absorption of the control beam.

CONCLUSIONS

This experimental work was a pilot study on the fatigue performance of the fiber reinforced cementitious matrix used to strengthen RC beams. In general, the results showed the use of the FRCM system to strengthen RC beams maintains the structural integrity and increases both the ultimate and fatigue strength of the strengthened beams. The following conclusions can be drawn from this study:

1. The new innovative FRCM system can be used to improve the RC beams' fatigue performance. All of the strengthened beams lasted for 2 million fatigue cycles without any observation of debonding in the FRCM system from concrete substrate.
2. A higher percentage of the stiffness degradation was observed at the first 250,000 cycles in all beam specimens then insignificant stiffness degradation observed at the end of 2 million cycles when the beam specimens stabilized under the constant fatigue loading.
3. The unexposed beam specimens had lower stiffness degradation than the exposed beam specimens and the sustained loads reduced the strengthened beam specimens' stiffness farther
4. Exposing the beam specimens to high temperature and humidity inside the environmental chamber concluded their higher ultimate load capacities. Also, the environmental exposure did not affect the beam specimens' failure mode. The slippage mode was observed for strengthened beam specimens with one ply and the debonding mode was observed for strengthened beam specimens with four plies.

5. Using four plies of the FRCM system greatly influenced both fatigue and flexure performance (ultimate load and displacement ductility). The beam specimens strengthened with four plies observed mostly the same percentage of stiffness degradation as the beam specimens strengthened with one ply, even though those beam specimens were under a high loading rate.
6. The flexural capacity of the beam specimens was not affected by the long-term fatigue cyclic loading.
7. ACI 549 conservatively predicted the ultimate flexural capacity of the strengthened beams with the FRCM system.

ACKNOWLEDGMENTS

The authors gratefully acknowledge the financial support provided by the Ruredil Company and the ReCAST Tier 1 University Transportation Center at Missouri S&T, as well as the personnel support from the Center for Infrastructure Engineering Studies and the Department of Civil, Architectural, and Environmental Engineering at Missouri S&T.

REFERENCES

AC 434, (2013). "Acceptance criteria for masonry and concrete strengthening using fabric-reinforced cementitious matrix (FRCM) composite systems." ICC-Evaluation Service, Whittier, CA.

ACI (American Concrete Institute). (1997). "Considerations for design of concrete structures subjected to fatigue loading." ACI 215, 71, 97-121.

American Association of Highway and Transportation Officials (AASHTO). (2012). "AASHTO-LRFD bridge design specifications." Washington, D.C., 3rd Edition.

ACI (American Concrete Institute). (2013). "Guide to design and construction of externally bonded fabric-reinforced cementitious matrix (FRCM) systems for repair and strengthening concrete and masonry structures." ACI 549, Farmington Hills, MI.

ACI (American Concrete Institute). (2014). "Building code requirements for structural concrete." ACI 318, Farmington Hills, MI.

Arboleda, D. (2014). "Fabric reinforced cementitious matrix (FRCM) composites for infrastructure strengthening and rehabilitation: Characterization methods." University of Miami, Florida.

ASTM A370 (2012a). "Standard test methods and definitions for mechanical testing of steel products." ASTM International, West Conshohocken, PA.

ASTM C109 (2013). "Standard test method for compressive strength of hydraulic cement mortars (Using 2-in. or [50-mm] cube specimens)." ASTM International, West Conshohocken, PA.

ASTM C1583 (2013). "Standard test method for tensile strength of concrete surfaces and the bond strength or tensile strength of concrete repair and overlay materials by direct tension (pull-off method)." ASTM International, West Conshohocken, PA.

ASTM C39 (2014). "Standard test method for compressive strength of cylindrical concrete specimens." ASTM International, West Conshohocken, PA.

ASTM C469 (2014). "Standard test method for static modulus of elasticity and poisson's ratio of concrete in compression." ASTM International, West Conshohocken, PA.

Babaeidarabad, S., Loreto, G. and Nanni, A. (2014). "Flexural strengthening of RC beams with an externally bonded fabric-reinforced cementitious matrix." Journal of Composites for Construction 18(5), 0401400.

D'Antino, T., Carloni, C., Sneed, L. H. and Pellegrino, C. (2014). "Matrix–fiber bond behavior in PBO FRCM composites: A fracture mechanics approach." Engineering Fracture Mechanics 117, 94-111.

Ekenel, M., Rizzo, A., Myers, J., and Nanni, A. (2006). "Flexural fatigue behavior of reinforced concrete beams strengthened with FRP fabric and precured laminate systems." Journal of Composite for Construction, 10, 443-442.

Ekenel M. and Myers J.J. (2009). "Fatigue Performance of CFRP Strengthened RC Beams under Environmental Conditioning and Sustained Load." Journal of Composites for Construction,13(2), 93-102.

Hojatkashani, A., and Kabir, M. Z. (2012). "Experimental examination of CFRP strengthened RC beams under high cyclic fatigue loading." International Journal of Civil Engineering 10 (4), 291-300.

Loreto, G., Leardini, L., Arboleda, D. and Nanni, A. (2014). "Performance of RC slab-type elements strengthened with fabric-reinforced cementitious-matrix composites." Journal of Composites for Construction 18(3), A4013003.

Masoud, S., Soudki, K., and Topper, T. (2001). "CFRP-Strengthened and corroded RC beams under monotonic and fatigue loads." Journal of Composites for Construction, 4, 228-236.

National Weather Service Forecast, http:// www.weather.gov.

National Climatic Data Center (NCDC), http://www.ncdc.noaa.gov/oa/ncdc.html.

Ombres, L. (2011). "Flexural analysis of reinforced concrete beams strengthened with a cement based high strength composite material." Composite Structures 94(1), 143-155.

Table 1. Mechanical properties of FRCM coupon specimens

PBO Property (Ruredil Company)	**Symbol**	**Mean results**
Ultimate tensile stress in main direction, kN/m (kip/ft)	F_{fu}	2,640 (1,947)
Ultimate tensile stress in the secondary direction, kN/m (kip/ft)	F_{fu}	665 (490)
FRCM Laboratory Tested Property	**Symbol**	**Mean results**
The uncracked specimen's modulus of elasticity, GPa (ksi)	E^*_f	1,360 (197,000)
The cracked specimen's modulus of elasticity, GPa (ksi)	E_f	127 (18,400)
Ultimate tensile strength, MPa (ksi)	F_{fu}	1,200 (174)
Ultimate tensile strain, mm/mm (in./in.)	ε_{fu}	0.007
Fiber area by unit width, mm^2/mm ($in.^2/in.$)	A_f	0.123 (0.005)

Table 2. Test matrix

Specimen ID	**Conditioning**	**FRCM**	**# ply**
B1-0	Laboratory conditions	N/A	
B2-0	Laboratory conditions	N/A	
B3-1	Laboratory conditions	FRCM	1
B4-1	Environmental cycles (*without sustained loading*)	FRCM	1
B5-1	Environmental cycles + sustained loading	FRCM	1
B6-4	Laboratory conditions	FRCM	4
B7-4	Environmental cycles (*without sustained loading*)	FRCM	4
B8-4	Environmental cycles + sustained loading	FRCM	4

Table 3. Applied fatigue loading

Beam description	**Specimen ID**	**Sustained loading**	**Applied fatigue loading**	
			Minimum	**Maximum**
RC-*Control beam*	B1-0	-	16 kN (3.6 kip)	31 kN (7 kip)
RC beams strengthened with one ply FRCM	B3-1, B4-1, B5-1	22 kN (5 kip)	18 kN (4.2 kip)	36 kN (9 kip)
RC beams strengthened with four ply FRCM	B2-0, B6-4, B7-4, B8-4	36 kN (8 kip)	31 kN (7.3 kip)	62 kN (14 kip)

Table 4. Load carrying capacity

Specimen ID	Experimental ultimate load kN (kip)	% Increase in load carrying capacity*	Standard predicted ultimate load, kN (kip)	Experimental load/Standard predicted load
B1-0	97 (22)	-	45 (10)	2.16
B3-1	110 (24)	13%	53 (12)	2.08
B4-1	132 (30)	36%	53 (12)	2.49
B5-1	112 (25)	15%	53 (12)	2.11
B6-4	119 (27)	23%	93 (21)	1.28
B7-4	157 (35)	62%	93 (21)	1.69
B8-4	155 (35)	60%	93 (21)	1.67

* compared to control specimen B1-0

Table 5. Ductility and energy absorption

Specimen ID	Yield Deflection (δ_y) mm (in.)	Ultimate Deflection (δ_u) mm (in.)	Displacement Ductility	Energy Absorption Index*
B1-0	2.8 (0.11)	30 (1.2)	11	1.00
B3-1	3 (0.12)	10 (0.4)	3	1.03
B4-1	3.9 (0.15)	20 (0.8)	5	1.30
B5-1	3.9 (0.15)	18 (0.7)	5	1.18
B6-4	4.3 (0.17)	13 (0.5)	3	1.14
B7-4	3.5 (0.14)	23 (0.9)	7	1.36
B8-4	5 (0.2)	22 (0.87)	4	1.31

* normalized to control specimen B1-0

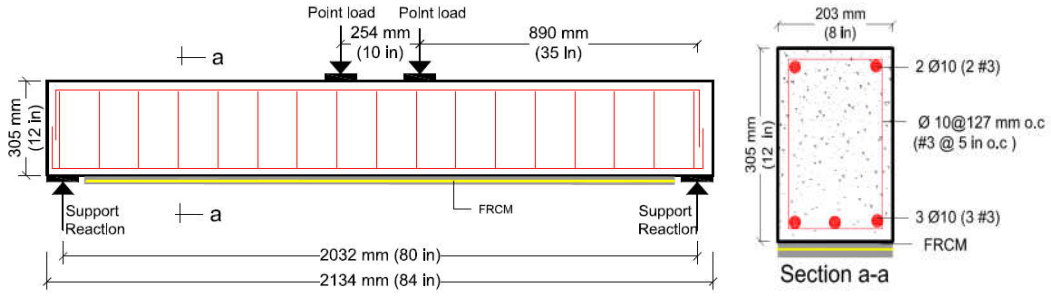

Fig. 1. Typical geometry and reinforcements of the beam specimen

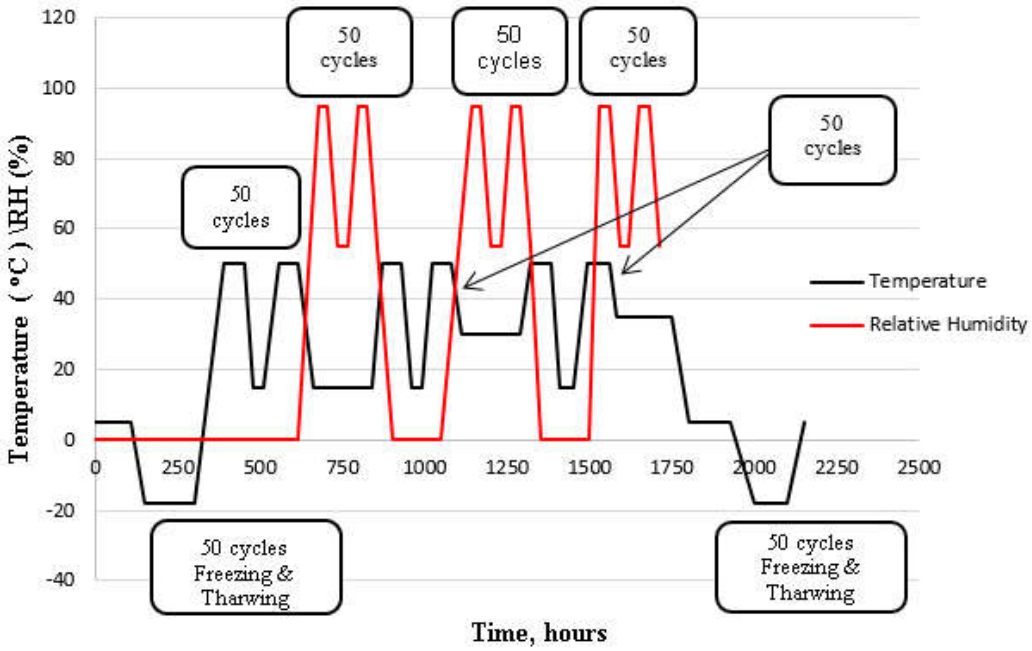

Fig. 2. Environmental conditioning regime

Fig. 3. Beam specimens inside the environmental chamber

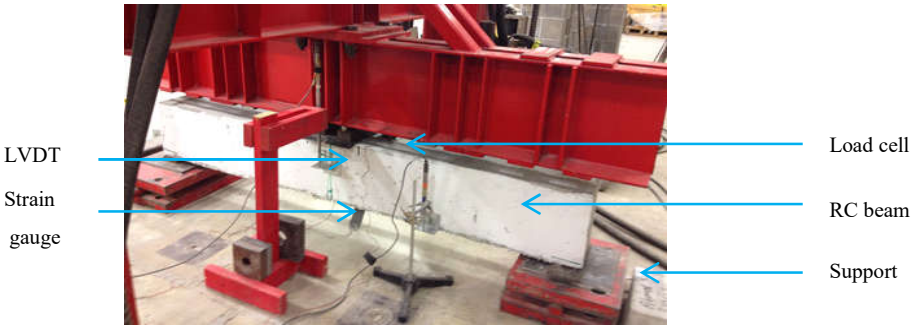

Fig. 4. Test setup

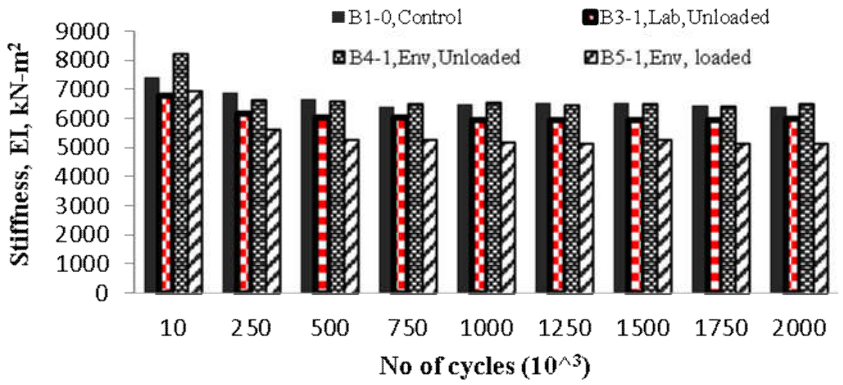

(a) Beam specimens strengthened with 1 ply FRCM

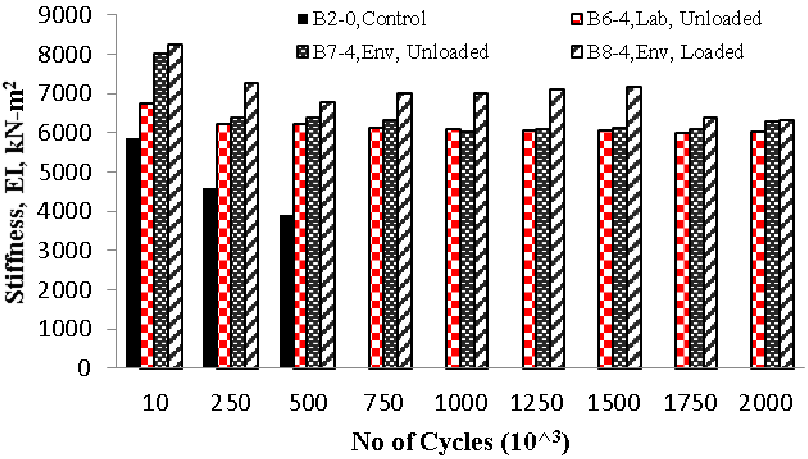

(b) Beam specimens strengthened with 4 plies FRCM

Conversion units: 1-in. = 25.4 mm; 1 kip = 4.45 kN

Fig. 5. Beam specimens' stiffness measurements

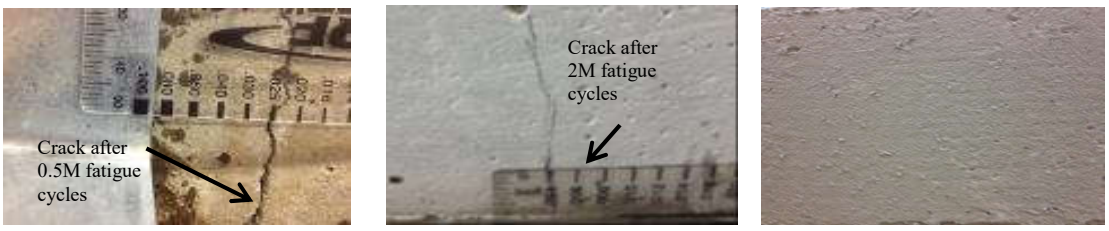

(a) Control beam (B2-0) (b) Strengthened beams c) FRCM Bottom View

Fig. 6. Fatigue cracks at the mid-span of the beam specimens

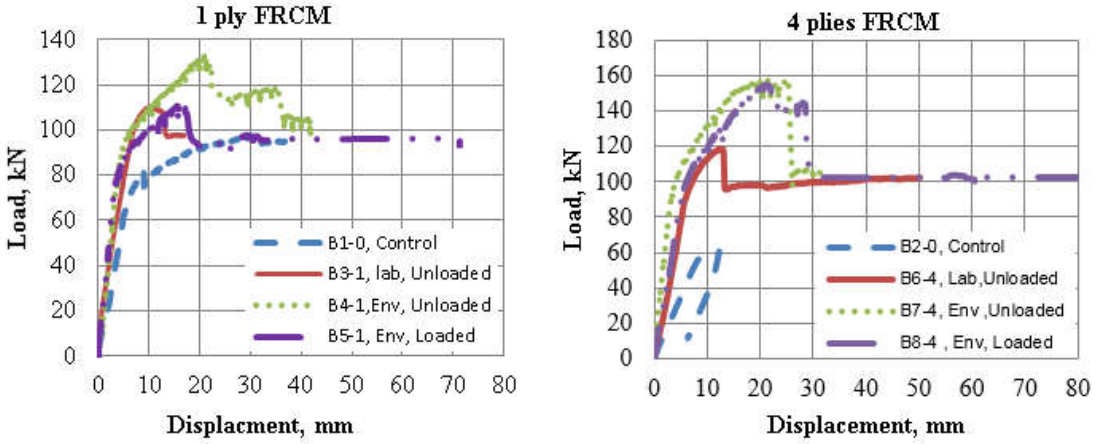

(a) 1 ply FRCM (b) 4 plies FRCM

Conversion units: 1-in. = 25.4 mm; 1 kip = 4.45 kN

Fig. 7. Load-displacement curves for flexure test preceding fatigue test

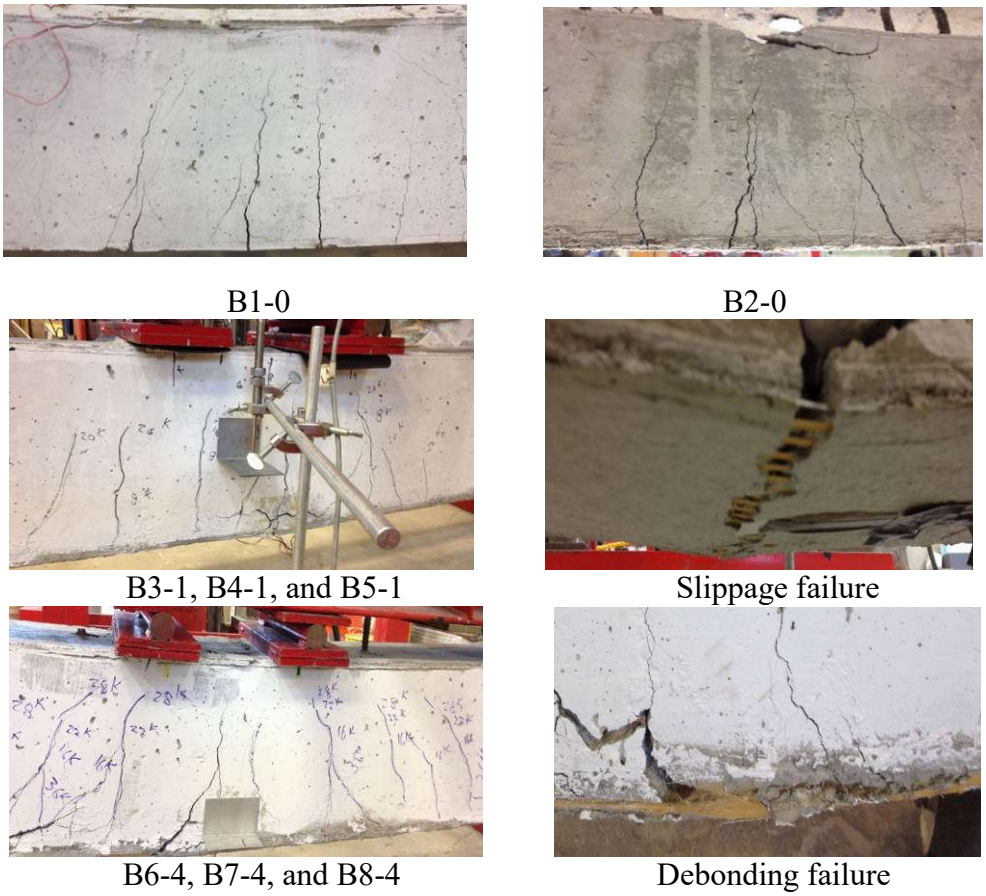

B1-0 B2-0

B3-1, B4-1, and B5-1 Slippage failure

B6-4, B7-4, and B8-4 Debonding failure

Fig. 8. Failed beam specimens

II. STRENGTHENING OF REINFORCED CONCRETE BEAMS IN SHEAR WITH A FABRIC-REINFORCED CEMENTITIOUS MATRIX

Zena R. Aljazaeri [1], John J. Myers [2*] F.ASCE
[1] Graduate Research Student, Missouri University of Science and Technology, 1304 Pine Street, 201 Pine Building, Rolla, MO 65409, USA. Email: zracnb@mst.edu
[2] Professor of Civil, Arch. and Envir. Engr, Missouri University of Science and Technology, 325 Butler-Carlton CE Hall, Rolla, MO 65409, USA.
Email: jmyers@mst.edu
*Corresponding author

ABSTRACT

The development and advancement of cement-based composites has shown promise in recent years. It is important to examine new materials and technologies so they can satisfy the ever-changing repair and strengthening application needs in the structural engineering field. An experimental study on the behavior of reinforced concrete beams strengthened in shear using an externally applied fiber reinforced cementitious matrix (FRCM) is presented. The first aim of this study was to investigate the effectiveness and the performance of the polyparaphenylene benzobisoxazole fiber reinforced cementitious mortar (PBO-FRCM) system for shear strengthening. The second aim was to study the shear performance of the PBO-FRCM system in terms of the availability and absence of internal transverse shear reinforcements. A comparison study with previous experimental work and the ACI 549 (2013) equations were done to evaluate the shear performance of the PBO-FRCM system.

The test results included the observed shear contribution of the PBO-FRCM system, the failure mode of the strengthen beams, and the influence of the internal transverse shear reinforcements on the shear performance of the PBO-FRCM system.

KEYWORDS

PBO-FRCM, reinforced concrete beams, transverse shear reinforcement, strengthening, strips, continuous, shear.

INTRODUCTION

Numerous reinforced concrete bridges and structures around the world are currently in need of repair or complete replacement as they approach the end of their service lives. Increases in traffic volume, traffic loads, and corrosion-induced deterioration are necessitating significant expenditures to strengthen and rehabilitate existing structures (Baggio et al. 2014). Of the 163,000 single span concrete bridges in the United States, 23% are considered structurally deficient or functionally obsolete (Baggio et al. 2014). In the last few decades, fiber reinforced polymer systems have been widely used for retrofitting and strengthening reinforced concrete structural members. Although the use of fiber reinforced polymers (FRP) has proven to demonstrate excellent performances both in terms of bonding and load carrying capacity, some drawbacks exist.

The epoxy resin, in fact, has a low permeability, diffusion tightness, poor thermal compatibility with the base concrete, poor fire resistance, susceptibility to ultraviolet (UV) radiation and low reversibility (Ombres 2011; Babaeidarabad et al. 2014).

As a result of these problems, alternative strengthening systems with cement based bonding agents were invented. These composite materials are previously known as textile-reinforced mortar (TRM) and have very recently been denoted as a fabric reinforced cementitious matrix (FRCM).

Triantafillou and Papanicolaou (2006) used TRM composite to increase the shear resistance of RC members in the forms of conventionally wrapped fabrics or helically applied strips. The experimental results of strengthen RC members concluded the substantial enhancement provided by the TRM jacketing and the percentage of enhancement was higher as the number of TRM layers increased.

Al-Salloum et al. (2012) used two different mortar types (cementitious and polymer-modified cementitious mortars) as a bonding agent for textile sheets. The study parameters included the effect of textile's reinforcement ratio and the orientation of the textile material. The experimental response of RC beams strengthened in shear concluded that the TRM composite provided a substantial gain in shear strength; that gain was higher as the textile's reinforcement ratio increased. A 45° orientated textile with polymer-modified cementitious mortar provided the highest shear strength enhancement. A comparison study with FE modeling was carried out by the authors. A good correlation was determined between the experimental and numerical results in terms of the ultimate loads of TRM composites.

Azam and Soudki (2014) studied experimentally the effectiveness of different types of FRCM composites to strengthen shear critical RC beams. The test parameters included the strengthening composite (glass-FRCM and carbon-FRCM) and the strengthening scheme (side bonded and U-wrapped).

The test results revealed that FRCM strengthening effectively enhanced the shear load of RC beams between 19% and 105%. Both strengthening schemes (side bonded and U-wrapped) provided similar behavior.

Tetta et al. (2015) presented an experimental work on strengthening rectangular RC beams in shear with advanced composite materials. The key study parameters included the strengthening system (TRM jacketing and FRP jacketing), the strengthening configuration (side-bonding, U-wrapping, and fully-wrapping), and the number of strengthening layers. The experimental comparison between TRM and FRP composites concluded that TRM composite was less effective than FRP composite in increasing the shear capacity of RC beams. However, the TRM composite's effectiveness depended on both the strengthening configuration and the number of TRM layers. The U-wrapped strengthening configuration was much more influential than side-bonding strengthening configuration in the case of TRM jackets, and the effectiveness of TRM jackets was noticeably amplified with the increasing in the number of TRM layers.

The new FRCM strengthening system made of a polyparaphenylene benzobisoxazole (PBO) fiber embedded into cementitious matrix was proposed to the market. The mechanical and durability properties of PBO-FRCM system have been validated by Arboleda (Arboleda 2014). The study specified the tensile mechanical properties of the PBO-FRCM and concluded that this system could address the problems regarding fire resistance, moisture resistance, and freezing and thawing.

The PBO-FRCM system flexural performance has been examined by several authors (Ombres 2011; Babaeidarabad et al. 2014; Loreto et al. 2013; Aljazaeri and Myers 2016).

The experimental studies results have shown the PBO-FRCM system enhanced the flexure carrying capacity of reinforced concrete (RC) beams in the range of 20% to 60% of the unstrengthen beams based on the PBO-FRCM' reinforcement ratio. In spite the fact that a shear failure mode in a concrete structure is a catastrophic failure where no or minimal warning is observed prior its occurrence (Li et al. 2001), finite experimental data are available on using the PBO-FRCM system to strengthen RC beams in shear.

Ombres (2015) conducted experimental study on the shear performance of the PBO-FRCM in strengthening RC beams under two loading schemes. The beams were strengthened with different PBO-FRCM's reinforcement ratio and two configurations (U-wrapped continuous and U-wrapped strips). The test results showed 25% increase in shear capacity for strengthen beam with continuous U-wrapped configurations while the strip U-wrapped configurations did not permit a contribution to the shear capacity.

Baggio et.al. (2014) used U-wrapped fiber reinforced cement matrix strips to strengthen reinforced concrete beams in shear with and without anchorage. The test results have shown that the FRCM system can effectively enhance the shear carrying capacity by 30%. Diagonal shear failures followed by debonding of the FRCM system were observed. No influence of anchorage system on the shear enhancement. Trapko et al. (2015) demonstrated a study on strengthening RC beams in shear with a PBO-FRCM composite and anchoring system. The beams differed in terms of the inclination angle of the PBO-FRCM composite and the anchoring type. The experimental test results showed that the application of the PBO-FRCM composite functionally improved the shear strength of RC beams. The anchoring type and anchoring shape had a great impact on the effectiveness of the PBO-FRCM composite.

However, the proposed method of anchoring external strips of FRCM composite did not ensure a complete utilization of the PBO mesh's tensile strength.

This study was conducted to investigate the shear performance of RC beams strengthened with externally bonded PBO-FRCM system in the availability or absence of internal transverse shear reinforcements. The absence of shear reinforcements can represent the case of corroded shear stirrups as a result of harsh environmental conditions or members without transverse shear reinforcement in need of upgrade. Furthermore, this study evaluated the effectiveness of the FRCM in enhancing the shear capacity of the RC beams. The crack propagations and beam failure behavior were inspected. The increases in the shear load and ductility performances of the PBO-FRCM system were discussed as well. A comparison study demonstrated the shear performance of the PBO-FRCM system among the conventional composites that have used in experimental and field applications. Carbon fiber reinforced polymer (CFRP), mineral-based composites (MBC), textile-reinforced cementitious mortar and textile polymer-modified cementitious mortar that were used for shear strengthening of RC beams with and without internal shear reinforcements were included in this comparison. Another comparison study between the ultimate shear loads was determined through this study and the theoretical ultimate shear loads to validate the ACI 549 (2013) equations was provided.

EXPERIMENTAL PROGRAM

Test Specimens and Materials

The beam dimensions used in this study were 2,133 mm (84-in.) long, 305 mm (12-in.) deep, and 203 mm (8-in.) wide. The distance between the supports was 1,905 mm (75-in.).

The center to center distance between the positions of load was 686 mm (27-in.). Two sets of five RC beams were fabricated. Set A beam specimens series had longitudinal and transverse reinforcements. The flexural reinforcements consisted of using three 22 mm (No. 7) diameter as bottom reinforcements and two 10 mm (No. 3) diameter as top reinforcements. The shear reinforcements consisted of 10 mm (No. 3) diameter stirrups placed at 127 mm (5-in.) spacing. Set B beam specimens series had the same longitudinal reinforcements as Set A and no transverse shear reinforcements at the regions of critical shear stresses. There were only four stirrups that provided to hang on the top longitudinal reinforcements. Fig. 1a and Fig. 1b show the dimensions and reinforcements' details for Set A and Set B beams, respectively.

The longitudinal steel reinforcement had a yield stress of 412 MPa (60 ksi) while the transverse shear reinforcement had a yield stress of 345 MPa (50 ksi). The yield strength of each reinforcement was determined from three tested coupon samples based on ASTM A370 (2012a).

The concrete properties were obtained from a series of standard cylindrical specimens with 100 mm (4-in.) diameters and 200 mm (8-in.) heights. ASTM C39/C39M (2014) and C469/C469M (2014) test methods were followed. The measured compressive strength and elastic modulus were 45 MPa (6,500 psi) and 33 GPa (4,800 ksi), respectively at the date of testing the beam specimens (90-days).

The PBO fabric was the proposed type of FRCM composite in this study. The PBO fabric was made of 5 mm (0.2-in.) and 3 mm (0.125-in.) wide yarns in the longitudinal and transverse directions, respectively.

The free space between the yarns was 5 mm (0.2-in.) and 22 mm (0.9-in.) in the longitudinal and transverse directions, respectively, and the nominal thickness of the yarns in each direction was 0.2 mm (0.008-in.) and 0.12 mm (0.045-in.) in the longitudinal and transverse directions, respectively. The cement-based mortar was made of a combination of portland cement, silica fume, and fly ash as a binder. It had less than 5 percent polymer. The cement-based mortar also contained glass fibers to improve the bond between the PBO mesh and the cement mortar. The tensile strength of the yarns in the longitudinal direction was 5,800 MPa (840 ksi) and it was five times the tensile strength of the yarns in the transverse direction, specified by the manufacturer. The modulus of elasticity of the yarns was 270 GPa (39,160 ksi) with an ultimate strain of 2.15%, and the weight of the PBO fiber in the mesh was 88 g/m^2 ($125*10^{-6}$ psi), specified by the manufacturer. The mechanical properties of the FRCM system were characterized based on AC 434 (2013) procedure, as shown in Table 1.

The five coupons were fabricated at the same time the FRCM system was prepared and applied for strengthening the beam specimens. The compressive strength of the cementitious mortar was found by testing five 50 mm (2-in.) cubes in accordance with ASTM C109 (2013) (having as average of 38 MPa (5,400 psi) at 28 days.

PBO-FRCM Strengthening Schemes

One unstrengthen beam served as a control specimen for each set. Vertical U-wrapped PBO sheets were used as it was considered the more effective strengthening configuration for reinforced concrete beams where access to fully wrap a member is not feasible. Two different configuration of strengthening were considered in this study.

For each set, two beams were strengthened with strips of the PBO-FRCM system that had a 102 mm (4-in.) width with 204 mm (8-in.) center to center spacing, as shown in Fig. 2a. The two remaining beams were strengthened with continuous strips of the PBO-FRCM system over a width of 560 mm (22-in.), as shown in Fig. 2b. The test matrix is represented in Table 2.

Specimen Preparation

The castings of the beams were made by ready-mix concrete in two batches. The specimens were left in room conditions and were strengthened after a concrete aging period of 28 days. To ensure a good bonding the bottom surface and the sides of each beam were sandblasted and cleaned by vacuum. The edges of the beam were rounded for 19 mm (0.75-in.) radius based on the recommendation of ACI 549 (2013) to prevent stress concentration failure at the edges. Before the application, the concrete surfaces were wet. The installation procedure of the PBO-FRCM systems was based on the recommendations of the manufacturer and ACI 549 (2013).

The first step involved applying the non-thixotropic mortar with polypropylene fibers (Exocem FP) to provide the perfect adhesive to the concrete surface. In the second step, the first mortar layer (X MORTAR 750) was laid on for about 3 mm (0.12-in.) in thickness. In the third step, The PBO mesh was applied and pressed slightly into the first mortar layer to ensure a good contact with the mortar. Finally, the second mortar layer was covered with the PBO mesh and leveled to have a smooth finishing surface. In the case of applying four plies of PBO mesh, the procedure was repeated until all the layers were applied and covered by the cementitious mortar. All strengthened beams were cured for 28 days under the laboratory environmental conditions before testing.

Fig. 3 shows the material and application steps for the PBO-FRCM strengthening system on the RC beams.

Instrumentation and Testing Procedure

All beams were loaded in a four point loading configuration using a vertically positioned MTS actuator, as shown in Fig. 4.

All beams were tested monotonically at a displacement rate control of 1.3 mm/min (0.05 in./min.) up to failure. Displacements were measured using a linear variable differential transducer (LVDT) seated at mid-span of the beam specimens.

A strain gauge (Type 250BG) with a 6.35 mm (0.25-in.) gauge length was used to record the strain data for longitudinal and transverse reinforcements and the PBO-FRCM.

One strain gauge was attached to the longitudinal rebar at mid-span. One strain gauge was attached to the closed stirrup from the support.

Three sets of strain gauges were attached to the PBO fibers on the last applied ply at each side of the beam on three different locations. The first strain gauge was located at 186 mm (7 in.) from the face of the support and 100 mm (4 in.) from the bottom of the beam section. The second strain gauge was located at 372 mm (15 in.) from the face of the support and 150 mm (6 in.) from the bottom of the beam section. The third strain gauge was located at 560 mm (22 in.) from the face of the support and 254 mm (10 in.) from the bottom of the beam section.

The measurements of the load versus mid-span deflection and strain gauge reading were collected from the data acquisition system for each tested beam.

EXPERIMENTAL TEST RESULTS

Beams with Transverse Shear Reinforcement

The load–mid span deflection relationships of Set A beams are shown in Fig. 5. The ultimate loads and deflections are represented in Table 3. There were no sudden brittle shear failures observed for the strengthened beams. All Set A beams observed an increase in ultimate load, as shown in Fig. 5. The percentage increase in the ultimate load of the strengthened beams relative to the control beam is presented in Table 3. The load-deflection curves of all the beams started in the linear behavior. Then, the control beam failed due to a sudden drop in the load carrying capacity. All the strengthen beams continued to carry loads with a stepped down drop in the loads as the loss in the beam specimens' stiffness occurred. The cracks developed and the crack widths increased with continually loading up to failure.

Beam specimens exhibited different failure modes under shear, as shown in Fig. 6. The control beam (BA-C) failed in shear through the formation of a single diagonal tensile crack in the shear span. The beam specimen that was strengthened with one ply U-wrapped strips of the PBO-FRCM (BA-S-1) failed via diagonal tensile shear cracks followed by slippage of the PBO-FRCM system. The slippage of the PBO-FRCM system was at the top of the second and third strips from supports.

Beam specimen (BA-S-4) observed a same load carrying capacity as beam (BA-S-1).The failure mode for beam specimen (BA-S-4) was diagonal tensile shear cracks followed by rupture of PBO fibers at the second strip from one support and debonding of other strips. The debonding of the PBO-FRCM system occurred between the PBO fibers and the attached cementitious matrix to the concrete substrate through all strips.

The lower carrying load capacity for beam specimen (BA-S-4) with respect to the provided FRCM' reinforcement ratio can be explained due to the following reasons. The first reason was the variation in the shear contribution provided by the aggregate interlock. The second reason was concluded after removing the PBO-FRCM system from the surface of the beam. Wider cracks in the beam specimen (BA-S-4) engaged the two plies of the PBO-FRCM system until rupture so the other outer plies no longer contributed in the shear carrying capability.

The beam specimens that were strengthened with continuous U-wrapped strips (BA-C-1and BA-C-4) failed by shear flexure cracks. First shear cracks were initiated and the internal shear reinforcement yielded. Then, flexural cracks propagated through the unwrapped regions, ultimately followed by crushing in the concrete. There was no evidence that the PBO-FRCM strengthening system was failed in beam specimens (BA-C-1and BA-C-4). The continuous U-wrapped strips turned the failure mode from shear cracks to flexure cracks where the higher displacement ductility observed. This includes the effective contribution of the continuous U-wrapped configuration as it provided higher strength, higher stiffness, and continuous confinement along the shear span.

The PBO-FRCM strengthening system enhanced the ultimate loads with respect to its provided reinforcement ratio in continuous U-wrapped configuration. Using four plies of the PBO-FRCM system provided double enhancement than a single ply. The strips U-wrapped configuration did not provide enhancement in the ultimate loads with respect to its reinforcement ratio that could explained as follow.

The shear performance is an unexpected phenomenon due to the wide-ranged behavior in terms of its aggregate interlock and its non-homogeneity which affects the development of shear cracks and how wide they could be. So, the authors recommended testing three beam specimens for each configuration in order to provide better assessment for shear performance of the PBO-FRCM system.

All the strengthen beams had gradually decrease in the load carrying capacity, as shown in Fig. 5. Unlike, the control beam exhibited a sudden shear failure. The ultimate defection of the strengthen beams with strips U-wrapped strengthening configuration was 25% higher than that of the control beam. The ultimate defection of the strengthen beams with continuous U-wrapped strengthening configuration was 85% higher than that of the control beam as the mode of failure changed to flexure cracks at the later loading stage. The higher ultimate deflection with the gradually decrease in the ultimate load proved that the PBO-FRCM strengthening systems developed ductile failure mode in terms of holding the beams against unwarned shear failure.

Beams without Transverse Shear Reinforcement

The load–mid span deflection relationships of Set B beams are shown in Fig. 5. As the beams reached their ultimate load, there was an abrupt drop in the load-deflection curves for Set B beams. The ultimate loads and deflections are represented in Table 3. Most of the strengthen beams in Set B had no significant increase in the ultimate loads or deflections as Set A beams did. The beam (BB-S-1) had no increase in the shear load. There was only a modest 21% increase in shear load for the beam (BB-C-1). Beams (BB-S-4 and BB-C-4) observed an insignificant increase in the shear load even though four plies of the PBO-FRCM strengthening system were used.

All beams in Set B failed due to the formation of a single diagonal tensile crack through the shear span, as shown in Fig. 6.

No evidence of shear failure through the PBO-FRCM strengthening system observed in the strengthen beams with four plies of the FRCM strengthening system. However, a slippage of the PBO fibers out of the cementitious matrix observed in the strengthen beam specimens with one ply. After peeling back the PBO-fabric of Set B beams, the crack pattern along the shear span and through the web was visible, as shown in Fig. 7a and 7b. It was evidence as the diagonal tensile crack started to propagate in concrete and become wider; it was passed through the adhesive cementitious matrix layer simultaneously. That concluded the concrete alone was not able to transfer the load through the strengthening system progressively. As well, the weakness of the cementitious matrix in carrying tensile stresses caused the matrix following the concrete crack path and preventing the high-tensile PBO fabric from being engaged.

Thus, there was not a significant increase in the shear load. Unlike Set A beams, there was a significant increase in the shear load where the internal shear reinforcements played an important role in distributing the shear stresses along the shear span and transferring the shear load through the strengthening system.

That revealed the effectiveness of the transverse PBO-FRCM strengthening was, in case of RC beams with no internal shear reinforcement, practically null. The test results of the ten beams showed a different shear performance of the PBO-FRCM strengthening system that determined in previous studies.

Loreto et al. (2015) and Ombres (2015) found that the shear failure of the PBO-FRCM system was unexpected, and the increasing in the ultimate shear load was not proportional to the reinforcement ratio of the strengthening system. It was hard to tell that the increase in the shear load of the beam specimen (BB-C-1) was due to the influence of PBO-FRCM strengthening action as the mode of failure was same as the control beam. A more experimental investigation would provide a database to assess the shear performance of the PBO-FRCM strengthening system in case of RC beams without internal shear reinforcement. Also, an average of three beam specimens for each configuration would prove the shear performance of FRCM strengthening system.

Strain measurements

The maximum recorded strains in the longitudinal and transverse reinforcements and the PBO-FRCM system are shown in Table 4. Strain gauge readings indicated that the transverse shear reinforcement yielded in beam specimens of Set A. The longitudinal reinforcement in Set A beams with the internal shear reinforcement exhibited higher strains in comparison to the longitudinal reinforcement in Set B as their beams experienced higher ultimate shear loads. Also, the failure mode changed to flexure at the later loading stage of beam specimens (BA-C-1 and BA-C-4) which contributed on higher strains in the longitudinal rebar.

The lower strain readings observed in the longitudinal reinforcement and PBO fibers for Set B beams without internal shear reinforcement. These beams did not experience a significant increase in the shear load capacity. Therefore, their dowel action and the PBO-FRCM system contributions were less in comparison with Set A beams.

The strain readings for the PBO fibers represented the higher recorded value out of six strain readings for each beam. Although, it was hard to know for certain if those values represented the maximum reachable strain value in the PBO fibers since the shear crack path was unexpected and the location of the strain gauges did not perfectly match the actual crack path or the slippage of PBO fibers. The lower shear enhancement between 18% to 32% for Set A beams validated the limited effective strain in the PBO-FRCM for shear strengthening to be less or equal to 0.4% (ACI 549 2013).

COMPARISION WITH OTHER STUDIES

Experimental results

In this study, a comparison with previous experimental studies was undertaken and presented as a further investigation due to the unpredicted shear failure phenomenon. A summary of the previous results is presented in Table 5 including results for strengthening RC beams with and without internal shear reinforcement using various strengthening systems. It has been well documented that the span-to-depth ratio plays a significant role in the shear resistance of RC beams (Taylor 1974). For this, investigating currently available experimental results was undertaken that had span-to-depth ratio which differed by less than or equal to 5% of this current study.

Ta¨ljsten, et al. (1999) conducted a study to determine the shear force capacity of the RC beams without internal shear reinforcement both before and after strengthening. The U-wrapped continuous, 45 degree carbon fiber reinforced polymer (CFRP) was used as the strengthening system. The shear load of the strengthened beam was enhanced by 250% as compared to the control one.

Pellegrino, et al. (2002) studied the shear behavior of RC beams strengthened with fully U-wrapped carbon fiber polymer laminates along the beam spans. The study was carried out on 11 beams with and without internal shear reinforcement that had different reinforcement ratios of the FRP shear strengthening. In the strengthened beams without internal shear reinforcement for one and three layers of the FRP, respectively, the FRP strengthening had increased the ultimate shear load by 160% and 180 % as compared to the control beam. The strengthened beams with internal shear reinforcement for one, two, and three layers of FRP, respectively, exhibited 130% increase in the ultimate shear loads than the control beam.

Barros et al. (2006) used carbon fiber reinforced polymer (CFRP) laminates to increase the shear resistance of the concrete beams. It was observed that a closer spacing between the strengthening strips had a great influence on increasing the shear load rather than using two strengthening layers with widely spaced strips.

Blanksvärd et al. (2009) studied reinforced concrete beams strengthened in shear with the use of the cementitious bonding agents and carbon fiber grids, denoted as mineral-based composites (MBC). The study included RC beams with and without internal shear reinforcements.

Shear failure was observed for the RC beams without internal shear reinforcements and the ultimate shear load was enhanced by 200% as compared to the control beam. Nevertheless, the flexure failure was noticed for RC beams with internal shear reinforcement.

Al-Salloum et al. (2012) conducted experimental and numerical study for the shear strengthening of RC beams using textile-reinforced mortar without internal shear reinforcements. Four beams were strengthened with textile-reinforced cementitious mortar; whereas, the other four beams were strengthened with textile polymer-modified cementitious mortar. For the RC beams strengthened by TRM with cementitious mortar in the absence of the internal shear reinforcements, the shear load was enhanced by an average of 150% that of the control beam. That is contributed to the effectiveness of the fibers' orientation (0/90) and (45/-45) degrees.

Loreto et al. (2015) conducted experimental work on strengthening RC beams in shear with U-wraps using the PBO-FRCM system. The test matrix included low and high strength concrete specimens with internal transverse shear reinforcement under three point loading. The enhancement in shear strength was proven not to be proportional to the increasing in the FRCM piles. The shear strength enhancement was found to be 121% and 151% for beams with low-strength concrete and 126 and 161% for beams with high-strength concrete in case of a single ply and four plies of the PBO-FRCM system, respectively. The observed failure mode was slippage of the PBO-fabric in the strengthened beams with one ply and the delamination from the concrete substrate in case of the strengthened beams with four plies.

In the experimental study done by Ombres (2015) on strengthening RC beams with PBO-FRCM system in shear, the internal transverse shear reinforcement was distributed at a distance equal to the effective RC beam depth (d) along the shear span. Test results clearly showed the interaction between the externally bonded FRCM strips and the internal steel stirrups.

The previous experimental results proved the effectiveness of the FRP strengthening in enhancing the shear performance of the RC beams in both the presence and the absence of the internal shear reinforcement. While the PBO-FRCM strengthening resulted in an increase in the ultimate shear load for RC beams with internal shear reinforcement only. In this study, a mainly ineffective enhancement performance for the PBO-FRCM strengthening was concluded in the case of the shear strengthening RC beams without internal shear reinforcement. This is related to the impact of lower tensile strength and modulus of elasticity of the cementitious mortar compared to the polymer curing agents used in other studies.

Comparison of experimental results to code provisions

A comparison of the experimental shear strength results with the theoretical shear strength results was performed in order to investigate the design shear strength estimated by ACI 549 (2013). The total shear strength of the strengthened RC beams based on ACI 549 (2013) was the sum of three contributions. The shear strength contribution from concrete (V_c), the shear strength contribution from steel stirrups (V_s), and the shear strength contribution from externally bonded strengthening material, FRCM (V_{FRCM}), as follows in Eq. (1).

$$V_u = V_c + V_s + V_{FRCM} \quad (1)$$

The shear strength contribution from the concrete (V_c) and steel stirrups (V_s) was calculated using ACI 318 (2014). The shear strength contribution from the continuously U-wrapped FRCM system was determined by Eq. (2) (ACI 440, 2008; ACI 549, 2013).

V_f was computed as the sum of the primary (PD) and secondary (SD) fiber strands where both directional reinforcement contributed to shear resistance.

$$V_f = 2\ n\ t_f f_{fv}\ d_f \quad (2)$$

The shear strength contribution from strips of the U-wrapped FRCM system was determined by Eq. (3) (ACI 440, 2008).

$$V_f = A_{fv} f_{fv}\ d_f / S_f \quad (3)$$

where:

n is the number of the mesh reinforcement layers; t_f is the thickness of the mesh reinforcement; A_{fv} is the effective area of the mesh reinforcements in shear based on Eq. (4); d_f is the effective depth of the FRCM shear reinforcement; and S_f is the center to center spacing between the FRCM' strips. The design tensile shear strength of the FRCM reinforcement (f_{fv}) was calculated in accordance with Eq. (5).

$$A_{fv} = 2\ n\ t_f\ w_f \quad (4)$$

$$f_{fv} = E_f\ \varepsilon_{fv} \quad (5)$$

where:

w_f is the FRCM's strip width. ε_{fv} is the design tensile strain in the FRCM shear reinforcement that was calculated by Eq. (6)

$$\varepsilon_{fv} = \varepsilon_{fu} \leq 0.004 \quad (6)$$

The actual concrete, steel, and PBO-FRCM reinforcement properties were used for the theoretical shear strength calculation.

For FRCM design considerations, the tensile modulus of elasticity of the cracked FRCM composite material (E_f) were used and the ultimate strain in the FRCM was 0.004 mm/mm (in./in.) which represented the maximum limit that is specified in ACI 549 (2013) to prevent a debonding failure mode.

The theoretical shear strength calculated without any reduction safety factor. The actual shear loads for the control and the strengthen beams ranged between 1.7 to 2.25 times the theoretical shear loads for Set A beams with internal shear reinforcement. The percentage of shear enhancement by the PBO-FRCM strengthening system determined from the experimental test results was in a good agreement with that expected from the theoretical equations of ACI 549 (2013).

However, the theoretical equations of ACI 549 (2013) anticipated a 50% to 200% shear enhancement by the PBO-FRCM strengthening system for Set B beams without internal reinforcement. In addition, the ratio of the experimental shear loads to the theoretical shear loads ranged from 1.57 to 3.85 where the experimental ultimate shear loads did not approve such enhancement. In fact, the test results indicated the insignificant shear performance of the PBO-FRCM strengthening system for RC beams without internal shear reinforcement.

The authors used a finite element modeling (FEM) to evaluate the ultimate loads of the control beam in Set A and Set B due to the higher difference between the experimental and theoretical ultimate loads. Response software program (Bentz 2000) was used and the ultimate loads are presented in column 7 of Table 3.

The actual properties of concrete and steel reinforcement were used. The FEM results found to be in a good correlation with respect to the theoretical results. The higher ratio of the experimental to theoretical shear loads for Set B beams revealed the very conservative formula of shear strength provided by the concrete as well the limitation of rebar's tensile properties to the yielding.

Thus, a restriction should point out that ACI 549 (2013) equations for shear enhancement are valid to design RC beams with internal transverse shear reinforcement only. Further investigation is necessary to accommodate the shear performance of PBO-FRCM strengthening system for RC beams in the absence of the internal shear reinforcement.

CONCLUSIONS

The PBO-FRCM technology is still a novel system under investigation and more experimental results are needed to better understand the performance of the PBO-FRCM system in shear strengthening applications. The limited tested specimens for each shear configuration in this work provided the following findings:

- The PBO-FRCM strengthened beams with internal shear reinforcement had a significant increase in the shear load and deflection (ductile behavior) near failure compared to the control beams and the strengthened beams without internal shear reinforcement. The strengthened RC beam without internal shear reinforcement exhibited an insignificant increase in the shear load capacity. The brittle failure modes of the strengthened beams were observed to be the same as the control beam.
- The continuous U-wrapping provided a more desirable ductile failure with an increase in the shear load capacity for RC beams with internal shear reinforcement. The continuity of the U-wrapped PBO-FRCM was able to minimize the stress concentration observed in the strip configuration layout.

- Without the presence of internal shear reinforcement, the non-homogenous property of concrete resulted in an unexpected crack path and larger crack width which contributed to reduce aggregate interlock contributions and lowering of the effectiveness of the PBO-FRCM system in shear strengthening.
- The relatively fragile cementitious matrix (Lower tensile strength) was another influence that prevented the PBO-FRCM strengthening system from enhancing the shear load capacity in RC beams without internal shear reinforcements.
- The presence of stirrups had a major impact on the shear behavior of the concrete beams, they helped to minimize the crack width by increasing aggregate interlock and more efficiently transfer the load through the PBO-FRCM strengthening system gradually.
- Additional research is needed to investigate varied fiber orientations and shear span on the shear performance of the PBO-FRCM strengthening system.
- Comparing the current experimental results with the pervious experimental results revealed that the comparative FRP systems are much effective than the PBO-FRCM system in terms of enhancing the shear strength of RC beams. However, the PBO-FRCM system is still a promising strengthening system as the ACI 549 (2013) limited the enhancement to be less than 50 percent in addition to its durability performance.
- ACI 549 (2013) predicted the shear strength using PBO-FRCM system conservatively for RC beams with internal shear reinforcement.

- A restriction is required to use ACI 549 (2013) equations and assumptions for shear strengthening of RC beams in the absence of internal shear reinforcement until supplementary experiment testing.
- Testing three specimens for each shear configuration would well evaluate the shear performance of FRCM strengthening system.

ACKNOWLEDGMENTS

The authors gratefully acknowledge the financial support provided by the Ruredil Company in Milan, Italy, and the ReCAST Tier 1 University Transportation Center at Missouri S&T as well as the support from the Center for Infrastructure Engineering Studies (CIES) and the Department of Civil, Architectural and Environmental Engineering at Missouri S&T in Rolla, Missouri.

REFERENCES

AC 434, (2013). "Acceptance criteria for masonry and concrete strengthening using fabric-reinforced cementitious matrix (FRCM) composite systems." ICC-Evaluation Service, Whittier, CA.

ACI (American Concrete Institute), (2008). "Guide for the design and construction of externally bonded FRP systems for strengthening concrete structures." ACI 440, Farmington Hills, MI.

ACI (American Concrete Institute), (2013). "Guide to design and construction of externally bonded fabric-reinforced cementitious matrix (FRCM) systems for repair and strengthening concrete and masonry structures." ACI 549, Farmington Hills, MI.

ACI (American Concrete Institute), (2014). "Building code requirements for structural concrete." ACI 318, Farmington Hills, MI.

Aljazaeri, Z., and Myers, J.J., (2016). "Fatigue and flexural behavior of reinforced concrete beams strengthened with a fiber reinforced cementitious matrix," ASCE Journal of Composites for Construction, 10.1061/(ASCE)CC.1943-5614.0000696.

Al-Salloum, Y.A., Elsanadedy, H. M., Alsayed, S.H., and Iqbal, R. A., (2012). "Experimental and numerical study for the shear strengthening of reinforced concrete beams using textile-reinforced mortar." ASCE Journal of Composites for Construction, 10.1061/(ASCE)CC.1943-5614.0000239, 16(1),74-90.

Arboleda, D., (2014). "Fabric reinforced cementitious matrix (FRCM) composites for infrastructure strengthening and rehabilitation: characterization methods." (Doctoral dissertation), University of Miami, Florida, Retrieved from: http://scholarlyrepository.miami.edu/oa_dissertations.

ASTM C39 (2014). "Standard test method for compressive strength of cylindrical concrete specimens." ASTM International, West Conshohocken, PA.

ASTM C109 (2013). "Standard test method for compressive strength of hydraulic cement mortars (Using 2-in. or [50-mm] cube specimens)." ASTM International, West Conshohocken, PA.

ASTM C469 (2014). "Standard test method for static modulus of elasticity and Poisson's ratio of concrete in compression." ASTM International, West Conshohocken, PA.

ASTM A370 (2012a). "Standard test methods and definitions for mechanical testing of steel products." ASTM International, West Conshohocken, PA.

Azam, R., and Soudki, K. (2014). "FRCM strengthening of shear-critical RC beams." Journal of Composites for Construction, 18(5), 04014012.

Babaeidarabad, S. Loret, G. and Nanni, A. (2014). "Flexural strengthening of RC beams with an externally bonded fabric-reinforced cementitious matrix." ASCE Journal of Composites for Construction, 10.1061/(ASCE)CC.1943-5614.0000473, 18(5), 04014009-1.

Baggio, D., Soudki, K. and Noël, M., (2014). "Strengthening of shear critical RC beams with various FRP systems." Construction and Building Materials, 66, 634–644.

Barros, J.A.O. , and Dias, S.J.E., (2006). "Near surface mounted CFRP laminates for shear strengthening of concrete beams." Cement & Concrete Composites, 28 (3), 276–292.

Bentz, E.C. (2000). "Sectional Analysis of Reinforced Concrete Members." PhD Thesis, Department of Civil Engineering, University of Toronto, 310 pp.

Blanksvärd, T., Täljsten, B., and Carolin, A., (2009). "Shear strengthening of concrete structures with the use of mineral-based composites." ASCE Journal of Composites for Construction, 10.1061/(ASCE)1090-0268,13(1), 25-34.

Li, A., Assih, J., and Delmas, Y., (2001). "Shear strengthening of RC beams with externally bonded CFRP sheets." ASCE Journal of Structural Engineering, 10.1061/ (ASCE) 0733-9445(2001)127:4, 374-380.

Loreto, G., Leardini, L., Arboleda, D. and Nanni, A., (2013). "Performance of RC slab-type elements strengthened with fabric-reinforced cementitious-matrix composites." ASCE Journal of Composites for Construction, 10.1061/ (ASCE) CC.1943-5614.0000415, 18(3), A4013003-1.

Loreto, G., Babaeidarabad, S., Leardini, L., and Nanni, A., (2015). "RC beams shear-strengthened with fabric-reinforced cementitious-matrix (FRCM) composite." Int. J Adv. Struct. Eng. (IJASE), 7(4), 341-352.

Ombres, L. (2011). "Flexural analysis of reinforced concrete beams strengthened with cement based high strength composite material." Composite Structures 94(1), 143-155.

Ombres, L., (2015). "Structural performances of reinforced concrete beams strengthened in shear with a cement based fiber composite material." Composite Structures, 122, 316–329, http://dx.doi.org/10.1016/j.compstruct.2014.11.059.

Pellegrino, C., and Modena, C., (2002). “Fiber reinforced polymer shear strengthening of reinforced concrete beams with transverse steel reinforcement.” ASCE Journal of Composites for Construction, 10.1061/(ASCE)1090-0268, 6(2), 104-111.

Ta¨ljsten, B., and Elfgren, L., (2000). “Strengthening concrete beams for shear using CFRP-materials: evaluation of different application methods.” Composites, Part B, 31(2), 87–96.

Taylor, H. P. J., (1974). “The fundamental behavior of reinforced concrete beams in bending and shear.” Shear in Reinforced Concrete, SP- 42, American Concrete Institute, Farmington Hills, MI, 43–78.

Tetta, Z. C., Koutas, L. N., and Bournas, D. A. (2015). “Textile-reinforced mortar (TRM) versus fiber-reinforced polymers (FRP) in shear strengthening of concrete beams.” Composites Part B: Engineering, 77, 338-348.

Trapko, T., Urbańska, D., and Kamiński, M. (2015). “Shear strengthening of reinforced concrete beams with PBO-FRCM composites.” Composites Part B: Engineering, 80, 63-72.

Triantafillou, T. C., and Papanicolaou, C. G. (2006). “Shear strengthening of reinforced concrete members with textile reinforced mortar (TRM) jackets.” Materials and structures, 39(1), 93-103.

Table 1. Mechanical properties of FRCM coupon specimens

FRCM laboratory properties	**Symbol**	**Mean**
Modulus of elasticity of the uncracked specimens, GPa (ksi)	E^*_f	2,705 (392,400)
Modulus of elasticity of the cracked specimens, GPa (ksi)	E_f	150 (21,850)
Ultimate tensile strength, MPa (ksi)	F_{fu}	1,480 (215)
Ultimate tensile strain, mm/mm (in./in.)	ε_{fu}	0.012
Fiber area by unit width, mm^2/mm ($in.^2/in.$)	A_f	0.123 (0.005)

Table 2. Test matrix

Set #	**Specimen ID**	**Stirrups**	**FRCM configuration**	**Ply number**	**Ply width w_f, mm (in.)**	**Strip spacing S_f, mm (in.)**
Set A	BA-C	Yes	N/A	N/A	N/A	N/A
	BA-S-1	Yes	Strips	1	102 (4)	204 (8)
	BA-S-4	Yes	Strips	4	102 (4)	204 (8)
	BA-C-1	Yes	Continuous	1	560 (22)	_
	BA-C-4	Yes	Continuous	4	560 (22)	_
Set B	BB-C	No	N/A	N/A	N/A	N/A
	BB-S-1	No	Strips	1	102 (4)	204 (8)
	BB-S-4	No	Strips	4	102 (4)	204 (8)
	BB-C-1	No	Continuous	1	560 (22)	_
	BB-C-4	No	Continuous	4	560 (22)	_

Table 3. Load carrying capacity and ultimate deflection

Specimen ID	Experimental Ultimate load, kN (kips)	% Increase in load carrying capacity	Theoretical* ultimate load, kN (kips)	Exp. load/ theoretical* load	Ultimate Deflection mm (in.)	**FEM ultimate load, kN (kips)
BA-C	325 (73)	-	160 (36)	2.04	9 (0.36)	180 (36)
BA-S-1	384 (86)	18%	170 (38)	2.24	13 (0.49)	
BA-S-4	384 (86)	18%	182 (40)	1.86	12 (0.45)	
BA-C-1	400 (90)	24%	250 (56)	2.20	16 (0.62)	
BA-C-4	427 (96)	32%	190 (43)	1.69	17 (0.67)	
BB-C	223 (50)	-	58 (13)	3.85	10 (0.40)	67 (15)
BB-S-1	198 (45)	N/A	69 (16)	2.85	8 (0.32)	
BB-S-4	231 (52)	4%	104 (23)	2.21	9 (0.38)	
BB-C-1	270 (61)	21%	81 (18)	3.31	10 (0.4)	
BB-C-4	238 (54)	7%	150 (34)	1.57	6 (0.23)	

*code predicted values.

**FEM by Response 2000 software.

Table 4. Strain readings in steel rebar's and PBO-FRCM system

Specimen ID	Strain reading mid-span rebar mm/mm, in./in.	Strain reading stirrups mm/mm, in./in.	Strain reading PBO-FRCM mm/mm, in./in.
BA-C	0.0022	0.0020	
BA-S-1	0.0074	0.0022	0.0013
BA-S-4	0.0074	0.0025	0.0028
BA-C-1	0.0070	0.0025	0.0020
BA-C-4	0.0060	0.0024	0.0020
BB-C	0.0012		
BB-S-1	0.0014		0.0015
BB-S-4	0.0016		0.0030
BB-C-1	0.0019		0.0014
BB-C-4	0.0016		0.0010

Table 5. Summary of previous studies involving strengthened RC beams in shear

Author/ Year	Specimen ID	Stirrups ρ_w	FRP type	Configuration	Sheets #	Sheets orientation	V_{test}, kN	$*V_n/V_{con.}$
Ta¨ljsten (1999)	R1	0	CFRP				212	
	R2	0					241	
	R3	0					226	
	S1	0		Continuous	2	45	681	2.80
	S2	0		Continuous	1	45	548	2.3
	S3	0		Continuous	4	45/-45	546	2.30
	S4	0		Continuous	1	45	662	2.70
	S5	0		Continuous	2	45	695	2.90
	SR1	0		Strips	1	45	390	1.80
	SR2	0		Continuous	1	45	486	2.00
Pellegrino (2002)	TR30C1	0	CFRP				74.7	
	TR30C2	0		Continuous	1	90	120	1.61
	TR30C3	0		Continuous	3	90	113	1.51
	TR30C4	0		Continuous	3	90	140	1.88
	TR30D1	0.013					162	
	TR30D10	0.013		Continuous	2	90	193	1.20
	TR30D2	0.013		Continuous	3	90	213	1.32
	TR30D20	0.013		Continuous	3	90	248	1.53
	TR30D3	0.013		Continuous	1	90	161	1.00
	TR30D4	0.013		Continuous	2	90	209	1.29
	TR30D40	0.013		Continuous	2	90	212	1.31
Barros (2006)	A10_C	0	CFRP				100	
	A10_M	0		8- Strips	2	90/90	122	1.22
	A10_VL	0		16- Strips	1	90	159	1.59
	A10_IL	0		14-Strips	1	45	158	1.58
	A12_C	0					117	
	A12_M	0		8- Strips	2	90/90	180	1.54
	A12_VL	0		16- Strips	1	90	235	2.01
	A12_IL	0		14-Strips	1	45	262	2.24
Blanksvärd (2009)	C40S0	0	MBC				124	
	C40S0-M2	0		Continuous	1	90	245	1.98
	C35s3	0.037					346	
	C35s3-M2	0.037		Continuous	1	90	337	0.97

Table 5. Summary of previous studies involving strengthened RC beams in shear (cont.)

Al-Salloum (2012)	BS 1	0	TRM, with cement Matrix Polymer-modified cement				60	
	BS 2	0		Continuous	2	0/90	85	1.42
	BS 3	0		Continuous	2	45/- 45	85	1.42
	BS 4	0		Continuous	4	0/90	90	1.50
	BS 5	0		Continuous	4	45/- 45	90	1.50
	BS 6	0		Continuous	2	0/90	80	1.33
	BS 7	0		Continuous	2	45/- 45	80	1.33
	BS 8	0		Continuous	4	0/90	90	1.50
	BS 9	0		Continuous	4	45/- 45	110	1.83
Loreto (2015)	L_0	0.008	FRCM				167	
	L_1	0.008		Continuous	1	90	203	1.22
	L_4	0.008		Continuous	4	90	251	1.51
	H_0	0.008					183	
	H_1	0.008		Continuous	1	90	231	1.26
	H_4	0.008		Continuous	4	90	296	1.61
Ombres (2015)	TRA0	0.019	FRCM				151	
	TRA1	0.019		Continuous	2	90	189	3.24
	TRA2	0.019		Strips	1	90	114	0.75
	TRB0	0.028					138	
	TRB1	0.028		Continuous	3	90	182	1.32
	TRB2	0.028		Continuous	3	90	125	0.91
	TRB3	0.028		Strips	3	90	125	0.91
	TRB4	0.028		Strips	3	90	130	0.94
	TRB5	0.028		Strips	3	90	130	0.94

* V_n/V_{con}. represents the ratio of shear strength provided by strengthened beam over the control beam.
** Conversion units: 1 kip = 4.45 kN

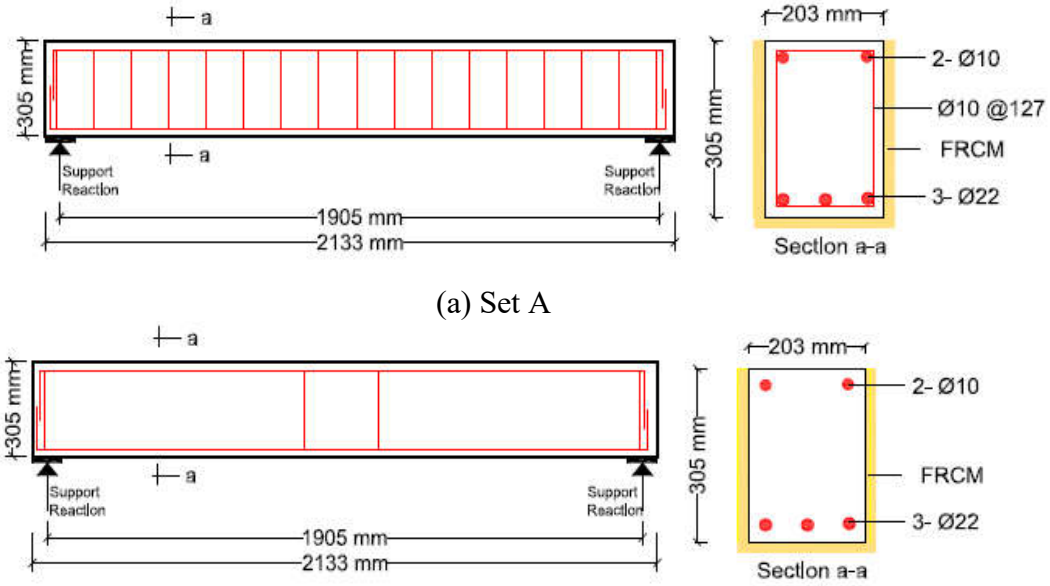

(a) Set A

(b) Set B

Conversion units: 1-in. = 25.4 mm

Fig. 1. Typical geometry and reinforcements of beam specimens

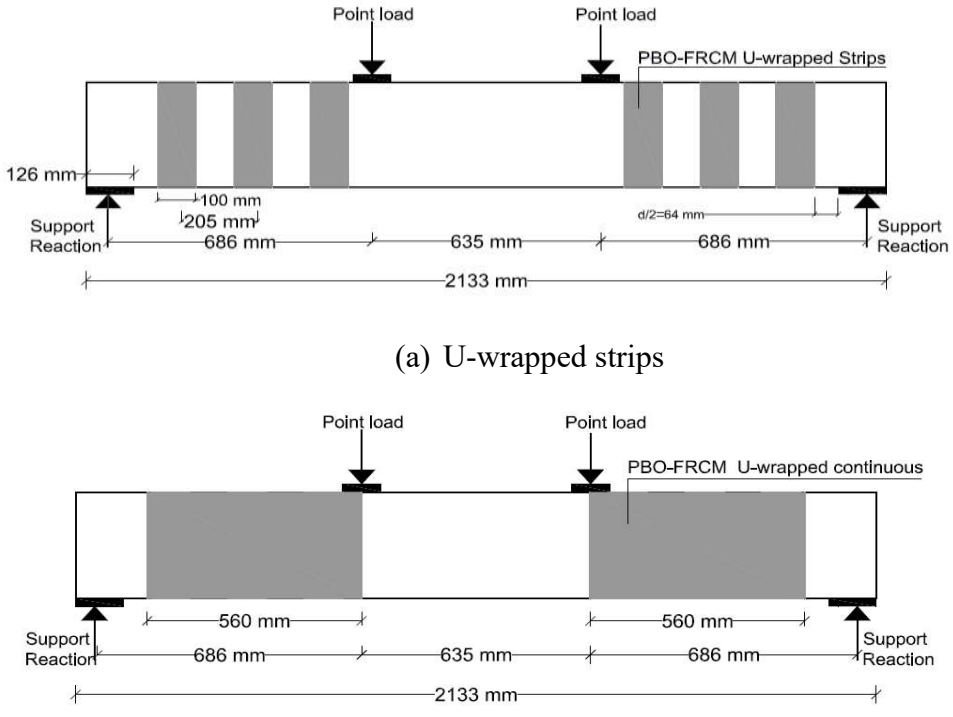

(a) U-wrapped strips

(b) U-wrapped continuous

Conversion units: 1-in. = 25.4 mm

Fig. 2. Shear strengthening configurations

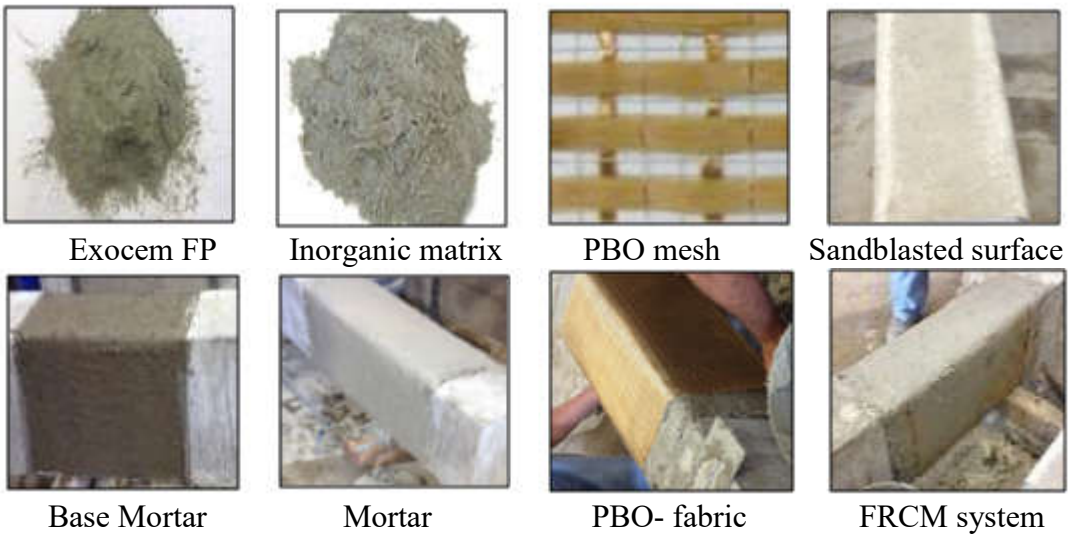

Fig. 3. Application of PBO-FRCM

Fig. 4. Beam test set-up

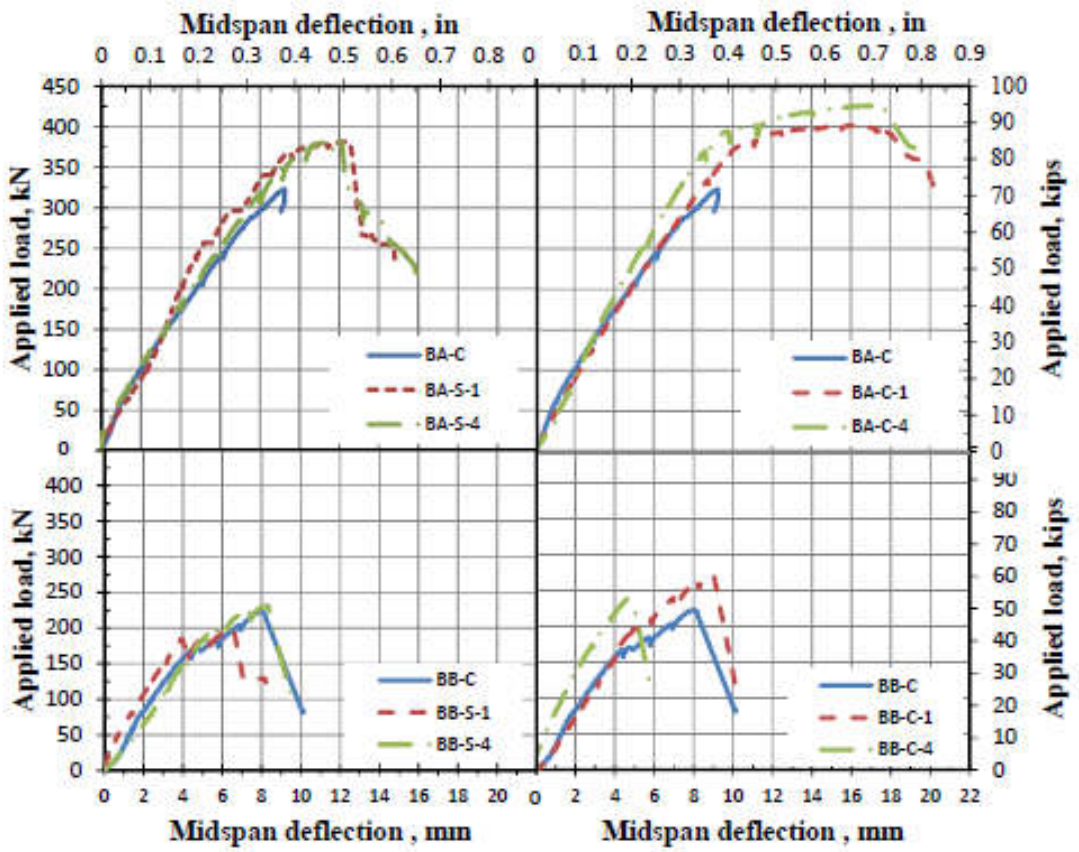

Fig. 5. Load- mid span deflection curves

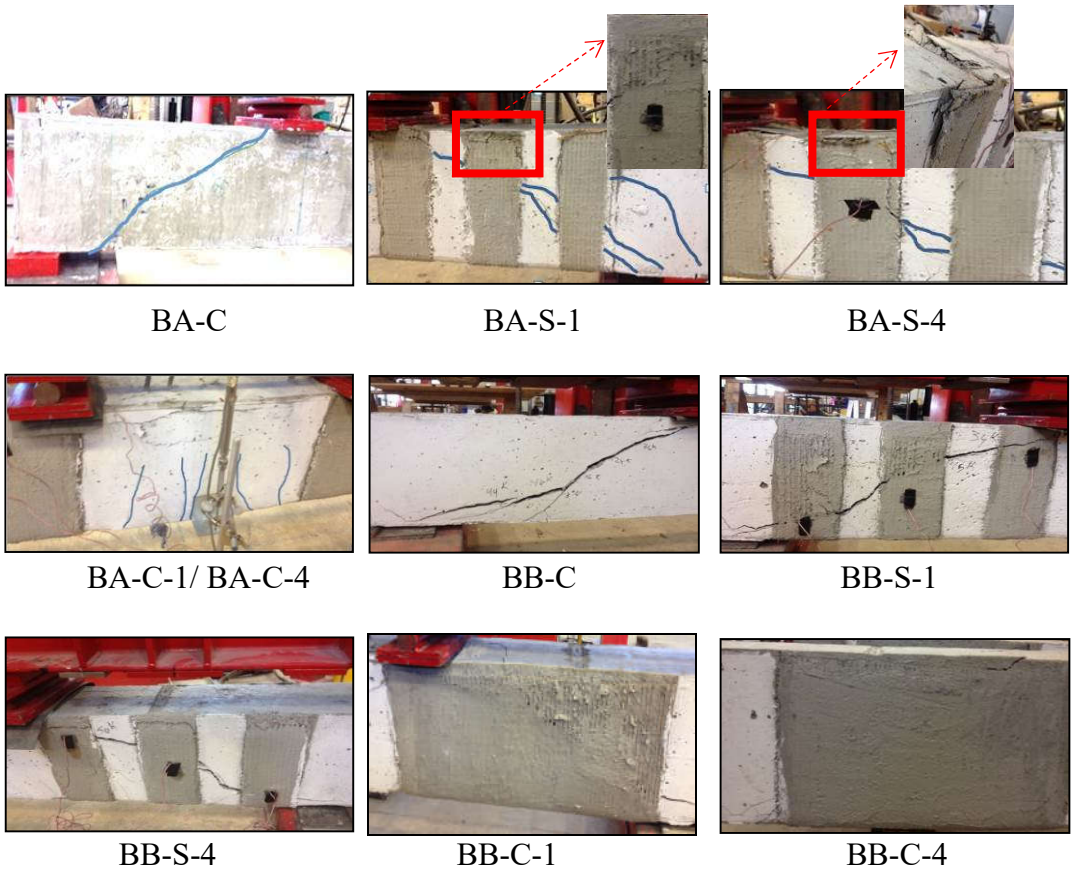

Fig. 6. Shear failures of beam specimens

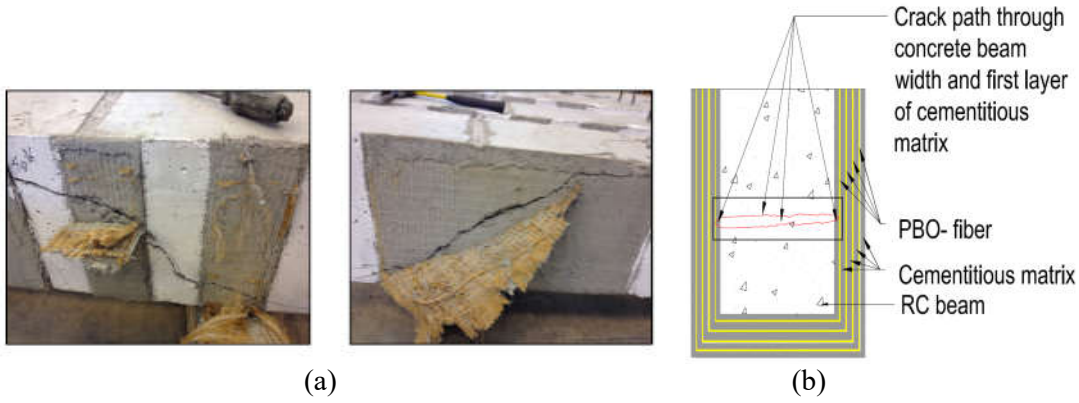

Fig. 7. Shear cracks through FRCM composite: (a) Cracks pattern of beam specimens (Set B) after peeling the PBO ply, (b) Crack path through the cross section

III. MECHANICAL AND DURABILITY PERFORMANCE OF REINFORCED CONCRETE ONE-WAY SLABS STRENGTHENING IN FLEXURAL: EVALUATION OF DIFFERENT COMPOSITE MATERIALS

Zena R. Aljazaeri [1*], John J. Myers [2]
[1] Graduate Research Student, Missouri University of Science and Technology, 1304 Pine Street, 201 Pine Building, Rolla, MO 65409, USA. Email: zracnb@mst.edu
[2] Professor of Civil, Arch. and Envir. Engr, Missouri University of Science and Technology, 325 Butler-Carlton CE Hall, Rolla, MO 65409, USA.
Email: jmyers@mst.edu
*Corresponding author

ABSTRACT

Composite materials are widely used in retrofitting bridge and building construction in order to improve the load-carrying capacity of under-strength or deficient structural members. This paper presents experimental research conducted on full-scale one-way reinforced concrete (RC) slabs strengthened using three different composites. Evaluation the flexure performance of a new innovative composite, fiber reinforced cementitious matrix (FRCM), in comparison with the conventional fiber reinforced polymers is presented for some specimens under laboratory condition and other specimens exposed to environmental conditioning before testing. The test results illustrated the impact of the composite materials on enhancing the flexural strength of RC slabs and their durability performance.

KEYWORDS

FRCM; CFRP-grid; SRP; RC slabs; one-way; strengthening; flexural behavior.

INTRODUCTION

There is an increasing need and a great challenge to repair and upgrade transportation infrastructures. There can be several reasons for the need to repair and/or upgrade structures, such as a structural insufficiency due to deterioration by de-icing-salts, freeze-thaw, or process of unsatisfactory concrete or design. In other cases, a structure may be upgraded to bear larger loads or to comply with new standards. In extreme cases, a structure may have to be repaired due to an accident or errors that were made during the design phase (Ta¨ljsten and Elfgren 2000; ACI 440, 2008; ACI 549, 2013).

Several composite systems are currently in use for repairing and/or strengthening RC structural members. One such composite that has been used quite extensively around the world during the last two decades is fiber reinforced polymers (FRP). This type of composite consists of two-components: the reinforcing mesh and the curing agent. The curing agent is an epoxy adhesive compound that bonds the fibers to the external surface of a structure. Experimental works have addressed the outstanding mechanical properties of the FRP in terms of high strength-to-weight ratio and corrosion resistance. Although, drawbacks exist with epoxy curing agent such as low impact resistance, poor thermal compatibility with the base concrete, poor fire resistance, and low reversibility have limited its use (Ombres 2011; Babaeidarabad et al. 2014).To address some of these limitations, a new family of composite materials based on cement-based matrix reinforced by continuous dry-fabric were developed.

These composites include textile reinforced concrete (TRC), textile reinforced mortar (TRM), fiber reinforced concrete (FRC), mineral based composites (MBC), and fabric reinforced cementitious mortar (FRCM) (Ombres 2011; Babaeidarabad et al. 2014). The FRCM composite is a new innovative material that has superior physical-durability properties. The FRCM composite with a cement-based curing agent is not influenced by outdoor temperature after it hardens like epoxy resins. Its fire resistance is similar to that of the concrete base as it is an inorganic material. FRCM composite does not produce toxic fumes under fire action as the epoxy curing agent does. FRCM composite can be applied on a wet surface, while FRP composites can only be applied on a dry substrate, as polyester and epoxy resins will not catalyze in the presence of water (Ombres 2011; ACI 549, 2013; Babaeidarabad et al. 2014).

In this experimental study, a unique evaluation for expending the use of the FRCM composite in strengthening one-way slabs are presented in comparison with two known composite systems. The first composite is the carbon fiber reinforced polymer grid (CFRP-grid) and the second composite is the steel reinforced polymer (SRP). The CFRP-grid and SRP composites have been used successively for experimental and field applications for repairing or strengthening existing structural members. Rahman et al. (2000) studied the service and ultimate load behavior of a bridge deck reinforced with CFRP-grid. The tested slab had a considerable reserve capacity after undergoing 4,000,000 fatigue cycles of simulated design service load and its ultimate load capacity was more than five times the AASHTO design wheel load.

Yost et al. (2001) evaluated the flexural performance of simply supported concrete beams reinforced with CFRP-grid.

The experimental results revealed that the flexural capacity of the strengthened RC beams with CFRP-grid were accurately predicted using ACI 318 (1995).

Salinas (2010) used glass, basalt, and carbon fiber polymer grids for strengthening reinforced concrete one-way slabs. The strengthened slabs with CFRP-grid exhibited a higher load carrying capacity and a higher displacement ductility performance before failure than the strengthened slabs with glass or basalt fibers.

On the other hand, Barton et al. (2005) investigated the effect of externally bonded steel reinforced polymers (SRP) for increasing the flexural capacity of RC beams. Analytical models were developed to predict the behavior of the retrofitted RC beams. Comparisons between the analytical model results and the experimental results showed a good correlation for the mid-span displacement until the reinforcing steel reaches the plastic region.

Pecce et al. (2006) demonstrated an experimental campaign for flexural strengthening of RC beams with carbon fiber polymers and steel fiber-reinforced polymers (SRP) and steel fiber-reinforced grout (SRG). Test results demonstrated that steel cords and carbon fibers, both impregnated with epoxy provided very similar ultimate loads. On the other hand, the steel cords bonded to the RC beams by cementitious grout had lower ultimate loads.

Mitolidis et al. (2012) tested three groups of full-scale RC beam specimens that strengthened in flexure or shear using steel reinforced polymers (SRP) and carbon fiber reinforced polymers (CFRP). The study showed that the flexural strengthening of RC beams with SRP strips led to a substantial increase in strength; the strength enhancement was about 90% for span specimens and about 80% for support specimens.

Moreover, a higher deformation capacity (up to 17%) was found for the strengthened specimens with SRP composite than the strengthened specimens with CFRP composite.

Balsamo et al. (2013) conducted an experimental investigation on prestressed-concrete beams strengthened in flexure using pultruded carbon laminate bonded with epoxy resin and steel wire bonded with different types of adhesive. The test results of the SRP strengthening composite showed a correlation flexural performance with the traditional CFRP plate and the conservatively of the ACI 440 (2008) approach in flexural strength.

Napoli and Realfonzo (2015) presented the results of 10 RC slabs strengthened with SRP composite under flexural loading. The test results provided valuable information in terms of maximum forces, deformability, and failure modes. The percentage of increase in load carrying capacity ranged from 40% to 90% based on the type of steel wires (low/high density), the number of layers, and the type of adhesive (epoxy/grout).

The performance of the PBO-FRCM composite for strengthening RC beams in flexure was evaluated by Tommaso et al. (2008) and Ombres (2011) in Europe. The ultimate capacity of the strengthened beams increased by a range of 10% to 44% compared to the control beam's ultimate capacity.

D'Ambrisi and Focacci (2011) conducted another experimental study on strengthening RC beams in flexure using different FRCM composite materials (carbon fabric or PBO fabrics). Different net shapes, cementitious matrices, and a number of net layers were considered.

The test results illustrated that depending on the fibers type and the matrix, different flexural debonding failure modes were identified. In most cases, fiber debonding was involved the fibers/matrix interface but did not involve the concrete, as were happened in the case of FRP-strengthened beams.

Ombres (2012) conducted a study on analyzing the debonding failure modes that had captured in pervious experimental works with FRCM composite using a nonlinear bond-slip law and a bi-linear bond slip law. The predicted results corresponding to the bi-linear bond slip law were more conservative than those results relative to the non-linear bond slip law mainly for high PBO-FRCM composite's reinforcement ratio.

Loreto et al. (2013) discussed the performance and analysis of RC slab-type elements strengthened with FRCM composite. The failure mode, ultimate load, and ultimate displacement ductility were evaluated. The test results showed that a 40% and 100% increase observed in the ultimate load for one ply and four plies of the FRCM composite, respectively.

Pellegrino and D'Antino (2013) conducted a study on the behavior of FRCM strengthened full-scale precast prestressed double-T beams through experimental testing. The experimental results determined an increase of 20% for strengthened beam with carbon-FRCM, and 24% for strengthened beam with steel fibers and cementitious matrix with respect to the unstrengthen control beam. However, the strengthened beam with carbon-FRCM exhibited a failure mode of fibers sliding inside the matrix near mid-span and a rupture of some fibers. While, the strengthened beam with steel-FRCM composite exhibited a debonding failure between the steel fiber and the cementitious matrix.

Babaeidarabad et al. (2014) demonstrated an experimental program consisting of testing 18 RC beams strengthened in flexure with two different FRCM schemes (one and four layers of fabrics). Test results showed that the FRCM composite provided a substantial gain in the flexure resistance of RC beams. Limited research studies are available on strengthening and repairing one-way RC concrete slabs, even though they represented a prevailing practice 40 to 50 years ago in the United States.

RESEARCH SIGNIFICANCE

The aim of this study was two-fold; the first aim was to study the flexure behavior of one-way reinforced concrete slabs before and after strengthening. The first aim examined the effectiveness of three composite materials in terms of the composite material's type and the number of composite layers. The second aim was to evaluate the durability performance of the composites on the flexural behavior of the strengthened RC slabs exposed to environmental conditioning. The second aim provided information about the environmental reduction factors that can be considered for implementation in design guidelines. The composite materials used in this study:

1. PBO fabric with a cement based curing agent (FRCM).
2. Carbon fiber grid with a polymer curing agent (CFRP-grid).
3. Steel reinforced polymer (SRP).

MATERIALS AND METHODS

Specimen construction details

A total of 14 reinforced concrete slabs were fabricated using ready-mix concrete in two batches. All of the slabs had a span length of 2438 mm (96-in.) with a rectangular cross section 457 mm (18-in.) wide and 152 mm (6-in.) deep.

The slab reinforcements included four 10 mm (No.3) diameter steel rebar in the longitudinal direction and 10 mm (No. 3) diameter steel rebar spaced at 305 mm (12-in.) center to center in the transverse direction. The details for the longitudinal and transverse sections through the slabs with reinforcements are shown in Fig. 1. The average 28-day compressive strength of two batches used to fabricate the panels was 38 MPa (5,512 psi) based on ASTM C39 (2014) with coefficient of variation (COV) 4%. The average modulus of elasticity of the concrete was 30,330 MPa (4,400 ksi) with coefficient of variation (COV) 0.8% based on ASTM C469 (2014). Grade 60 steel rebar were used to reinforce the one-way slabs to be under flexural failure per ACI 318 (2014).Three coupons of steel rebar were tested to specify its tensile properties based on ASTM A370 (2012). The average yielding strength of the rebar was 482 MPa (70 ksi) and the average ultimate tensile strength of the rebar was 726 MPa (105 ksi).

Description, configurations and application of the strengthening composites

Three composite materials were used in this study. Their reinforcement meshes are shown in Fig. 2. The first composite was the polyparaphenylene benzobisoxazole (PBO) fabric with a cement based curing agent. The PBO-fabric had a 5 mm (0.2-in.) width in the longitudinal direction and a 3 mm (0.125-in.) width in the transverse direction. The free spacing between the strands was approximately 5 mm (0.2-in.) and 22 mm (0.9-in.) in the longitudinal and transverse directions, respectively.

The nominal thickness of the strands was 0.2 mm (0.008-in.) and 0.12 mm (0.0045-in.) in the longitudinal and transverse directions, respectively. The curing agent used to adhere the PBO-fabric was cement based mortar with a low dosage of polymer (X MORTAR 750). The second composite was the carbon fiber grid with a polymer curing agent.

The carbon fiber grid was produced in the form of 2D strands. Each strand had a width of 6.5 mm (0.25-in.) and the grid spacing was 38 mm (1.5-in.) and 32 mm (1.25-in.) in the longitudinal and transverse direction, respectively. The grid thickness was 1.0 mm (0.04-in.) and 1.3 mm (0.05-in.) in the longitudinal and transverse direction, respectively. The curing agent used to adhere the carbon fiber grid to the concrete substrate was Sikadur 30. Sikadur 30 is a two-component structural epoxy paste adhesive that has a high-modulus and high-strength.

The third composite was the steel reinforced polymer (SRP). It is unidirectional high carbon steel cord that is made by twisting five individual wires together with a micro fine brass coating. The steel cords have some inherent ductility that was provided by the twisted wires (Huang et al. 2005; Lopez et al. 2007). The low density steel wire with category number (3x2-4-12) was used. The selected steel cords were non-galvanized steel wires in order to examine its performance under environmental exposure. The steel wire's thickness was 1.2 mm (0.047-in.) and the spacing between the steel wires was 6.4 mm (0.25-in.). The low density steel wire mesh was selected to provide equivalent strength with other types of used composites in this study. Epoxy adhesive (Sikadur 330) was the curing agent that was used for bonding the steel wire mesh to the concrete substrate. The mechanical properties for these composites are listed in Table 1.

The test matrix of this work was divided into three groups based on the type of composite material, as presented in Table 2. One RC slab served as a control slab in this experimental study. The other thirteen slab specimens were strengthened with different composites' reinforcement ratios. In first group, the slabs were strengthened with FRCM composite. In second group, the slabs were strengthened with CFRP-grid. In third group, the slabs were strengthened with SRP composite. Each group consisted of four slabs. Three of the four strengthened slabs were tested under laboratory conditions directly after curing while the fourth strengthened slab was tested after being exposed to environmental conditioning.

The selected number of strengthening layers (n) was based on the design perspective that limited the flexural enhancement to not exceed 50 percent of the existing structural strength (ACI 440, 2008; ACI 549, 2013). This limit is imposed to guard against a collapse of the structure due to bond or other failure of the fiber reinforced composites that may occur due to damage, vandalism, fire, or other causes. The identification symbol used for describing each group in the test matrix was made-up of three symbols. The first symbol denoted the group number: G1 for the FRCM composite, G2 for the CFRP composite, and G3 for SRP composite. The second symbol denoted the exposure condition: L for laboratory conditioning and E for environmental conditioning. The third symbol denoted the number of applied composite layers: 0, 1, 2, and 3.

In addition, one slab was reinforced with two layers of the SRP composite in an overlap custom over the entire width of the slab which was represented in the test matrix by G3-L-Lap.

The strengthening composites were provided along the clear span length of RC slabs. The strengthening composite width (w_f) was 457 mm (18-in.) for the FRCM and CFRP-grid composites application. The steel wire sheet was produced with a width of 305 mm (12-in.) which was laid over at the central width of the slab's tensile face. The reinforcement ratio of the composites (ρ_f) was based on the provided fiber's area per unit width (A_f), as presented in Table 2. The axial stiffness of each strengthening composite was determined as the product of ($n\ A_f\ E_f$) based on ACI 440 (2008) and ACI 549 (2013), as presented in Table 2. Where n is the number of composite layers, and E_f is the elastic modulus of the reinforcement fibers. The difference in the tensile and geometrical properties of the three composite types illustrates the variation in their axial stiffness and reinforcement ratio. So, the comparison between the three composite types was formulated on limiting the maximum number of strengthening layer to be not greater than three for reasons explained above.

After curing all RC slabs for 28 days, the slabs were precracked to 65% of their ultimate design capacities based on ACI 440 (2008) and ACI 549 (2013) to simulate their condition if strengthened in a field application for example. Then, the slabs' concrete substrate surfaces were sandblasted to expose the coarse aggregate in order to achieve an optimal bond condition between the concrete substrate and the strengthening composites.

The hand-layup procedure was used to apply the strengthening composites. The CFRP-grid application was executed on a dry surface by applying the epoxy paste onto the concrete surface with a trowel or spatula to a nominal thickness of 1.5 mm (0.06-in.). Then, the CFRP-grid was laid and pressed into the epoxy paste until the epoxy paste was forced out on the free spacing between the CFRP-grid's strands.

The CFRP-grid was covered with a second layer of the epoxy paste, and the surface was finished with a trowel to remove excess paste. The application procedure of the steel wire polymer (SRP) was executed following the CFRP-grid application procedure.

The FRCM composite application was performed on a wet surface in four steps. In the first step, the non-thixotropic mortar with polypropylene fibers (Exocem FP) was applied on the concrete substrate with a trowel to fill the crack openings. In the second step, the first cementitious mortar layer (X MORTAR 750) was laid over for about 3 mm (0.12-in.) in thickness. In the third step, The PBO mesh was applied and pressed slightly into the first mortar layer to ensure a good contact with the mortar. Finally, the second cementitious mortar layer was covered the PBO-mesh and leveled to have a smooth finishing surface. The application procedures were repeated successively for two or three layers of the strengthening composites. The CFRP-grid and SRP strengthened slabs were cured for only 7 days while the FRCM strengthened slabs required 28 days curing. All of the slabs were maintained for curing under the laboratory conditions before any exposure or testing. Three of the strengthened slabs with one composite layer were placed inside an environmental chamber for 72 exposure days prior to testing, as shown in Fig. 3.The exposure cycles included 50 cycles of freezing and thawing, 150 cycles of high temperature, and 150 cycles of high relative humidity. The fluctuating temperature of the environmental regime cycles is presented in Fig. 4. It was based on collected data from the National Weather Service and Worldwide Weather Station for Missouri weather in the United States from 1980 to 2013. The environmental regime was developed to represent 10 years of peak Missouri conditions.

Test procedure

The flexural test was conducted on simply supported one-way slabs that were loaded by two concentrated point loads, as shown in Fig. 1. The distance between the supports was 2286 mm (90-in.) and the concentrated load was applied 762 mm (30-in.) from the support's center. All tests were implemented monotonically at a displacement control rate of 1.3 mm/minute (0.05 in./minute). Two types of instruments were used: linear variable differential transformer (LVDT) and strain gages. One LVDT located at the mid-span was used to monitor the vertical displacement. For each slab, the strain gauges were attached to the internal and external reinforcements to measure their strain readings.

TEST RESULTS AND DISCUSSION

Load-displacement response

A summary of test results for all slabs based on yielding loads, ultimate loads, displacement at yielding and ultimate load stage, and failure mode are presented in Table 3 and Table 4. All of the strengthened slabs exhibited a flexural strength higher than the flexural strength of the control slab.

The ultimate loads determined from the experimental testing were compared with the theoretical ultimate loads (columns 3 to 5, Table 3). The theoretical ultimate loads were based on ACI 440 (2008) and ACI 549 (2013).

The strengthened slabs observed higher experimental ultimate loads than their theoretical ultimate loads. The ultimate load results were normalized for composites width difference (column 6, Table 3).

The flexural strength enhancement was determined as the ratio between the normalized ultimate loads of the strengthened slabs to the ultimate load of the control slab (column 7, Table 3).

As illustrated in previous research studies that the displacement ductility index indicated the ability of the strengthened RC structural members to endure reasonable flexural displacements when the strengthening composites reached their ultimate loads (Loreto et al. 2013; Babaeidarabad et al. 2014). The slabs' displacement ductility index was calculated as the ratio between the mid-span displacements at ultimate load stage to the mid-span displacements at steel rebar's yielding stage (column 4, Table 4).

Fig. 5 shows the load-displacement responses for the control slab and strengthened slabs with one, two, and three layers of the FRCM, CFRP-grid, and SRP composites, respectively. The load-displacement response had a linear elastic behavior at the beginning. Then, the response turned to nonlinear behavior as the steel rebar's yielded and the cracks extended toward the neutral axis. The control slab reached its ultimate load and continued through the plastic displacement stage until concrete crushing occurred. The strengthened slabs uphold higher ultimate loads than the control slab. Then, a sudden drop in load-displacement response was observed when the strengthening composites failed at ultimate load stage. After that, all of strengthened slabs followed the same trend of the load-displacement response as the control slab. Test results showed that the SRP composite had increased the ultimate loads of the strengthened slabs by 100% to 150% of the unstrengthen slab. The strengthened slab with two overlapped layers of SRP composite had the same flexural behavior as the strengthened slab with two central layers of SRP composite.

The FRCM composite revealed a 32% to 46% increase in the ultimate loads of the strengthened slabs. The CFRP-grid showed only 30% increase in the ultimate loads of the strengthened slabs with two and three strengthening layers. No increase in the ultimate load for strengthened slab with one layer of CFRP-grid.

Effect of composites' reinforcement ratio, axial stiffness, and material type

The normalized ultimate loads per unit width of the strengthening composites in relation with their reinforcement ratio (layers number) are presented in Fig. 6. The effect of composite reinforcement ratio was essentially investigated by the ultimate load, stiffness, and displacement ductility behavior of the strengthened slabs.

The three composite materials exhibited different enhancement in the ultimate load and stiffness of RC slabs as their reinforcement ratio increased. The ultimate load enhancement was unproportioned to the composite's reinforcement ratio. The elastic stiffness represents the linear behavior of the load-displacement response was not influenced by the strengthening composites. The inelastic stiffness represents the nonlinear behavior of the load-displacement response was highly influenced by the strengthening composites. The displacement ductility of the strengthened slabs directly declined as the composite' reinforcement ratio increased.

The SRP composite had a superior flexural behavior in terms of ultimate load, stiffness, and displacement ductility in comparison with the flexure behavior of other composites. The strengthened slabs with the FRCM composite had lower ultimate loads compared to the SRP composite due to the premature debonding failure mode in case of using two or three layers of the FRCM composite.

The strengthened slabs with FRCM composite were exhibited lower displacement ductility with the increase in the reinforcement ratio. Unlike, the strengthened slabs with SRP composite were exhibited higher displacement ductility with the increase in the reinforcement ratio. The difference in the performance of the flexural enhancement (ultimate loads and displacement ductility) between FRCM and SRP composites revealed the influence of the bond curing agents (cementitious matrix and epoxy polymers).

The axial stiffness of the composite showed less impact on the flexural performance of the composite material. The comparison between the ultimate loads determined by strengthened RC slabs with FRCM, CFRP, and SRP composites and the composites' axial stiffness are shown in Fig. 7. The axial stiffness of the FRCM composite was approximately 1.5 times that of the SRP and Carbon-grid composites, as presented in Table 3. However, the FRCM composite did not significantly enhance the flexure capacity of one-way slabs due to the premature debonding failure mode. The SRP and carbon-grid composites have a better enhancement with respect to their axial stiffness due to the improved bond performance provided by the epoxy curing agents in comparison with the cementitious matrix.

The reinforcement ratio of the fibers determined to be less influential on the composites performance. Even though, the carbon grid had double reinforcement ratio that of the steel wire, the strengthened slabs with CFRP grid determined lower ultimate loads that of the SRP composite. The composite material types and the geometrical strand's spacing influenced the composites performance. The steel wire cords had a higher tensile strength and spaced very close through its mesh.

Unlike, the carbon fiber grid had an only fifth the tensile strength of the steel wire cords and its strands were widely spaced through its mesh. That was contributed to less influence on the CFRP-grid composite's flexural enhancement.

Failure mode

Different failure modes were observed for the strengthened slabs, which were influenced by the composite material type and composite's reinforcement ratio, as shown in Fig. 8. The detailed type failure mode of the strengthening composites is presented in Table 4. A slippage of the FRCM composite was observed for strengthened slabs with one layer. Debonding failure mode was observed in strengthened slabs with two or three layers of the FRCM composite. All strengthened slabs with a CFRP-grid had a rupture failure mode. The slabs that were strengthened with one layer of the SRP composite had also a rupture failure mode, while the strengthened slabs with two or three layers of the SRP composite had a debonding failure mode with concrete cover delamination. In some of strengthened slabs, a shear failure mode was performed at the final loading stage when higher flexure ultimate loads were perceived.

Durability performance

The previous experimental studies that involved the influence of different composite materials on strengthening RC one-way slabs were focused only on the mechanical performance (flexure or shear) of the strengthening composites. In particular, little work to date has related to the effect of severe environmental conditioning on the flexural performance of full-scale structural members. This study provided information on the validation of the reduction factor that has been used for design perspective in ACI 440 (2008) and ACI 549 (2013).

A comparison between the unexposed and exposed slabs to environmental regime cycles is presented in Fig. 9. The flexural strength of exposed slabs was equal to the flexural strength of the unexposed slabs. However, the exposed slabs appeared to have a different displacement ductility behavior than the unexposed slabs. The exposed slab that strengthened with FRCM composite observed better ductile behavior due to the effect of high temperature and relative humidity cycles on curing the FRCM composite. Oppositely, the high temperature cycles indicated the degradation on the epoxy curing agent bond performance that lowered the displacement ductility of exposed slabs were strengthened with CFRP-grid or SRP composites.

Strain gauges measurements

The strain gauges' measurements in the steel rebar reinforcements and the externally bonded composites are summarized in Table 5. The measurements represent the strain readings at the ultimate load stage. The steel rebar had an strain reading varying between 0.006 to 0.012 mm/mm (in./in.) depending on how much the strengthening composite engaged in increasing the ultimate loads of RC slabs.

The strengthening composites were observed to have a lower ultimate strain reading than the ultimate strains which was determined from the tensile coupon test in Table 1. The lower strain in the composite materials revealed the recommendation of the ACI 440 (2008) and ACI 549 (2013) for limiting the effective strain in the FRP and FRCM composites due to the influence of bonding agent material's properties on controlling the fiber reinforcement from reaching its ultimate capacity.

CONCLUSIONS

Based on the results of the experimental investigation presented in this study, the following conclusions can be drawn:

- The flexural strength of RC one-way slabs improved by strengthening with FRCM, CFRP-grid, and SRP composites. The increase in the strengthened slabs' ultimate loads were approximately 1.3 to 2 times that of the unstrengthen slab.
- Impregnation of the PBO-fabric with cementitious mortar for strengthening one-way RC slabs exhibited reasonable flexure enhancement with the SRP composite. Therefore, the FRCM composite can overcome the problems of fire endurance and decrease the application cost substantially.
- Increase the number of strengthening composite layers would not correspondingly increased the flexural strength of the strengthened slabs due to the premature debonding failure mode. However, the test results indicated the ineffectiveness of using one layer of the CFRP-grid in comparison with using two or three layers.
- The composite properties (composite material type, reinforcement ratio, and mesh spacing) played important roles on the flexural behavior of strengthened RC slabs.
- Strengthening RC slabs with one layer of the FRCM composite revealed a better ductile failure mode, whereas failure due to rupture was detected in one layer of SRP or CFRP-grid strengthening composites.
- Using overlapped SRP strengthening layers determined to have the same flexural strength as if two central layers were used.
- No delamination or debonding of the strengthening composites appeared in the exposed slabs to environmental conditioning.

- The strengthened slabs subjected to environmental conditioning yielded the same flexural strength that was determined in the unconditioned slabs. However, the displacement ductility of the strengthened slabs was partially influenced based on the type of bonding agent. These results validate the reduction factor for environmental exposure in the ACI 440-08 and ACI 549-13 codes.
- The durability performance of the three different curing agents influenced the stiffness resistance of strengthening composites. High temperature cycles inside the environmental chamber had a benefit of added curing benefits to the FRCM composite and increased its stiffness resistance. While the lower stiffness resistance of SRP or CFRP-grid composites proved the sensitivity of the epoxy curing agents to high temperatures.
- ACI 440 (2008) and ACI 549 (2013) predicted the ultimate flexural capacities of the externally bonded RC one-way slabs conservatively.

ACKNOWLEDGMENTS

This research work was funded by a grant received from the Re-CAST Tier 1 University Transportation Center at Missouri S&T in Rolla, Missouri. The experimental work was conducted at the Center for Infrastructure Engineering Studies (CIES) Engineering Research Laboratory (ERL) and the Structural Engineering Research Laboratory (SERL) at Missouri S&T. The Ruredil Company and Sikadur Company provided donations for the composite materials. The writers express their gratitude and sincere appreciation for all the support.

REFERENCES

ACI (American Concrete Institute). (2008). "Guide for the design and construction of externally bonded FRP systems for strengthening concrete structures." ACI 440, Farmington Hills, MI.

ACI (American Concrete Institute). (2013). "Guide to design and construction of externally bonded fabric-reinforced cementitious matrix (FRCM) systems for repair and strengthening concrete and masonry structures." ACI 549, Farmington Hills, MI.

ACI (American Concrete Institute). (2014). "Building code requirements for structural concrete." ACI 318, Farmington Hills, MI.

ASTM A370 (2012a). "Standard test methods and definitions for mechanical testing of steel products." ASTM International, West Conshohocken, PA.

ASTM C39 (2014). "Standard test method for compressive strength of cylindrical concrete specimens." ASTM International, West Conshohocken, PA.

ASTM C469 (2014). "Standard test method for static modulus of elasticity and poisson's ratio of concrete in compression." ASTM International, West Conshohocken, PA.

Babaeidarabad, S. Loret, G. and Nanni, A. (2014). "Flexural strengthening of RC beams with an externally bonded fabric-reinforced cementitious matrix Journal of Composites for Construction." 10.1061/(ASCE)CC.1943-5614.0000473, 18(5), 04014009-1.

Balsamo, A., Nardone, F., Iovinella, I., Ceroni, F., and Pecce, M. (2013). "Flexural strengthening of concrete beams with EB-FRP, SRP and SRCM: Experimental investigation." Composites Part B: Engineering, 46, 91-101.

Barton, B., Wobbe, E., Dharani, L.R., Silva, P., Birman, V., Nanni A., Alkhrdaji, T., Thomas, J., and Tunis, G., (2005). "Characterization of reinforced concrete beams strengthened by steel reinforced polymer and grout (SRP and SRG) composites, Materials Science and Engineering." A, 412(1), 129–136.

D'Ambrisi, A., and Focacci, F. (2011). "Flexural strengthening of RC beams with cement-based composites." Journal of Composites for Construction, 15(5), 707-720.

Huang, X., Birman, V., Nanni, A., and Tunis, G. (2005). "Properties and potential for application of steel reinforced polymer and steel reinforced grout composites." Composites: Part B: Engineering, 36 (2005) 73–82.

Loreto, G., Leardini, L., Arboleda, D. and Nanni, A. (2013). "Performance of RC slab-type elements strengthened with fabric-reinforced cementitious-matrix composites." Journal of Composites for Construction, 10.1061/ (ASCE) CC.1943-5614.0000415, 18(3), A4013003-1.

Lopez, A., Galati, N., Alkhrdaji, T., and Nanni, A. (2007). "Strengthening of a reinforced concrete bridge with externally bonded steel reinforced polymer (SRP)." Composites Part B: Engineering, 38(4), 429-436.

Mitolidis, G. J., Salonikios, T. N., and Kappos, A. J. (2012). "Test results and strength estimation of R/C beams strengthened against flexural or shear failure by the use of SRP and CFRP." Composites Part B: Engineering, 43(3), 1117-1129.

Napoli, A., and Realfonzo, R. (2015). "Reinforced concrete beams strengthened with SRP/SRG systems: Experimental investigation." Construction and Building Materials, 93, 654–677.

National Weather Service Forecast, http:// www.weather.gov.

National Climatic Data Center (NCDC), http://www.ncdc.noaa.gov/oa/ncdc.html.

Ombres, L. (2011). "Flexural analysis of reinforced concrete beams strengthened with cement based high strength composite material." Composite Structures 94(1), 143-155.

Ombres, L. (2012). "Debonding analysis of reinforced concrete beams strengthened with fiber reinforced cementitious mortar." Engineering Fracture Mechanics, 81, 94-109.

Pecce, M., Ceroni, F., Prota, A., and Gaetano Manfredi, G., (2006). "Prediction of RC beams externally bonded with steel-reinforced polymers." Journal of Composites for Construction, DOI: 10.1061/ (ASCE) 1090-0268(2006)10:3(195).

Pellegrino, C., and D'Antino, T. (2013). "Experimental behavior of existing precast prestressed reinforced concrete elements strengthened with cementitious composites." Composites Part B: Engineering, 55, 31-40.

Rahman, A. H., Kingsley, C. Y., and Kobayashi, K. (2000). "Service and ultimate load behavior of bridge deck reinforced with carbon FRP grid." Journal of Composites for Construction, 4(1), ISSN 1090-0268/00/0001-0016–0023.

Salinas, A.J.O., (2010). "Use of grancrete as adhesive for strengthening reinforced concrete structures." Thesis, North Carolina State University, Raleigh, NC, US.

Ta¨ljsten, B., and Elfgren, L. (2000). “Strengthening concrete beams for shear using CFRP-materials: evaluation of different application methods.” Composites, Part B, 31(2), 87–96.

Tommaso, D.A., Focacci, F., and Mantegazza, G. (2008). “PBO-FRCM composites to strengthen RC beams: mechanics of adhesion and efficiency.” In Proceedings of the international conference on FRP composites in civil engineering (CICE), Zurich, Switzerland.

Yost, J.R., Charles H. Goodspeed, C.H., and Schmeckpeper, E. R. (2001). “Flexural performance of concrete beams reinforced with FRP grids.” Journal of Composites for Construction.” 5(1), 18–25.

Table 1. Composite materials' properties

Reinforcement type	**Tensile strength MPa (ksi)**	**Elastic modulus MPa (ksi)**	**Ultimate strain mm/mm (in./in.)**
PBO-FRCM, Coupon test	1,170 (170)	168,000 (18,400)	0.0215
CFRP-strand, Coupon test			
- Transverse direction	496 (72)	67,570 (9,800)	0.007
- Longitudinal direction	393 (57)	55,850 (8,100)	0.0055
3x2 wire , Hardwire Company	2,482 (360)	162,000 (23,500)	0.021
Curing agent type	**Flexure strength MPa (ksi)**	**Elastic modulus MPa (ksi)**	**Tensile strength MPa (ksi)**
Inorganic mortar, Ruredil Company	4 (0.6)	7 (1.015)	
Epoxy adhesive (Sikadur 30),	47 (6.8)	11,700 (1,700)	24.8 (3.6)
Epoxy adhesive(Sikadur 330),	60.6 (8.8)	3,500 (500)	33.8 (4.9)

Table 2. Test matrix for strengthening configuration and properties of composites

Composite type	**Specimen ID**	**n**	**Exposure conditions**	**A_f mm^2/mm**	**w_f, mm**	**$A_{f,total}$ mm^2**	**ρ_f %**	**Stiffness kN*10^3**
Control	C-0		Laboratory					
FRCM	G1-L-1	1	Laboratory	0.123	457	56	0.092	7
	G1-L-2	2	Laboratory	0.123	457	112	0.184	14
	G1-L-3	3	Laboratory	0.123	457	169	0.277	21
	G1-E-1	1	Environmental	0.123	457	56	0.092	7
CFRP	G2-L-1	1	Laboratory	0.150	457	69	0.112	5
	G2-L-2	2	Laboratory	0.150	457	137	0.225	9
	G2-L-3	3	Laboratory	0.150	457	206	0.337	14
	G2-E-1	1	Environmental	0.150	457	69	0.112	5
SRP	G3-L-1	1	Laboratory	0.100	305	31	0.050	5
	G3-L-2	2	Laboratory	0.100	305	61	0.100	10
	G3-L-3	3	Laboratory	0.100	305	92	0.150	15
	G1-E-1	1	Environmental	0.100	305	122	0.200	5
	G3-L-Lap	2	Laboratory	0.100	305	61	0.100	10

*Conversion units: Conversion units: 1-in. = 25.4 mm; 1 kip = 4.45 kN

Table 3. Slab's specimens test results: Ultimate load

Specimen ID	Yielding load kN (kips)	Experimental ultimate load kN (kips)	Theoretical ultimate load kN (kips)	$P_{u, exp.}/P_{u, th.}$	Normalized ultimate load kN/m (kips /ft.)	Enhancement, $P_{norm.}/P_{cont.}$ %
C-0	45 (10)	62 (14)	40 (9)	1.56	142 (9.7)	
G1-L-1	49 (11)	85 (19)	55 (12)	1.58	188 (12.9)	1.32
G1-L-2	49 (11)	89 (20)	63 (14)	1.43	199 (13.6)	1.40
G1-L-3	53 (12)	98 (22)	75 (17)	1.29	208 (14.3)	1.46
G1-E-1	49 (11)	89 (20)	55 (12)	1.67	198 (13.5)	1.39
G2-L-1	53 (12)	67 (15)	46 (10)	1.50	144 (9.90	1.01
G2-L-2	53 (12)	85 (19)	55 (12)	1.58	185 (16.7)	1.30
G2-L-3	53 (12)	89 (20)	59 (13)	1.54	195 (13.4)	1.37
G2-E-1	49 (11)	68 (15)	46 (10)	1.50	143 (9.8)	1.01
G3-L-1	53 (12)	89 (20)	67 (15)	1.33	286 (19.6)	2.01
G3-L-2	49 (11)	98 (22)	94 (21)	1.05	321 (22.0)	2.26
G3-L-3	49 (11)	111 (25)	94 (21)	1.19	355 (24.4)	2.50
G3-E-1	49 (11)	89 (20)	67 (15)	1.33	290 (19.9)	2.04
G3-L-Lap	49 (11)	102 (23)	94 (21)	1.10	224 (15.4)	1.58

Table 4. Slab's specimens test results: Displacement and failure mode

Specimen ID	Yielding disp., δy mm (in.)	Ultimate disp., δu mm (in.)	Ductility index (δu/δy)	Steel yielded Y/N	Failure mode
C-0	10.0 (0.40)	74 (2.90)	7.25	Y	Flexure
G1-L-1	10.0 (0.40)	59 (2.20)	5.50	Y	Slippage of FRCM
G1-L-2	9.7 (0.38)	41 (1.60)	4.20	Y	Debonding of FRCM
G1-L-3	10.0 (0.40)	36 (1.40)	3.50	Y	Endplate debonding of FRCM
G1-E-1	10.0 (0.40)	64 (2.50)	6.25	Y	Debonding of FRCM at the max load regions
G2-L-1	12.0(0.46)	20 (0.80)	1.75	Y	Rupture of CFRP-grid at mid-span
G2-L-2	8.50 (0.34)	23 (0.90)	2.65	Y	Rupture of CFRP-grid and concrete crushing
G2-L-3	12.0 (0.46)	17 (0.68)	1.48	Y	Rupture of CFRP-grid through the slab width
G2-E-1	10.0 (0.40)	17 (0.68)	1.70	Y	Rupture of CFRP-grid
G3-L-1	11.0 (0.43)	45 (1.75)	4.00	Y	Rupture of SRP at mid-span with cover delamination
G3-L-2	10.0 (0.40)	53 (2.10)	5.25	Y	Debonding of SRP along the span with cover delamination
G3-L-3	11.0 (0.43)	48 (1.90)	4.42	Y	Debonding of SRP along the span with cover delamination
G1-E-1	11.0 (0.43)	39 (1.53)	3.56	Y	Rupture of SRP at mid-span with cover delamination
G3-L-Lap	9.0 (0.36)	53 (2.10)	5.83	Y	Rupture of SRP longitudinally at the overlap with cover delamination

Table 5. Strain readings in steel, FRCM, CFRP-grid, and SRP

Composite Type	Specimen ID	Strain reading at ultimate load	
		mid-span rebar mm/mm, in./in.	FRCM/ CFRP /SRP mm/mm, in./in
Control	C-0	0.01	
FRCM	G1-L-1	0.012	0.01
	G1-L-2	0.012	0.0035
	G1-L-3	0.006	0.01
	G1-E-1	0.009	0.01
CFRP	G2-L-1	0.006	0.0035
	G2-L-2	0.006	0.0020
	G2-L-2	0.006	0.0020
	G2-L-3	0.006	0.002
	G2-E-1	0.007	0.0040
SRP	G3-L-1	0.013	0.0032
	G3-L-2	0.012	0.006
	G3-L-3	0.01	0.006
	G1-E-1	0.007	0.0032
	G3-L-Lap	0.012	0.005

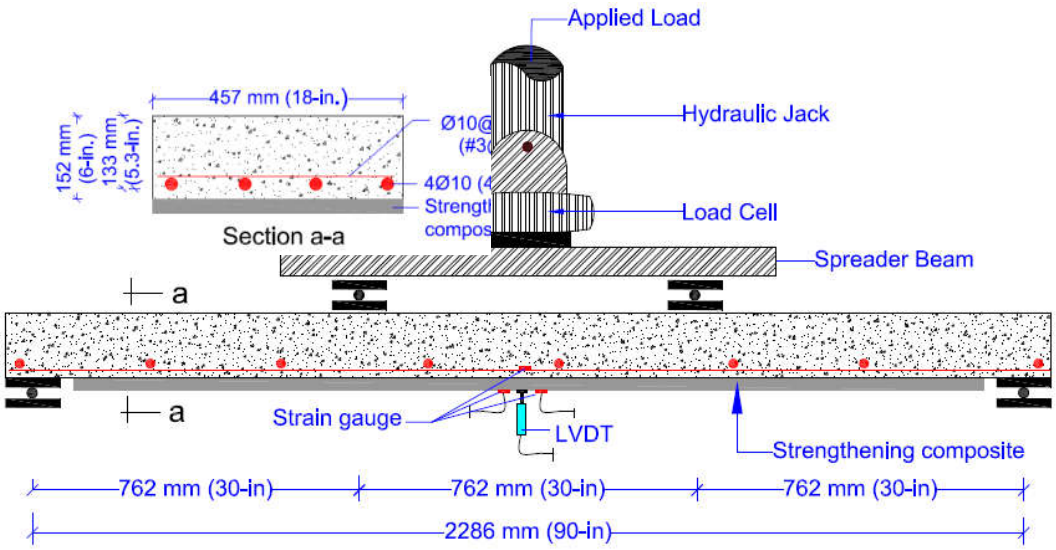

Fig. 1. Cross-section, reinforcement details, and test set-up

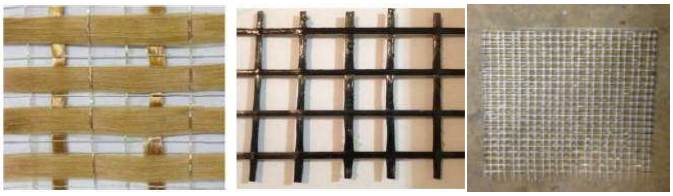

PBO mesh CFRP grid Steel wire

Fig. 2. Composite reinforcement meshes

Fig. 3. Representative specimens placed inside the environmental chamber

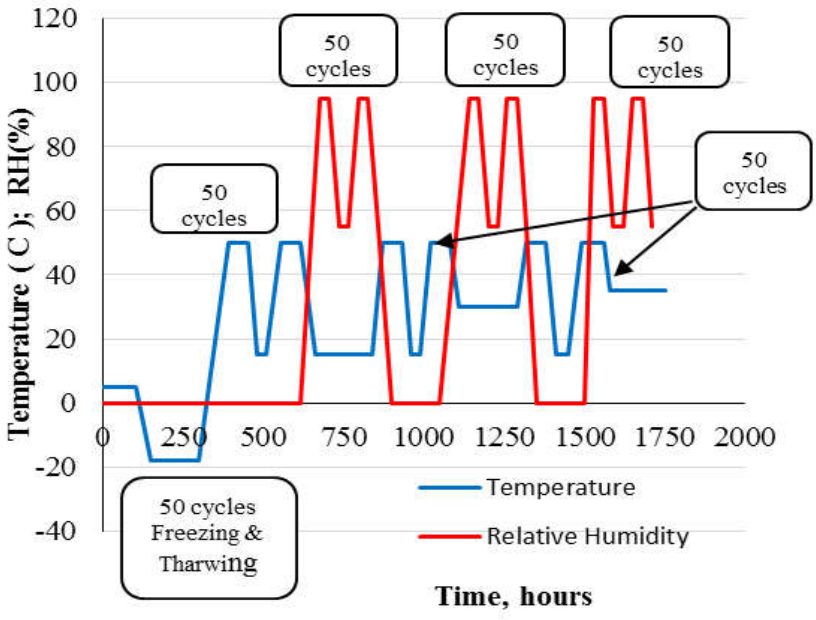

Fig. 4. Environmental conditioning regime

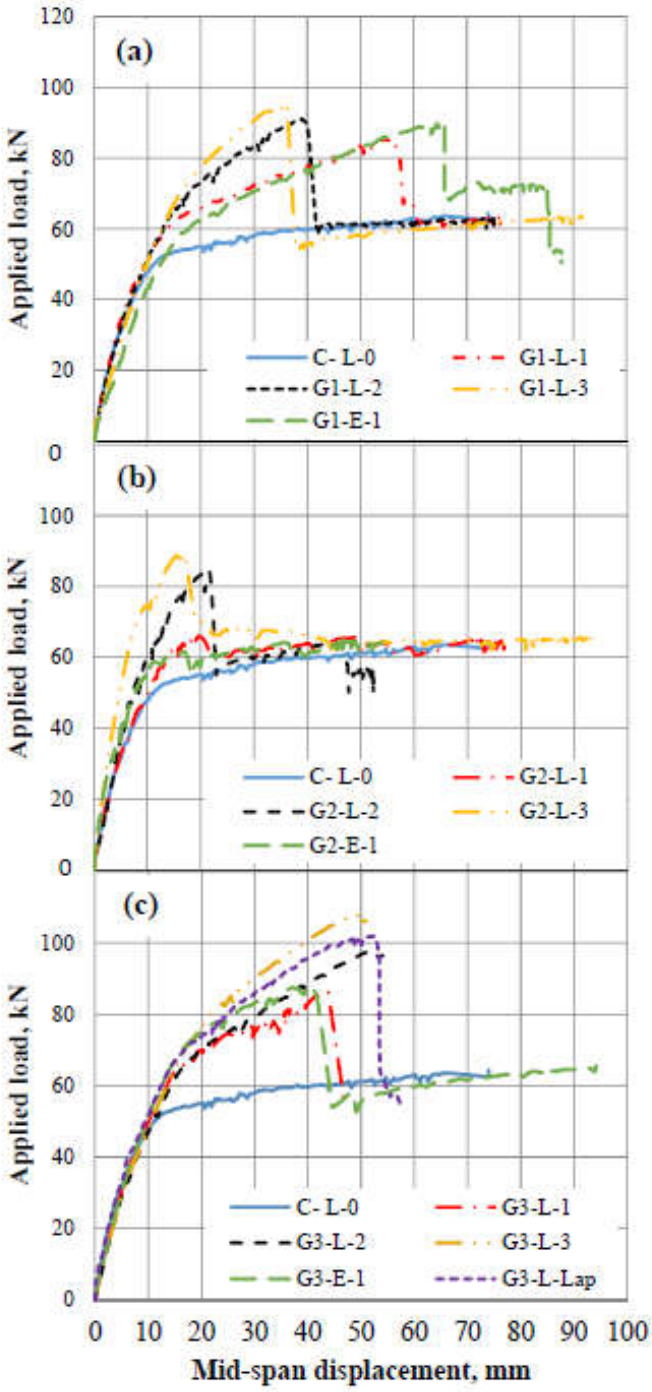

Conversion units: 1-in. = 25.4 mm; 1 kip = 4.45 kN

Fig. 5. Load-mid span displacement responses: (a) FRCM composite, (b) CFRP composite, and (c) SRP composite

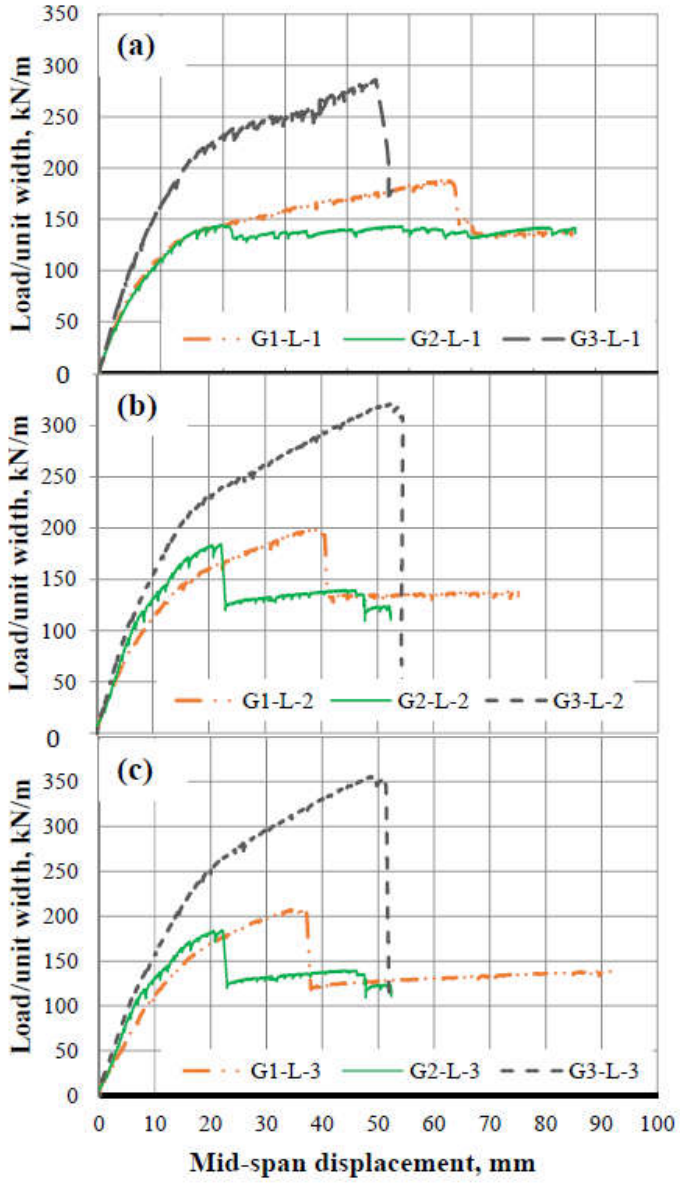

Conversion units: 1-in. = 25.4 mm; 1 kip = 4.45 kN

Fig. 6. Load carrying capacities of three composites: (a) One layer, (b) Two layers, and (c) Three layers

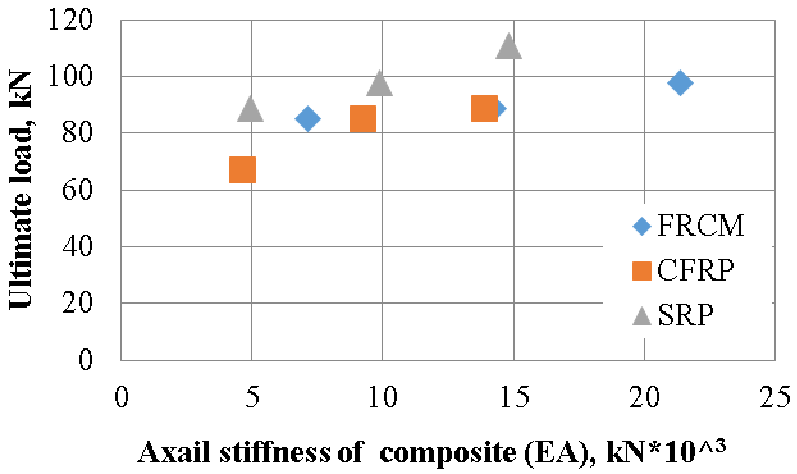

Conversion units: 1-in. = 25.4 mm; 1 kip = 4.45 kN

Fig. 7. Ultimate loads in comparison with composites' axial stiffness

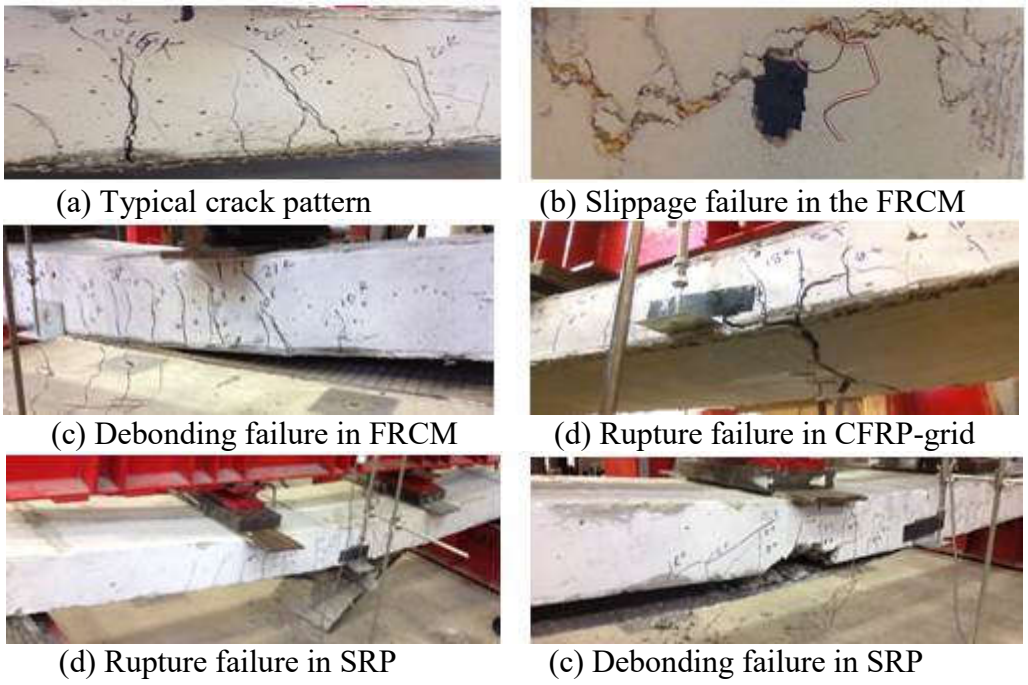

(a) Typical crack pattern (b) Slippage failure in the FRCM

(c) Debonding failure in FRCM (d) Rupture failure in CFRP-grid

(d) Rupture failure in SRP (c) Debonding failure in SRP

Fig. 8. Crack pattern and failure mode of strengthened RC slabs

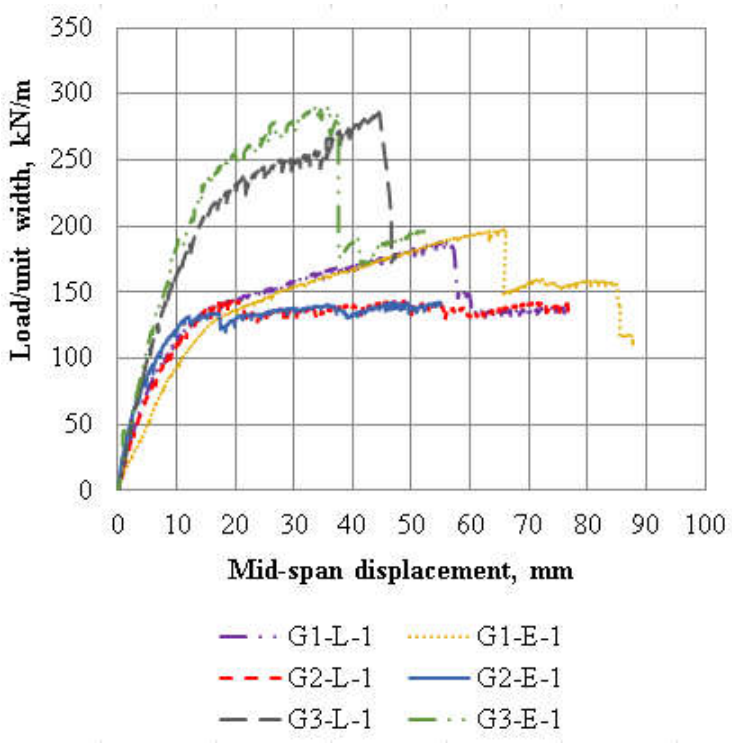

Conversion units: 1-in. = 25.4 mm; 1 kip = 4.45 kN

Fig. 9. Effect of environmental regime cycles on strengthened RC slabs

IV. DURABILITY PERFORMANCE OF FRCM COMPOSITE BONDED TO CONCRETE UNDER DIFFERENT ENVIRONMENTAL AGING CONDITIONS

Zena R. Aljazaeri [1], John J. Myers [2]
[1] Graduate Research Student, Missouri University of Science and Technology, 1304 Pine Street, 201 Pine Building, Rolla, MO 65409, USA. Email: zracnb@mst.edu
[2] Professor of Civil, Arch. and Envir. Engr, Missouri University of Science and Technology, 325 Butler-Carlton CE Hall, Rolla, MO 65409, USA.
Email: jmyers@mst.edu

ABSTRACT

From the perspective that an aggressive environment may cause damage to cementitious materials, curing agents of fiber reinforced cementitious matrix (FRCM) composite allows chemical agents to attack the reinforcement fabrics. In such cases, the accelerated interfacial FRCM debonding mechanisms interfere which reduce its mechanical performance. This task was conducted to investigate the long-term durability performance of the FRCM composite. In this study, environmental aging conditions were the freeze-thaw cycles, high humidity cycles, high temperature cycles, immersion into salt solution, and immersion into alkaline solution. Different FRCM reinforcement ratio and two surface roughness of concrete were also included. Two test methods were used to evaluate the FRCM composite's bond performance (pull-off test and bending test). The bending test results revealed that the FRCM composite bond performance was not influenced by the environmental exposure. While the test results for the pull-off strength were scattered, possibly due to the environmental degradation or a lack of proper quality control during the initial FRCM composite application or applying the load.

KEYWORDS

FRCM composite, Bond, Pull-off test, Bending test, Environmental conditioning.

INTRODUCTION

Using fiber reinforced cementitious matrix (FRCM) to repair deteriorated, damaged, or structurally unsafe concrete members, is an increasingly popular technique. The previous experimental works have been proving that FRCM composite application is economic, durable, convenient, and labor friendly (Babaeidarabad et al. 2014; Ombres 2011; Loreto et al. 2014). The long-term in-situ performance of the FRCM composite-concrete interfacial bonding is a primary concern due to the potential for age-related environmental degradation. A study on the bond strength-slip relations for the PBO-FRCM composite externally bonded to concrete blocks was reported by D'Ambrisi et al. (2012).

Carloni et al. (2013) conducted an experimental study on the applicability of a fracture mechanic based approach to understand the stress transfer mechanism of FRCM composites externally bonded to a concrete substrate. Results were analyzed to determine the effective bond length, which can be used to establish the load-carrying capacity of the interface to design the strengthening system. Results also determined the interfacial behavior between fibers and matrix and highlight the role of the cementitious matrix in the stress transfer.

D'Ambrisi et al. (2013) experimentally analyzed the bond between FRCM composite made out of a polyparaphenylene benzobisoxazole (PBO) net embedded in a cement based matrix and the concrete.

The results allowed estimating the effective anchorage length and evidence that the debonding occurs at the fibers/matrix interface after a considerable fibers/matrix slip.The results also confirm the effectiveness of the FRCM materials as external reinforcements for concrete and the obtained experimental results can be used to calibrate a local bond-slip relation in the design of the external reinforcement.

One other study related to D'Ambrisi et al. (2013) is an experimental and analytical investigation on bond between carbon-FRCM composite and masonry. Experimental results of double shear tests involving different bond lengths can be used to calibrate a local bond-slip relation that is essential in the modeling of the structural behavior of masonry elements strengthened with carbon-FRCM.

D'Antino et al. (2014) conducted a single-lap shear test on specimens with FRCM composite strips bonded to concrete blocks. Test parameters included different FRCM composite attachment area and reinforcement ratio and the stress-transfer mechanism that characterized the FRCM composite was determined.

Arboleda et al. (2014) studied the durability of FRCM composite in terms of different environmental exposure under bond pull-off testing. Two types of FRCM composites were investigated (carbon fabric and PBO fabric with cement based matrix). Test results for tensile and bond strength retention percentages after environmental exposure revealed no significant degradation concerns.

Sneed et al. (2015) demonstrated a comparison study between single-lap and double-lap shear test on the bond failure mechanism of PBO-FRCM composite. Ombres (2015) shaded the light on a comparison between experimental results and theoretical predictions of the bond-slip law for PBO-FRCM composite attached to concrete.

The comparison results concluded that the nonlinear proposed model described analytically the bond-slip law is influenced by experimental results and the available experimental data are not sufficient for a reliable calibration of parameters that define the model. This experimental work was looked up other aspect of view to investigate the long-term durability performance of bonded FRCM composite to concrete substrate. The environmental aging conditions were the freeze-thaw cycles, high humidity cycles, high temperature cycles, immersion into salt solution, and immersion into alkaline solution that were based on the recommendations of AC 434 (2013).

EXPERIMENTAL PROGRAM

Description of FRCM composite

The FRCM composite that considered in this study was consisted of polyparaphenylene benzobisoxazole (PBO) fabric and cement based matrix. Fig. 1 shows the PBO-fabric and the cementitious matrix. The PBO fabric was made of spaced strands in two directions. The PBO fabric strand has a width of 5 mm (0.2-in.) in the longitudinal direction and a width of 3 mm (0.12-in.) in the transverse direction. The free spacing between the strands is approximately 5 mm (0.2-in.) and 22 mm (0.9-in.) in the longitudinal and transverse directions, respectively. The nominal thickness of the strands is 0.2 mm (0.008-in.) and 0.12 mm (0.0045-in.) in the longitudinal and transverse directions, respectively. As reported by the manufacturer, the PBO fabric's ultimate tensile strength per unit width is 276 kN/m (18.9 kip/ft) in the longitudinal direction which is about 3.5 times its' tensile strength in the transverse direction. The bonding agent is a cement based mortar that has less than 5 percent polymer.

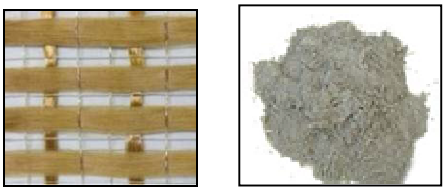

(a) (b)

Fig. 1. Materials of FRCM composite: (a) Polyparaphenylene Benzobisoxazole (PBO) mesh, (b) Inorganic Matrix

Specimen preparations

Two test methods were used to evaluate the FRCM composite's bond performance (pull-off test and bending test). The test matrix was divided into two phases of specimen preparations. In the first phase, the specimens were prepared for pull-off test. In the second phase, the specimens were prepared for bending test.

Specimen preparation and conditioning for pull-off test

In this phase, concrete blocks with a 508 mm (20-in.) length, a 150 mm (6-in.) width, and 150 mm (6-in.) height were casted for attaching one layer of FRCM composite. The average compressive strength of the three tested cylinders was 41 MPa (6000 psi) at 28 days based on ASTM C39 (2014). All of concrete substrate surfaces were roughened in order to provide better bond performance with FRCM composite. The sandblasting method was used for concrete surface roughness to a level of 1.2 to 3 mm (50 mils to 0.125 in.). That penetration level simulated the surface profiles of CSP3 to CSP5 when the concrete specimens were lightly sandblasted (Technical guidelines No.03732 and No.03730, International Concrete Repair Institute (ICRI), 1997). For FRCM composite installation, the hand lay-out method was followed with respect to the guidelines of ACI 549 (2013). The installation method consisted of four steps.

The first step was to wet the concrete surface. The second step was to apply the first layer of the cementitious mortar (X MORTAR 750) with a nominal typical thickness of 3 mm (0.1-in.). The third step was to place the PBO-fabric and press it gently into the cementitious mortar. The fourth step was to apply the second layer of the cementitious mortar to the same thickness, and level FRCM composite surface.

All of the concrete specimens cured for 28 days under laboratory conditions before any exposure or testing. The environmental exposure and aging were the main parameters for this test. The exposure conditions and aging were based on the recommendations in the AC 434 (2013). The specimen's matrix for pull-off test included five exposure conditions, as represented in Table 1.

In the first conditioning, specimens were mentioned under laboratory conditions that served as control specimens. In the second conditioning, specimens were exposed to an environmental regime that included 50 cycles of freezing and thawing, 150 cycles of humidity, and 150 cycles of high temperature. In the third conditioning, specimens were placed inside a moisture chamber under 100% relative humidity. In the fourth conditioning, specimens were immersed into a salt solution that demonstrated the case of exposure to seawater (PH level of 7). In the fifth conditioning, specimens were immersed into an alkaline solution that demonstrated the case of ocean water (PH level of 13).

The aging condition was the third study parameter. Some of the specimens were tested after one environmental regime cycle (72 days) and other specimens were tested after an aging time of 166 days based on the recommendation of AC 434 (2013).

Table 1. Specimens' matrix for pull-off test

Specimen ID	Tested specimen number	Conditions	Plies number	Exposure time, days	
P-L-1	5	Laboratory conditions	1		
P-E-1	5	Environmental regime cycles	1	72	
P-H-1	5	100% humidity at 72 ° F	1	72	
P-S-1	5	Saltwater at 72 ° F	1	72	166
P-A-1	5	Alkaline solution at 72 ° F	1	72	166

The environmental regime was established according to Missouri state weather conditions. The data was collected from the National Weather Service and Worldwide Weather Station during a time frame from 1980 to 2013. The environmental regime is presented in Fig. 2.

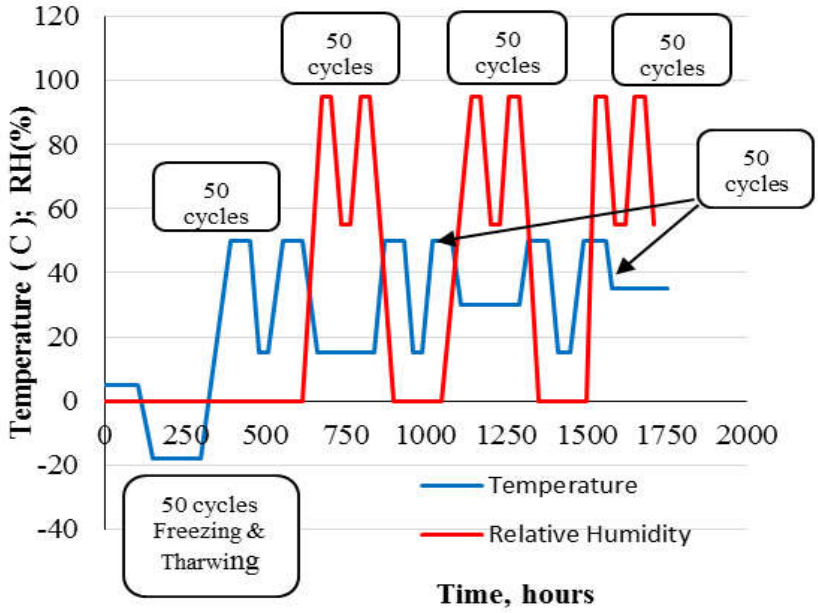

Fig. 2. Environmental conditioning regime

In the test matrix, the defined specimen name is represented by two letters and one number. The first letter, P, represents the test type (pull-off). The second letter, L, E, H, S, or A, represents the exposure condition (laboratory, environmental, humidity, saltwater, or alkaline solution). Finally, the number, 1, represents the number of ply. The salt solution was prepared by mixing NaCl of 3% by the weight of required solution to immerse the specimens. While, the alkaline solution was prepared by adding NaOH of 0.4% by the weight of the required solution.

Specimen preparation and conditioning for bending test

One test specimen consisting of two concrete blocks were spaced 12.5 mm (0.5-in.) by wood piece and a strip of the FRCM composite was attached to one face of the connected concrete blocks. The concrete blocks were casted to have a 254 mm (10-in.) length, a 150 mm (6-in.) width, and a 150 mm (6-in.) height. The average compressive strength of the three tested cylinders was 41 MPa (6000 psi) at 28 days based on the ASTM C39 (2014).

Two different surface preparations were considered in order to examine the effect of concrete surface roughness on FRCM composite bond performance. The first roughness level of 1.2 to 3 mm (50 mils to 0.125 in.) simulated the surface profiles of CSP3 to CSP5 when the concrete specimens were lightly sandblasted. The second roughness level of 3 to 6 mm (1/8 to 1/4 in.) simulated the surface profiles of CSP6 to CSP9 when the concrete specimens were heavy sandblasted. These penetration levels were based on technical guidelines No.03732 and No.03730 specified by International Concrete Repair Institute (ICRI, 1997).

The FRCM composite strip had a 100 mm (4-in.) width and 432 mm (17-in.) length. The FRCM composite installation procedure and curing were as preceded for the pull-off test specimens, except that the installation procedure was repeated successively for the specimens with four plies of FRCM composite. The specimens' matrix for bending test included two exposure conditions (laboratory condition and environmental regime cycles), as represented in Table 2.

The environmental regime cycles are represented in Fig. 2. In the test matrix, the defined specimen name is represented by three letters and one number. The first letter, B, represents the test type (bending). The second letter, L or E, represents the exposure condition (laboratory or environmental). The third letter, L or H, represents the surface roughness (light or heavy). Finally the number, 1 or 4, represents the number of plies.

Table 2. Specimens' matrix for bending test

Specimen ID	Specimen tested number	Conditions	Surface Roughness	# of plies	Exposure time days
B-L-L-1	3	Laboratory conditions	Light	1	
B-L-H-1	3		Heavy	1	
B-E-L-1	3	Environmental regime cycles	Light	1	72
B-E-H-1	3		Heavy	1	72
B-L-L-4	3	Laboratory conditions	Light	4	
B-L-H-4	3		Heavy	4	
B-E-L-4	3	Environmental regime cycles	Light	4	72
B-E-H-4	3		Heavy	4	72

TEST METHODS

Pull-off test

This test method was implemented in order to examine various environmental exposures on the bond performance of FRCM composite. The pull-off test was performed based on the general procedure of the ASTM C1583 (2013). A minimum of five specimens for each FRCM composite exposure were tested as recommended by ACI 549 (2013). After specimens were aged in exposure conditions, they were left in laboratory conditions for seven days to dry out, and then a 50 mm (2-in.) diameter bit was used to perform 12.5 mm (0.5-in.) depth cores. A vacuum cleaner was used to get rid of all the concrete dust then steel disks attached to FRCM composite surfaces by epoxy adhesive. The specimens were left to cure the epoxy adhesive for at least three days before testing.

The pull-off tester was used to pull the attached steel disks to the cored specimens. The incremental load was applied to produce an approximate stress rate of a 35 kPa/second (5 psi/second). The ultimate load was recorded by the dial gauge of the testing machine. Fig. 3a. shows a representative specimen under pull-off testing. The pull-off test revealed the pull-off strength and the bond failure mode.

Bending test

This test method was selected to reveal the impact of surface roughness and environmental regime cycles on multilayers of FRCM composite. The test setup was designed to simulate a reinforced concrete beam in bending with a preexisting crack at the mid-span (Pellegrino et al. 2008; Silva et al. 2008). All of the specimens were loaded at two points that spaced 150 mm (6-in.) apart and simply supported at each end thereby subjecting the FRCM composite to a direct tension.

Two linear variable differential transducers (LVDT) were used to measure the mid-span displacements. All of the specimens were subjected to a constant load rate of 0.25 mm/minute (0.01 in/minute). A representative specimen under a bending test is seen in Fig. 3b. The bending test results revealed the FRCM composite's tensile strength, mid-span displacements, and failure mechanism.

(a) (b)

Fig. 3. Specimens under testing: (a) Pull-off test, (b) Bending test

RESULTS AND DISCUSSIONS

Pull-off test results

The pull-off strength of five specimens based on the exposure condition is represented in Fig. 4a. The pull-off strength was computed by dividing the ultimate load over the net cross-sectional area that specified by ACI 549 (2013).

Bond failure was observed in all specimens at the interface between the PBO fabric and the cementitious matrix, as seen in Fig. 4b. All of the specimens had pull-off strength greater than the 1.4 MPa (200-psi) defined as a minimum value by ACI 549 (2013).

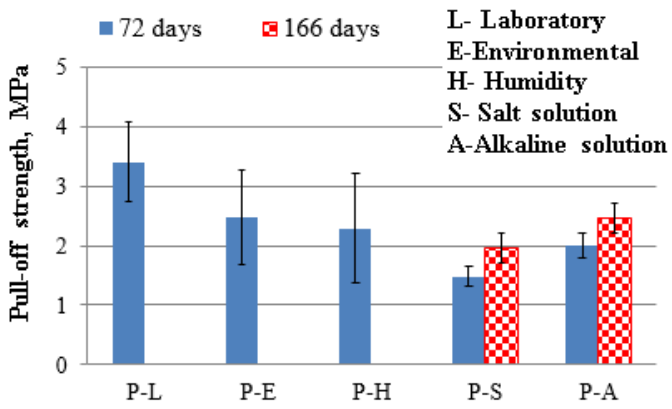

(a)

(b)

Conversion units: 1-in. = 25.4 mm; 1 kip = 4.45 kN

Fig. 4. Pull-off test results: (a) Pull-off strength result, (b) Failure mode

The test results had a large scatter for the same group specimens with all types of exposure, which might be due to the manual control in applying the load.The specimens exposed to the salt solution and alkaline solution had lower pull-off strength in comparison with other exposure conditions at 72 days aging, while the aged specimens to 166 days had higher pull-off strength. Comparison between exposures conditions was appeared to be less influential on the bond strength of the FRCM composite.

Bending test results

The bending test results were determined as the average bond strength of three tested specimens, which is represented in Fig. 5a. The normal bond strength was calculated from Eq. (1) in order to determine the effect of the FRCM reinforcement ratio:

$$\sigma = \frac{p}{nbt} \tag{1}$$

where, σ is the normal bond strength, MPa (psi), P is ultimate load divide by two in order to account for the two attached strips, (N or lb), n is the number of PBO fabric plies, b is the total width of PBO fabrics within a strip width of 100 mm (4-in.), and t is the thickness of PBO fabrics, which was equal to 0.2 mm (0.008-in.) that were represent the PBO fabrics' thickness in the main direction of the mesh.

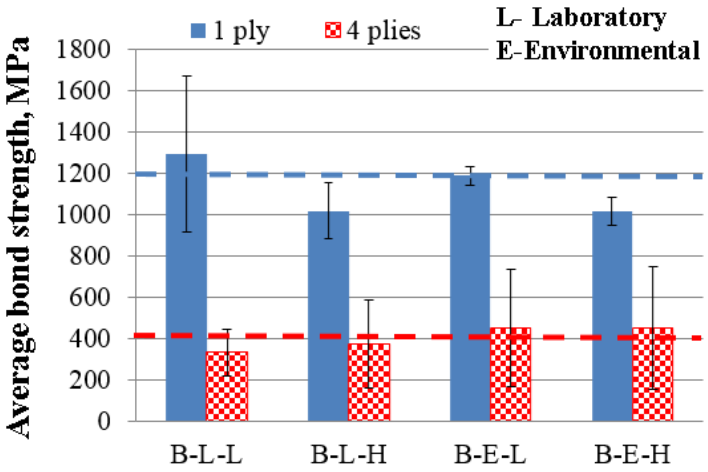

(a)

b)

c)

Conversion units: 1-in. = 25.4 mm; 1 kip = 4.45 kN

Fig. 5. Bending test results: (a) Bending test strength with respect to the exposure, (b) Slippage in the PBO-FRCM composite for one ply, and (c) Debonding of FRCM composite for four plies

The normal bond strength results revealed that the plies number of FRCM composite was the most influential factor on the failure mode type and bond strength of the tested specimens. The specimens that had a heavy roughened surface have lower bond strength with respect to those with light roughed surface by 23% reduction in the attachment of one ply of the FRCM. However, the insignificant bond strength reduction observed in the attachment of four plies of the FRCM. The environmental regime cycles showed insignificant effect on the bond strength of the tested specimens.

The strengthened concrete blocks with one ply of FRCM composite exhibited a slippage bond failure mode, as seen in Fig. 5b., while the strengthened concrete blocks with four plies of FRCM composite failed due to the FRCM composite‘s debonding from the concrete substrate, as seen in Fig. 5c.

The representative applied loads with specimens’ global slip at the min-span are seen in Fig. 6a. and 6b., respectively. The global slip is defined as a maximum slippage occurred in the PBO fabric at the mid span when the ultimate load capacity was reached.

The applied load-global slip relationships were influenced by the number of FRCM composite’ plies used. For concrete blocks with one ply of FRCM composite, the load started to increase linearly up to the point where the loss in the composite stiffness due to slippage in the PBO fabrics into the cementitious matrix were enlarged. The specimen reached its’ ultimate load capacity. Then, the load capacity was incrementally dropped when debonding of the PBO fabrics from the cementitious matrix were developed. The specimens were continuously extended a global slip at a constant load due to the friction force that developed between the PBO fabrics and the cementitious matrix.

This phenomenon was observed in single lap shear test that was conducted in previous research (D'Antino, 2014).However, for concrete blocks with four plies of FRCM composite, the specimens exhibited a rapid linear drop in their load capacities when the FRCM composite debonded from the concrete substrate, as seen in Fig. 6b.

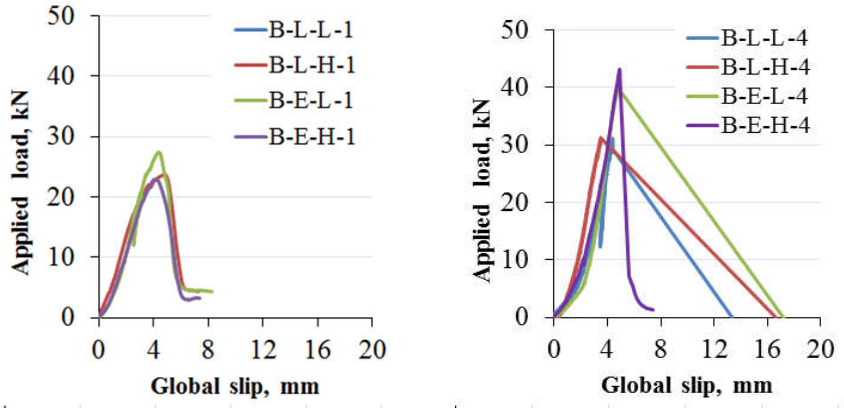

(a) (b)

Conversion units: 1-in. = 25.4 mm; 1 kip = 4.45 kN

Fig. 6. Applied load-global slip relationship by bending test: (a) one ply, (b) four ply

The bending test was able to predict the failure mode with respect to the FRCM composite's reinforcement ratio, as it was observed for testing full-scale reinforced concrete beams in flexure (Babaeidarabad et al. 2014; Ombres 2011; Loreto et al. 2014).

The average loads of bonded four plies of FRCM composite to concrete blocks were only 1.25 times for bonded one ply of FRCM composite to concrete blocks due to the premature failure of FRCM composite. The comparison between the two test methods revealed that the ultimate bond strength of the tested specimens under bending were highly greater than that produced due to the pull-off test.

The reason behind that is a pulling-off load was applied perpendicularly to the PBO fabric alignment, while in the bending test a direct tensile load was applied parallel to the PBO fabric alignment. In addition, a comparison of the normal bond strength from bending test with direct tensile coupons test for FRCM composite, that was done by the authors in another research (Aljazaeri and Myers, 2015), was revealed a good agreement between their ultimate strength and strain of the PBO fabrics. Even more, the bending test method revealed the same failure modes determined in strengthened full-scale RC beams under flexure loading (slippage of the PBO fabric for one ply strengthening and debonding of the FRCM composite for four plies strengthening).

CONCLUSIONS

An experimental study on the bond performance between externally applied FRCM composite and the concrete block is presented. The differences of the pull-off test results for various exposure conditionings were discharged due to partially scattering of the experimental data. The exposure conditionings did not influence the failure modes of FRCM composite. All exposed and unexposed specimens to various environmental exposures issued that debonding failure mode between the PBO fabric and the cementitious matrix. Higher pull-off strengths were determined for the specimens aged to 166 days in comparison with 72 days as the specimens continuously cured. The bending test method revealed the same failure mode associated in large scale strengthened beams under flexure test. The Variations in the applied load and the global slip were determined in the bending test, and the translation of the ultimate loads during delamination was experimentally observed.

Failure mode of FRCM composite was observed to be highly dependent on the number of FRCM composite's plies. The concrete surface preparations were influential factor in FRCM application of one ply. The bond strength of light roughened specimens was 23% higher than the heavy roughened specimens. Insignificant concrete surface roughness observed with FRCM application of four plies due to the debonding failure mode between the fiber/matrix interfaces.

ACKNOWLEDGMENTS

The authors gratefully acknowledge the financial support provided by the Ruredil Company and the ReCAST Tier 1 University Transportation Center at Missouri S&T, in addition to the generous support from the Center for Infrastructure Engineering Studies and the Department of Civil, Architectural, and Environmental Engineering at Missouri S&T.

REFERENCES

AC 434, (2013). "Acceptance criteria for masonry and concrete strengthening using fabric-reinforced cementitious matrix (FRCM) composite systems." ICC-Evaluation Service, Whittier, CA.

ACI (American Concrete Institute). (2013). "Guide to design and construction of externally bonded fabric-reinforced cementitious matrix (FRCM) systems for repair and strengthening concrete and masonry structures." ACI 549, Farmington Hills, MI.

Arboleda, D., Babaeidarabad, S., Hays, C. D., and Nanni, A. (2014). "Durability of fabric reinforced cementitious matrix (FRCM) composites." The 7th International Conference on FRP Composites in Civil Engineering International Institute for FRP in Construction, Canada, August 20-22.

ASTM C1583 (2013). "Standard Test Method for Tensile Strength of Concrete Surfaces and the Bond Strength or Tensile Strength of Concrete Repair and Overlay Materials by Direct Tension (Pull-off Method)." ASTM International, West Conshohocken, PA.

ASTM C39 (2014). "Standard test method for compressive strength of cylindrical concrete specimens." ASTM International, West Conshohocken, PA.

Aljazaeri, Z., and Myers, J.J., (2016). "Fatigue and flexural behavior of reinforced concrete beams strengthened with a fiber reinforced cementitious matrix." ASCE Journal of Composites for Construction, 10.1061/(ASCE)CC.1943-5614.0000696.

Babaeidarabad, S., Loreto, G. and Nanni, A. (2014). "Flexural strengthening of RC beams with an externally bonded fabric-reinforced cementitious matrix." Journal of Composites for Construction 18(5), 0401400.

Carloni, C., Sneed, L., and D'Antino, T. (2013). "Interfacial bond characteristics of fiber reinforced cementitious matrix for external strengthening of reinforced concrete members." Proceedings of the 8th International Conference on Fracture Mechanics of Concrete and Concrete Structures, Elsevier B.V.

D'Ambrisi, A., Feo, L., and Focacci, F. (2012). "Bond-slip relations for PBO-FRCM materials externally bonded to concrete." Composites Part B: Engineering, 43(8), 2938-2949.

D'Ambrisi, A., Feo, L., and Focacci, F. (2013). "Experimental analysis on bond between PBO-FRCM strengthening materials and concrete." Composites Part B: Engineering, 44(1), 524-532.

D'Ambrisi, A., Feo, L., and Focacci, F. (2013). "Experimental and analytical investigation on bond between Carbon-FRCM materials and masonry." Composites Part B: Engineering, 46, 15-20.

D'Antino, T., Carloni, C., Sneed, L. H. and Pellegrino, C. (2014). "Matrix–fiber bond behavior in PBO FRCM composites: A fracture mechanics approach." Engineering Fracture Mechanics 117, 94-111.

International Concrete Repair Institute (ICRI), Technical Guideline No.03732, (1997). "Selecting and Specifying Concrete Surface Preparation for Sealers, Coatings, and Polymer Overlays." Technical Guideline No.03730, "Guide for Surface Preparation for the Repair of Deteriorated Concrete Resulting from Reinforcing Steel Corrosion." 38800 Country Club Drive Farmington Hills, MI 48331, (248) 848-3809.

Loreto, G., Leardini, L., Arboleda, D. and Nanni, A. (2014). "Performance of RC slab-type elements strengthened with fabric-reinforced cementitious-matrix composites." Journal of Composites for Construction 18(3), A4013003.

National Weather Service Forecast, http:// www.weather.gov.

National Climatic Data Center (NCDC), http://www.ncdc.noaa.gov/oa/ncdc.html.

Ombres, L. (2011). "Flexural analysis of reinforced concrete beams strengthened with a cement based high strength composite material." Composite Structures 94(1), 143-155.

Ombres, L. (2015). "Analysis of the bond between fabric reinforced cementitious mortar (FRCM) strengthening systems and concrete." Composites Part B: Engineering, 69, 418-426.

Sneed, L. H., D'Antino, T. Carloni, C., and Pellegrino, C., (2015). "A Comparison of the Bond Behavior of PBO-FRCM Composites Determined by Double-Lap and Single-Lap Shear Tests." Cement and Concrete Composites Cement and Concrete Composites 64 (2015) 37- 48.

V. A NOVEL AND EFFECTIVE ANCHORAGE SYSTEM FOR ENHANCING THE FLEXURAL CAPACITY OF RC BEAMS STRENGTHENED WITH FRCM COMPOSITES

Zena R. Aljazaeri [1], Micheal Janke [2], and John J. Myers [3] F.ASCE
[1] Graduate Research Student, Missouri University of Science and Technology, 1304 Pine Street, 201 Pine Building, Rolla, MO 65409, USA. Email: zracnb@mst.edu
[2] Greenberg Scholar Researcher, Missouri University of Science and Technology, Email: majd38@mst.edu
[3] Professor of Civil, Arch. and Envir. Engr, Missouri University of Science and Technology, 325 Butler-Carlton CE Hall, Rolla, MO 65409, USA. Email: jmyers@mst.edu

ABSTRACT

Experimental works revealed that anchorage systems were able to increase the efficiency of fiber reinforced polymers (FRP) in terms of the flexure or shear capacities and ductility performance of structural members. This task was conducted to investigate the suitability and effectiveness of two anchorage systems for enhancing the bond performance of fiber reinforced cementitious matrix composite (FRCM) composite on behalf of improving its flexural performance. The two anchorage systems were included in this study: a glass spike anchor and novel U-wrapped anchor. Real-scale simply supported RC beams were examined under the effect of strengthening with different reinforcement ratios and with and without anchorage systems engagement. Test results revealed the contribution of anchorage systems in preventing or delaying the FRCM debonding failure mechanism and enhancing the flexural performance of strengthened beams.

KEYWORDS

Anchor; U-wrapped PBO anchor; glass spike; FRCM strengthening; flexural behavior.

1. INTRODUCTION AND BACKGROUND

Different types of anchorage systems have been used to delay the premature debonding failure mode associated with FRP composites. The successful anchorage systems have allowed FRP's composite materials to continuously carry a load in shear or flexure in which extra benefits from high-strength fabrics were achieved. Thus, proper anchorage systems can reduce the required cross-sectional area of the expensive fabric materials. Some of the important anchor types are mechanical anchorages, U-wrapped sheets, anchor spikes, and FRP rods. Many experimental studies have illustrated the efficiency and applicability of these anchorage systems.

Khalifa et al. [1] invented a novel u-anchor that was used to reduce the stress concentration of FRP systems at the ends. Khalifa et al. [1] stated that "the u-anchor system provides an effective solution for cases in which the bonded length of FRP composites is not sufficient to develop its full capacity.''

Wu and Huang [2] and You et al. [3] used mechanical anchorages with FRP composites. The authors concluded that mechanical anchors for prestressed FRP strips determined higher flexural loads of RC beams and ductile behavior enhancement. It was also concluded that the anchored beams experienced a rupture in the FRP strips as the anchors were successfully holding the FRP strips against debonding.

Kim et al. [4] replaced the mechanical anchors for prestressed FRP sheets with nonmetallic anchorages (non-anchored U-wrap and anchored U-wrap).

The results concluded the efficiency of the replaced nonmetallic anchors on maintaining a considerable amount of prestressing force in FRP sheets.

Bae and Belarbi [5] determined the improving effect of three mechanical anchorage types in shear-strengthened RC beams. Piyong et al. [6] and Smith et al. [7] used the glass fiber spikes to enhance the flexural performance of concrete slabs strengthened with nonprestressed and prestressed carbon-FRP sheets. The test results indicated that the glass anchor spikes significantly increased the ultimate strength and ductility of strengthened slabs, and the rupture of fibers was captured at the ultimate stage instead of the fibers debonding.

Smith et al. [7], Ekenel et al. [8], and Ekenel and Myers [9] conducted studies on the glass spikes to anchor FRP sheets for flexural strengthening RC beams. All of the studies determined the effectiveness of using glass anchor spikes on upgrading the flexural strength of RC beams. However, the anchor spikes did not contribute to the flexural stiffness of strengthened RC beams subjected to fatigue loading [9].

A novel textile-based anchor was developed by Tetta et al. [10] and used to improve the textile reinforced mortar (TRM) composite in the shear strengthening of T-section RC beams. The effect of the anchorage number, position of anchors, textile type, and textile layers was studied. The test results defined the great influence of textile anchorage in shear strength gain.

2. RESEARCH SIGNIFICANCE

This work is a pilot study on using anchorage systems with cement-based composites.

The idea behind using anchorage systems is based on the observed debonding failure mode that captured in many experimental works for strengthened RC beams with multilayers of FRCM composite. The aim of this study was to determine the influence of anchorage systems on improving the flexural performance of FRCM composite, delay or prevent the debonding in FRCM composite at the maximum moment regions and at the ends, and assign the failure mode of FRCM composite under the action of anchoring.

3. EXPERIMENTAL WORK

3.1. Materials properties

The experimental program included a total of seven large-scale beams. The RC beams had nominal cross-sectional dimensions of 305 mm (12-in.) depth and 203 mm (8-in.) width with a total length of 2.133 m (7-ft). The concrete was ready-mixed concrete with 28-day target strength of 41.4 MPa (6,000 psi). Concrete cylinders that had 100 mm (4-in.) in diameter and 200 mm (8-in.) in height were used to specify the concrete properties.

The compressive strength and young's modulus of elasticity of concrete were based on ASTM C39 [11] and ASTM C469 [12], respectively. The concrete's average compressive strength of three tested cylinders was about 45.5 MPa (6,600 psi) at the date of the beam specimens' testing, and the concrete's modulus of elasticity was about 36,425 MPa (5,283 ksi). A steel rebar of 10 mm (No. 3) in diameter was used as longitudinal and transverse reinforcements.

The tensile yield and ultimate strengths were determined by testing three coupon specimens based on ASTM A370 [13].

The average yielded strength of the three coupons was 482 MPa (70 ksi), and the average ultimate rupture of three coupons was 726 MPa (105 ksi).

The PBO fabric was used as external flexure reinforcement with a tensile strength of 5,800 MPa (840 ksi), elastic modulus of 270,000 MPa (39,160 ksi), and ultimate strain of 0.0215 mm/mm (in./in.). All of the beams were designed to fail in flexure based on the ACI 549-13 [14] and ACI 318-08 [15]. The internal reinforcement details are presented in Fig. 1.

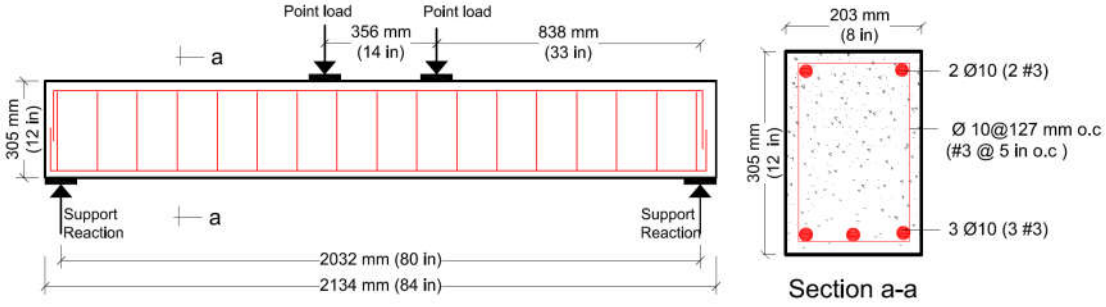

Fig. 1. Typical geometry and reinforcements of the beam specimen

3.2. Strengthening schemes

Two different anchorage systems were considered in this study. The first anchorage system was the glass spike. The glass spike was used in previous research and successfully enhanced the FRP composite's flexural performance [6] and [9]. The second anchorage system was a novel U-wrapped PBO strip. The novel U-wrapped PBO strips made of a PBO-fabric strip, where the PBO strips' ends were anchored into the concrete. The idea behind anchoring the ends of the U-wrapped PBO strip was to rely on the high tensile strength of the PBO strip to enhance the flexural performance of the FRCM composite. Two strengthening reinforcement ratio were considered in this study.

Two sheets of FRCM strengthening with anchoring systems were selected in order to reduce the number of required sheets of FRCM strengthening. Four sheets of FRCM strengthening with anchoring systems were designated to increase the effectiveness of using four sheets. Table 1 summarizes the test matrix of seven RC beams.

Table 1. Test matrix for strengthening configuration and anchorage

Specimen ID	Layers number	Anchors number	Anchorage configuration	Anchored layer	Anchor type
Con-RC					
G1-2	2				
G1-2-Glass	2	7	Along the span length	2	Glass
G1-2-PBO	2	7	Along the span length	2	PBO
G2-4	4				
G2-4-Glass	4	7	Along the span length	4	Glass
G2-4-PBO	4	7	Along the span length	4	PBO

One RC beam specimen served as the control beam. The other beam specimens were divided into two groups. Each groups consisted of three beam specimens. In group one, beams were strengthened with two layers of FRCM composite. In group two, beams were strengthened with four layers of FRCM composite. In each group, one beam was strengthened with FRCM composite without anchorages, one beam was strengthened with FRCM composite and anchored with glass spikes, and one beam was strengthened with FRCM composite and anchored with U-wrapped PBO strips.

The number of anchors was selected to be seven along the span length of strengthened RC beams. The number of anchors was intended to well distribute the load through the effective span length at the maximum moment regions through the mid-span and at the ends of FRCM strengthening where not enough development length was provided. The center-to-center spacing between the anchors was 280 mm (11-in.). The distribution and detail of glass spikes are presented in Fig. 2a. The central position of glass spikes were extended 25.4 mm (1.0-in.) from the center line of RC beams in a staggered form in order to prevent drilling at the location of longitudinal rebar's. The glass spike width was 150 mm (6-in.) The U-wrapped PBO strips' width was 114 mm (4.5-in.).

The U-wrapped PBO strips were anchored into the sides of RC beams at a depth of 100 mm (4.0-in.) from the top concrete surface to be away from the maximum tensile and compressive stresses areas, as shown in Fig. 2b. The anchors material mechanical properties are presented in Table 2. The detailed schemes for anchorage systems are presented in Fig. 3. The anchor's diameter was 15 mm (0.6-in.) and the embedded length inside the concrete was 50 mm (2-in.) for two anchorage systems.

Table 2. Anchors material' properties

Reinforcement type	**Tensile strength MPa (ksi)**	**Elastic modulus MPa (ksi)**	**Ultimate strain mm/mm (in./in.)**
PBO fibers, Ruredil Company	5,800 (840)	270,000 (39,160)	0.0215
Glass fibers, D-BASF Company	3,400 (490)	73 (10)	0.045

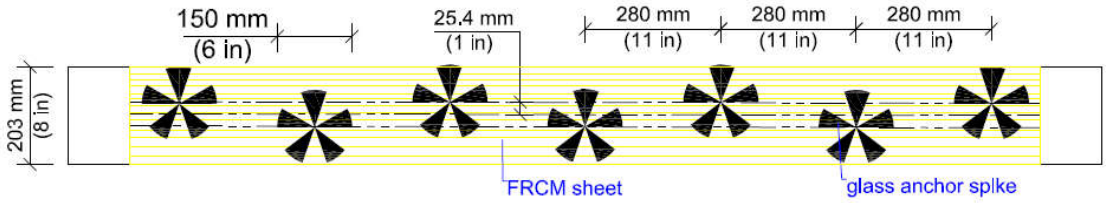

(a) Glass anchor spikes across the span, bottom view

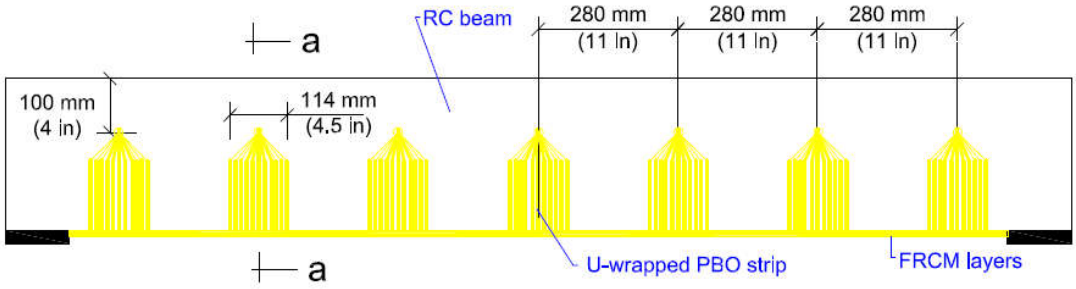

(b) U-wrapped PBO-strips across the span, side view

Fig. 2. Anchorage systems distribution

(a) Glass spike (b) Section a-a, U-wrapped PBO strip

Fig. 3. Anchorage systems' details

3.3. Anchorage systems preparation and strengthening application

Before the FRCM strengthening system was applied on the RC beam 'substrates, all beams were pre-cracked to 65% of their expected ultimate load capacity.

This level of load represented an approximate service loading level. Then, the beams were sandblasted to remove the smooth layer of concrete surface and provide better surface to adhere the FRCM composite as recommended by the ACI 549-13 [14].

The edges of two RC beams were rounded to 20 mm (0.75-in.) in order to reduce the stress concentrations around the U-wrapped PBO strips as recommended by the ACI 549-13 [14].

Holes that were 50 mm (2-in.) long and 18 mm (0.7-in.) in diameter were drilled into the concrete at the interested points for installing the anchorage systems. All of the holes were cleaned with air pressure and all of the beams' surfaces were vacuumed to remove the dust.

The anchorage systems were prepared as follows. The first anchor type was the glass spike. The glass spike was made by cutting a strip of the glass filament from the roving roll and folding several times to provide the required diameter, as shown in Fig. 4a. The folded ends of the glass strip were cut and one end was saturated by epoxy agent (Mbrace-saturant) to the desired bonded length, as shown in Fig. 4b and 4c. After one day of curing the glass spikes' ends, the glass spikes were attached to the concrete holes by epoxy agent and left again to cure for one day, as shown in Fig. 4d.

Then, the installation of the FRCM composite began by wetting the concrete substrate to eliminate the water absorption from the applied cement-based mortar. The FRCM strengthening in the form of two or four PBO sheets were applied to the concrete substrate. The cement-based mortar was used successively to attach the PBO sheets, as shown in Figs. 5a, 5b, and 5c. The PBO sheets had a width of 200 mm (7.5- in.) and a length of 1830 mm (72-in.).

Then, the glass anchor spikes were fanned over the last layer of the PBO sheet in a circular pattern, as shown in Fig. 5d, and covered with the cement-based mortar, as shown in Fig. 5e.

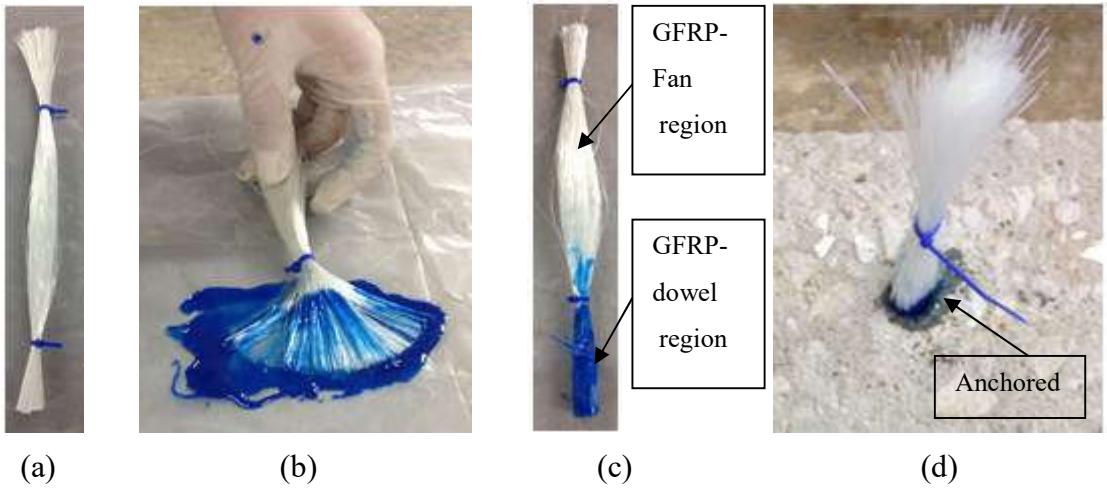

(a) (b) (c) (d)

Fig. 4. Glass spikes preparation: (a) Folded glass fabric, (b) Saturation of glass-fabric end, (c) glass spike, and (d) Anchor glass spike inside concrete hole

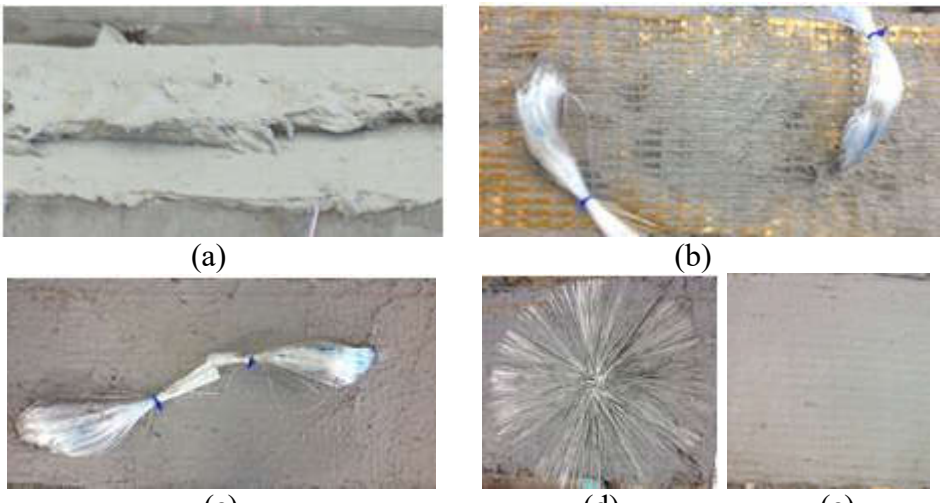

(a) (b)

(c) (d) (e)

Fig. 5. FRCM composite application with glass spikes: (a) Cement-based mortar application,(b) PBO-sheet embedment into mortar, (c) Covering PBO-sheet with mortar,(d) Fun glass spikes, and (e) Covering glass spikes with mortar

The second anchor type was the novel U-wrapped PBO strip. The U-wrapped PBO strip was made by cutting the PBO fabric in strips and removing the PBO fabric in the transverse direction, as shown in Figs. 6a and 6b. Then, the ends of the PBO strips were saturated with epoxy agent (Mbrace-saturant) for a length of 50 mm (2-in.) to be anchored in RC beams, as shown in Figs. 6c, 6d, and 6e. The installation of the U-wrapped PBO strips were done immediately after applying the successive layers of the FRCM composite, as shown in Figs. 7a, 7b, and 7c. Then, the U-wrapped PBO strips' ends were adhered into concrete holes using a high viscosity gel epoxy (MasterEmaco, ADH 1420), as shown in Fig. 7d. The final shape of the U-wrapped PBO strip is presented in Fig. 7e.

(a) (b) (c) (d) (e)

Fig. 6. Anchored U-wrapped PBO strip preparation: (a) Removal transverse PBO-fabrics, (b) Geometrical shape of U-wrapped PBO strip, (c) PBO-fabric ends saturation, (d) Injection of saturator around PBO strip's end, and (e) U-wrapped PBO strip's end

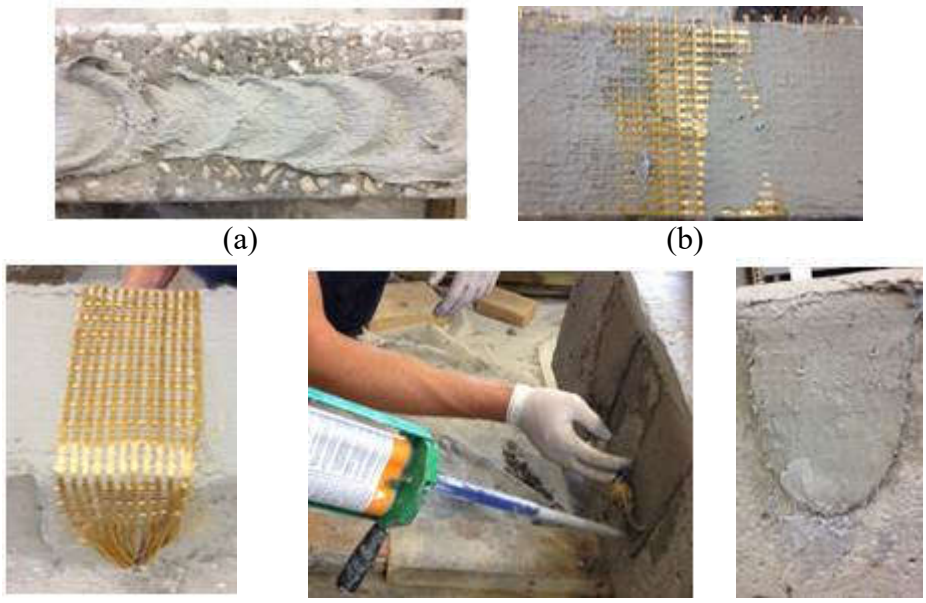

Fig. 7. FRCM composite application with anchored U-wrapped PBO strips: (a) Cement-based mortar application, (b) PBO-sheet embedment into mortar, (c) Applying U-wrapped PBO strip, (d) Injection gel epoxy into concrete hole for fixing U-wrapped PBO strip's ends, and (e) Anchored U-wrapped PBO strip

All of the strengthened RC beams were cured with water for three days and covered with plastic sheets to prevent the loss of moisture. Then, the strengthened RC beams were cured under laboratory conditions for 25 additional days before testing.

3.4. Test set-up and instrumentation

The four-point loading was selected to determine the anchorages' efficiency. The loads were applied on a displacement rate control of 1.3 mm/minute (0.05 in/min). A linear variable differential transducer (LVDT) was used to measure the displacement in the RC beams. Strain gauges were used to determine the strain reading of the internal longitudinal rebar and the external applied FRCM composite. The distribution schemes of strain gauges are presented in Fig. 8.

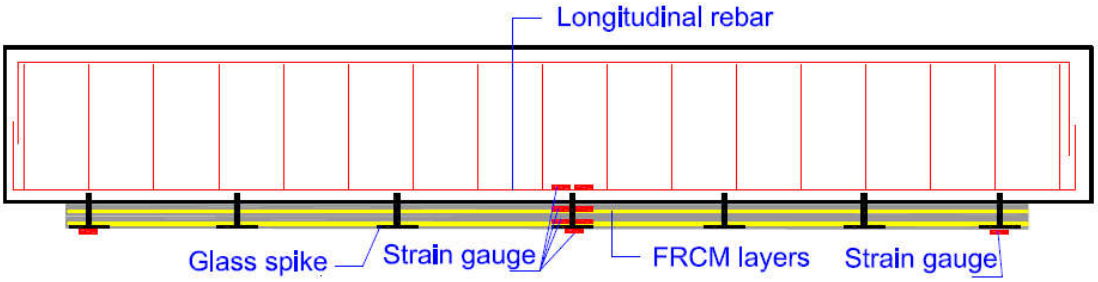

(a) Strain gauges distribution for anchored RC beams with glass spike

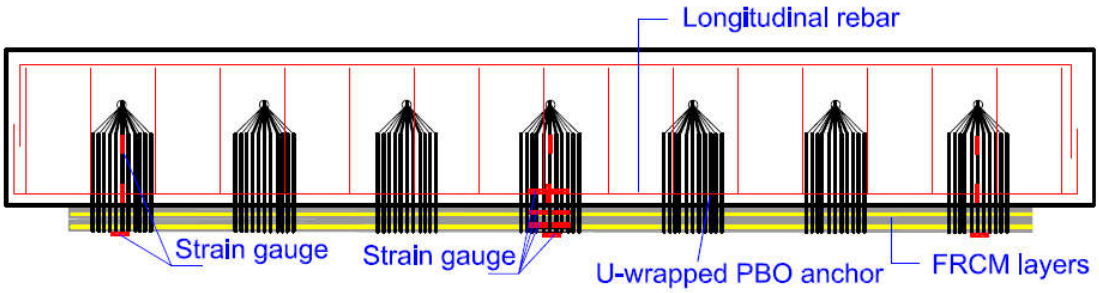

(b) Strain gauges distribution for anchored RC beams with U-wrapped PBO

Fig. 8. Strain gauges scheme

For all RC beams, two strain gauges were bonded to the longitudinal rebar at the mid-span, two strain gauges were bonded to first and last sheets of the FRCM composite at the mid-span, and three strain gauges were attached to the external surface of the FRCM composite (at the mid-span and at the ends), as shown in Fig. 8a. For the U-wrapped PBO strips, five strain gauges were attached to each PBO strip to determine its effective strain at the bottom, the edge region, and area close to the anchored ends, as shown in Fig. 8b.

The data acquisition system was used to record the load displacement curve and the strain gauge readings.

4. EXPERIMENTAL RESULTS

4.1. Load displacement

The load displacement curves of all specimens tested is presented in Fig.9. Table 3 include the key results: ultimate load, percentage increase in ultimate load, displacement at yielding rebar's, displacement at ultimate load, and displacement ductility index. The load displacement curve for the control RC beam was a classic response. The yielded rebar's were announced at 16 kips followed by an ultimate load of 27.4 kips. Then, the load displacement response turned to the plastic-ductile stage, and the concrete crushing terminated the test. The strengthened beams exhibited a gain in the flexure strength through the inelastic loading stage followed by a drop in their carrying loads as the FRCM strengthening and anchorage systems reached their ultimate loads. Then, the strengthened beams went through the plastic-ductile stage as the control beam. The strengthened beams with two and four PBO sheets determined higher ultimate loads of 34.6 kips and 31.6 kips, respectively.

Table 3. Ultimate loads and deflections

Specimen ID	Experimental ultimate load, kN (Kips)	% Increase in load carrying capacity	Yield displacement (δy) mm (in)	Ultimate displacement (δu) mm (in)	Displacement ductility index (δu/δy)
Con-RC	122 (27.4)		6.6 (0.26)	51.0 (2.0)	7.7
G1-2	154 (34.6)	26%	4.3 (0.17)	25.4 (1.0)	5.9
G1-2-Glass	146 (33.0)	20%	4.6 (0.18)	30.5 (1.2)	6.7
G1-2-FRCM	148 (33.3)	22%	5.1 (0.2)	25.4 (1.0)	5.0
G2-4	141 (31.6)	15%	5.1 (0.2)	17.8 (0.7)	3.5
G2-4-Glass	154 (34.6)	26%	4.6 (0.18)	28 (1.1)	6.1
G2-4-FRCM	175 (39.2)	43%	4.1 (0.16)	25.4 (1.0)	6.3

*Conversion units: Conversion units: 1-in. = 25.4 mm; 1 kip = 4.45 kN

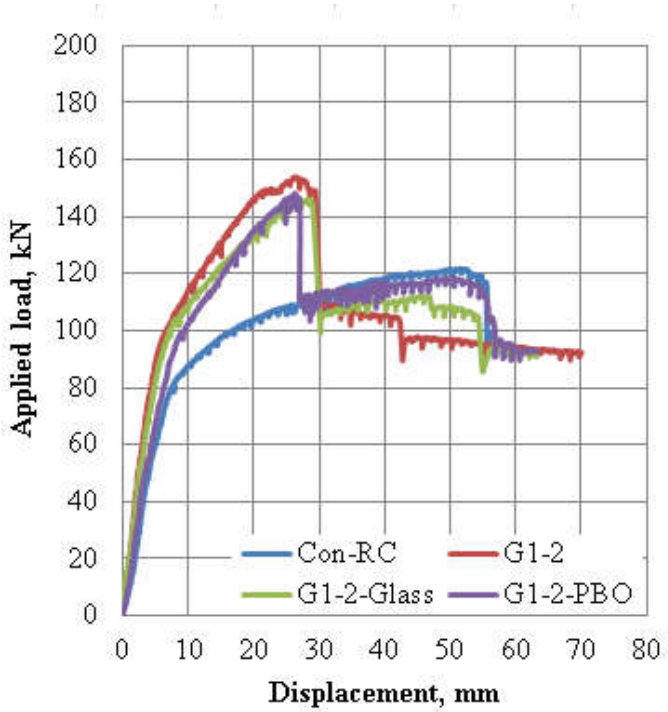

(a) Group1 beams with 2-ply

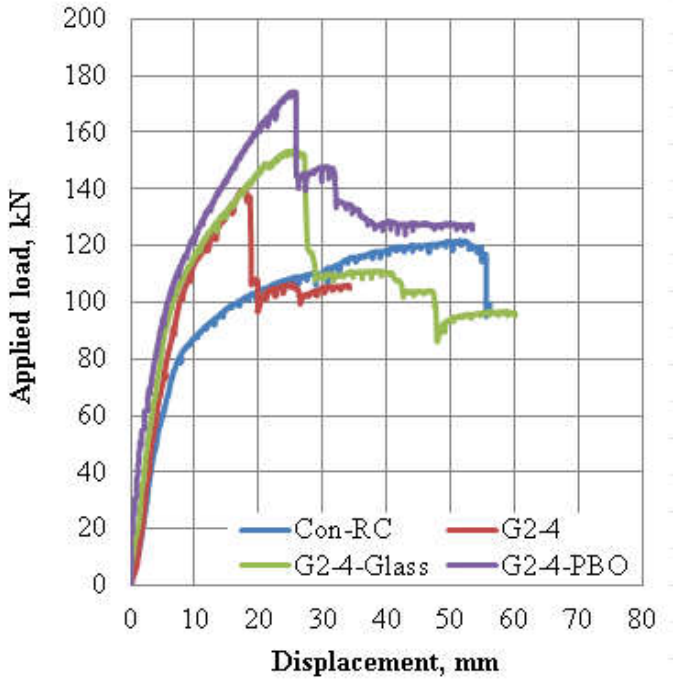

(b) Group2 beams with 4-ply

Conversion units: 1-in. = 25.4 mm; 1 kip = 4.45 kN

Fig. 9. Load displacement curves

The anchored beams with glass spikes carried an ultimate load of 33 kips and 34.6 kips for two and four PBO sheets, respectively. The anchored U-wrapped beams were carried an ultimate load of 33.3 kips and 39.2 kips for two and four PBO sheets, respectively. It is concluded that the anchorage systems were more effective when the higher external PBO sheets reinforcement ratio (four sheets) was provided.

As a measurement for the ductility performance of the strengthened beams with and without anchorages, the displacement ductility index was determined. The displacement ductility index represented the ratio of the beam's displacement at the ultimate load to the beam's displacement at the yielded load. The strengthened beams with and without anchorages obtained lower displacements at the yielded and ultimate load stages with respect to the control beam. However, the displacement ductility index showed that the strengthened beams maintained reasonable displacement ductility up to FRCM strengthening failure. The anchorage systems played influential role on the displacement ductility performance of strengthened beams with four PBO sheets than two PBO sheets.

4.2. Crack pattern, failure mode, and number of sheets

All of the beams failed due to flexural cracks that were observed from the tensile face toward the top face of the beams preceded by FRCM strengthening failure, as shown in Fig. 10. In addition, concrete crushing was noticed at the final loading stage. The non-anchored beams that were strengthened with two or four sheets of FRCM composite exhibited intermediate debonding at the maximum loaded area and the endplate debonding at the free end.The debonding was at the interface between the PBO sheets and the cementitious matrix.

Con-RC

G1-2 (debonding)

G1-2-Glass (slippage in PBO)

G1-2-FRCM (slippage in PBO)

G2-4 (debonding)

G2-4-Glass (debonding)

G2-4-FRCM (debonding)

Slippage in PBO

Fig. 10. Crack pattern and failure mode

The anchored beam with glass spikes that was strengthened with two sheets of FRCM composite was exhibited a slippage of the PBO sheets out of the cementitious matrix at the mid span with no debonding of the PBO sheets along the span length.

The anchored beam with glass spikes that was strengthened with four sheets of FRCM composite was revealed intermediate debonding and endplate debonding of the PBO sheets out of the cementitious matrix.

The anchored beams with U-wrapped PBO strips that were strengthened with two sheets of FRCM composite exhibited a slippage of the PBO sheets and U-wrapped PBO strips out of the cementitious matrix at the mid span. A slippage failure mode of the PBO sheet usually indicated that the PBO fabric developed a higher percentage of its tensile strength. In such a case, anchorage systems could not contribute more in upgrading the flexural performance of strengthened beams. However, the mode of failure was improved from intermediate debonding and end plate debonding to the slippage of PBO sheets, while anchorage systems contributed to delaying the premature debonding failure mode and improving the ultimate loads in strengthened beams with four PBO sheets.

The ultimate load of the strengthened beam with four PBO sheets and anchored with glass spikes was 10% higher than the non-anchored strengthened beam with four PBO sheets. The ultimate load of the strengthened beam with four PBO sheets and anchored with U-wrapped PBO strips was 24% higher than the non-anchored strengthened beam with four PBO sheets.

4.3. Anchorage's configuration and material

Test results of anchored beams determined different flexural performance. The external reinforcement ratio of the PBO sheets was influenced the contribution of the anchorage systems. The glass spikes contributed to reducing the stress concentration in the direction of the PBO sheets and preventing or delaying the debonding failure mode.

The anchored U-wrapped PBO strips performance was verified the research idea interms of relying on the high-tensile strength of PBO strips. The anchored ends of the PBO strips into the concrete prevented the debonding of the U-wrapped PBO strips and developed a slippage failure mode in the PBO strips. The anchored U-wrapped PBO strips resulted in greater enhancement than glass spikes in the ultimate load and the displacement ductility of the strengthened beam with four PBO sheets. The anchorage confinement of the anchored U-wrapped PBO strips concluded its greater impact. In addition, the anchors' material type could also play role in the efficiency of the anchorage systems. Glass spikes had lower tensile properties than the PBO strips which could be another reason why the U-wrapped PBO strips performed better. More experimental investigation would assist in the efficient selection of the anchorage systems in terms of the material type and configuration.

4.4. Strain measurements

Measurements of the strains in the rebar's, FRCM strengthening, and U-wrapped PBO strips are presented in Table 4. The strain reading of the rebar's determined that it was yielded in all tested RC beams. The ultimate strain in the rebar's ranged between 0.005 mm/mm (in./in.) to 0.006 mm/mm (in./in.) based on the measurement of two beams. The strain reading in the first applied PBO sheet at the mid-span ranged between 0.002 mm/mm (in./in.) to 0.005 mm/mm (in./in.), while higher strain readings were determined in the last applied PBO sheet at the mid span. The anchorage systems reduced the strain reading of the PBO sheets at the edges. Glass spikes reduced the strain reading of the PBO sheets by half of that measured in strengthened beams without glass spikes.

The U-wrapped PBO strips at the edges declared zero strain reading in the PBO sheets. The non-strain reading of the PBO sheets at the edges indicated the influence of the anchorage systems in preventing the PBO sheets' endplate debonding.

Table 4. Strain readings in rebars, FRCM sheets, and anchorage

Specimen ID	Strain reading, mm/mm (in./in.)					
	Rebar	FRCM sheets at mid span		FRCM at edge	U-wrapped PBO	
	mid span	First sheet	Last sheet	last sheet	Center	edge
Con-RC	0.005					
G1-2		0.002	0.005	0.007		
G1-2-Glass		0.005	0.010	0.004		
G1-2-FRCM		0.005	0.004		0.004	0.000
G2-4	0.006		0.006	0.005		
G2-4-Glass		0.004	0.006	0.003		
G2-4-FRCM			0.010		0.010	0.000

5. CONCLUSIONS

The effectiveness of two anchorage systems in increasing the strength and displacement ductility of FRCM strengthened RC beams is reported as follows:

- The anchorage systems can enhance the flexural performance of strengthened RC beams with FRCM composite based on the provided strengthening reinforcement ratio.
- The anchorage systems successfully prohibited the endplate debonding failure mode where not enough development length could be provided.

- The anchorage systems were proved to prevent or delay the intermediate debonding failure mode in the FRCM strengthening based on the FRCM strengthening reinforcement ratio.
- The non-anchored and anchored strengthened RC beams with two PBO sheets obtained the same flexural strength but the anchorage systems changed the mode of failure from debonding to slippage of the PBO sheets.
- The novel anchored U-wrapped PBO strips increased the ultimate load by 24% more than the non-anchored strengthened beam with four PBO sheets.
- The anchored U-wrapped PBO strip had a superior flexural enhancement compared to the glass spike due to its high tensile property and confining action.

ACKNOWLEDGMENTS

This work was supported by Ruredil Company and the ReCAST Tier 1 University Transportation Center at Missouri S&T. The authors acknowledge greatly both resources for their financial support. As well as to the academic support from the Center for Infrastructure Engineering Studies and the Department of Civil, Architectural, and Environmental Engineering at Missouri S&T.

REFERENCES

[1] Khalifa, A., Alkhrdaji, T., Nanni, A., and Lansburg, S. (1999). "Anchorage of surface mounted FRP reinforcement." Concrete International, 21(10), 49-54.

[2] Wu, Y. F., and Huang, Y. (2008). "Hybrid bonding of FRP to reinforced concrete structures." Journal of Composites for Construction, 12(3), 266-273.

[3] You, Y. C., Choi, K. S., and Kim, J. (2012). "An experimental investigation on flexural behavior of RC beams strengthened with prestressed CFRP strips using a durable anchorage system." Composites Part B: Engineering, 43(8), 3026-3036.

[4] Kim, Y. J., Wight, R. G., and Green, M. F. (2008). "Flexural strengthening of RC beams with prestressed CFRP sheets: Development of nonmetallic anchor systems." Journal of Composites for Construction, 12(1), 35-43.

[5] Bae, S. W., and Belarbi, A. (2012). "Behavior of various anchorage systems used for shear strengthening of concrete structures with externally bonded FRP sheets." Journal of Bridge Engineering, 18(9), 837-847.

[6] Piyong, Y., Silva, P. F., & Nanni, A. (2003). "Flexural strengthening of concrete slabs by a three-stage prestressing FRP system enhanced with the presence of GFRP anchor spikes." In Proceedings of the International Conference Composites in Construction (CCC2003-Vol. 239244).

[7] Smith, S. T., Hu, S., Kim, S. J., and Seracino, R. (2011). "FRP-strengthened RC slabs anchored with FRP anchors." Engineering Structures, 33(4), 1075-1087.

[8] Ekenel, M., Rizzo, A., Myers, J., and Nanni, A. (2006). "Flexural fatigue behavior of reinforced concrete beams strengthened with FRP Fabric and precured laminate systems." Journal of Composite for Construction, 10, 443-442.

[9] Ekenel M. and Myers J.J. (2009)."Fatigue performance of CFRP strengthened RC beams under environmental conditioning and sustained load." Journal of Composites for Construction, 13(2), 93-102.

[10] Tetta, Z. C., Koutas, L. N., and Bournas, D. A. (2015). "Textile-reinforced mortar (TRM) versus fiber-reinforced polymers (FRP) in shear strengthening of concrete beams." Composites Part B: Engineering, 77, 338-348.

[11] ASTM C39 (2014). "Standard test method for compressive strength of cylindrical concrete specimens." ASTM International, West Conshohocken, PA.

[12] ASTM C469 (2014). “Standard test method for static modulus of elasticity and poisson’s ratio of concrete in compression.” ASTM International, West Conshohocken, PA.

[13] ASTM A370 (2012a). “Standard test methods and definitions for mechanical testing of steel products.” ASTM International, West Conshohocken, PA.

[14] ACI (American Concrete Institute). (2013). “Guide to design and construction of externally bonded fabric-reinforced cementitious matrix (FRCM) systems for repair and strengthening concrete and masonry structures.” ACI 549, Farmington Hills, MI.

[15] ACI (American Concrete Institute). (2014). “Building code requirements for structural concrete.” ACI 318, Farmington Hills, MI.

SECTION

3. SUMMARY, CONCLUSIONS AND RECOMMENDATIONS

3.1. SUMMARY OF RESEARCH

This research was conducted to determine the mechanical and durability performance of FRCM composite to be implemented for repairing and strengthening infrastructural buildings.

The first paper represented a unique up-to-date study for flexure and fatigue performance of RC beams strengthened with FRCM composite. Three study parameters included the FRCM composite reinforcement ratio, environmental exposure, and sustained stress influence.

The second paper represented the performance of FRCM composite for shear strengthening RC beams. The study parameters included RC beams with and without transverse internal reinforcements, FRCM composite reinforcement ratio, and different strengthening configurations.

The third paper demonstrated a comparison study on three different composites to be used for strengthening RC slab systems. The study determined the mechanical and durability performance of three composites in terms of material standpoint (reinforcing fabrics and bonding agents). The ultimate loads, energy absorption, and failure modes of strengthened RC slabs were examined.

The fourth paper investigated the durability performance of FRCM composite as this strengthening or repairing system would be used in different applications when a structure can be exposed to various environmental conditions. Two different test sets up were conducted.

The pull-off test was to reveal the environmental conditioning effect and the failure mode of FRCM composite. The bending test was to evaluate the effect of concrete surface roughness and the effect of increasing FRCM composite's reinforcement ratio on the load carrying capacity.

The fifth paper represented the influence of using anchorage systems to enhance the flexural performance of FRCM composite in strengthening RC beams. The anchorage system types were glass spikes and U-wrapped PBO strips. Different FRCM composite reinforcement ratio was included. The flexure test results specified the ultimate loads, energy absorption, and mode of failure of the anchored-strengthened RC beams.

3.2. CONCLUSIONS

In general, the experimental investigations validated the performance of FRCM composite for structural rehabilitation and strengthening.

3.2.1. FRCM Composite under Fatigue and Flexure Loads. The innovative FRCM composite can be used to upgrade RC beams under the effect of cyclic loading conditions for the following reasons:

- All of the strengthened beams survived 2 million fatigue cycles without any debonding in the FRCM composite.
- The monitored stiffness degradation was highly recognized at the first 250,000 fatigue cycles in all beam specimens, while insignificant stiffness degradation was observed at the end of 2 million cycles due to balanced displacements under constant fatigue loading.

- The environmental exposure had a lower impact on the stiffness degradation of the beam specimens than the sustained load, and the ultimate load capacities of exposed beam specimens were higher than unexposed beam specimens due to the effect of curing inside the environmental chamber.
- The flexure failure mode was based on the strengthening reinforcement ratio. A slippage mode failure was exhibited for strengthened beam specimens with one ply, and a debonding mode failure was exhibited for strengthened beam specimens with four plies.
- The applied fatigue loading was within the limit of elastic stage. Thus, the flexural capacity of the beam specimens was not affected by long-term cyclic loading.
- ACI 549 (2013) conservatively expected the ultimate flexural capacity of the strengthened beams with the FRCM composite.

3.2.2. FRCM Composite under Shear Loads. The strengthened beams with FRCM composite determine that this type of strengthening system can be applied in the case of reinforced concrete beams that have adequate distribution of internal shear reinforcements only. The main findings of this work are summarized as follows:

- FRCM strengthening is applicable for beams with internal shear reinforcement, as a significant increase in the shear load and deflection (ductile behavior) near failure compared to the control beams were observed.

- The continuous U-wrapping through the shear span of the RC beam determined the ductile failure mode of strengthened beams due to its impact on confining the RC beams and reducing the stress concentration around corners.
- The strengthened beams without internal shear reinforcement exhibited the same brittle failure mode and ultimate load as the control beam. Thus, FRCM strengthening was not practical for of RC beams without internal shear reinforcements. The absence of the internal shear reinforcement, the non-homogenous property of concrete and lower tensile strength of the cementitious matrix resulted in an unexpected crack path and larger crack width which contributed to reduce aggregate interlock and lower FRCM composite effectiveness.
- The presence of stirrups had a major impact on the shear behavior of the concrete beams; they helped to minimize the crack width by increasing aggregate interlock and gradually transfer the load through the FRCM strengthening system.
- The comparison study between the results of FRCM composite strengthened RC beams with previous experimental results of FRP composite strengthened RC beams revealed that FRP systems greatly impact the enhancement of shear capacity. However, the FRCM system is still a promising strengthening system, as the ACI 549 (2013) limited the enhancement to be less than 50 percent in addition to its durability performance.

- The experimental values of ultimate loads validated the applicability of shear strengthening equations and assumptions in ACI 549 (2013) for RC beam with internal shear reinforcement.
- Further investigation should address the applicability of the FRCM system in shear strengthening RC beams in the absence of internal shear reinforcement.

3.2.3. Evaluation of Different Composites for Flexural Strengthening of One-Way Slabs. Based on the results of the experimental investigation presented in paper III, the following conclusions can be drawn:

- The FRCM, CFRP-grid, and SRP composites proved to be capable of improving the flexural performance of RC one-way slabs. The increases in the strengthened slabs' ultimate loads were approximately 1.3 to 2 times that of the unstrengthened slab.
- The FRCM composite can be considered an alternative solution for upgrading infrastructures as it was found to be competitive to the SRP composite, while the CFRP-grid composite was less influential in enhancing the flexural strength of RC one-way slabs.
- The failure mode of the strengthened one-way slabs depended on the type of composite and its reinforcement ratio. Application of one layer of FRCM composite failed due to slippage of the PBO-fabric out of the cementitious matrix while the one layer of SRP or CFRP-grid composites detected the rupture mode. For strengthening with more than one layer, FRCM and SRP composite exhibited a debonding failure mode and the CFRP-grid composite was ruptured at the mid span.

- The composite properties (composite material type, reinforcement ratio, and mesh spacing) played important roles on the flexural behavior of strengthened RC slabs.
- The bonding curing agents were approved under the effect of different exposure conditions inside the environmental chamber with no delamination or debonding of the strengthening composites. However, the high temperature cycles positively influenced the energy absorption of strengthened slab with FRCM composite and negatively influenced the energy absorption of strengthened slabs with SRP and CFRP-grid composites. The lower energy absorption of the exposed slabs revealed the sensitivity of epoxy curing agents to high temperatures.
- The exposed strengthened slabs had the same flexural strength that was determined in unexposed slabs, and ACI 440 (2008) and ACI 549 (2013) predicted the ultimate flexural capacities of the externally bonded RC one-way slabs conservatively.

3.2.4. Durability Performance of FRCM Composite. Some conclusions are presented here from the experimental study on the bond performance between externally attached FRCM composite to concrete blocks:

- The pull-off test determined the efficiency of the FRCM composite against various environmental conditioning.

- The bending test demonstrated the load versus the global slip of the FRCM composite attached to concrete blocks. The increase in the reinforcement ratio of FRCM composite did not lead to proportional enhancement in ultimate loads.
- In the pull-off test, the interfacial debonding of the PBO-fabric from the cementitious matrix was observed for all FRCM-concrete specimens, while the bending test determined the slippage of the FRCM composite attached in one layer and debonding of the FRCM composite attached in four layers as exhibited in large-scale tested RC beams.
- The heavy and light concrete surface preparations did not influence the failure mode of the FRCM composite-concrete blocks, and the same ultimate tensile strength of the FRCM composite was determined.
- The impermeable property of the cementitious matrix that contains silica fume concluded the FRCM composite's bond performance under different exposure conditioning.

3.2.5. FRCM Composite Performance with Anchorage Systems. The experimental results have revealed the following remarks:

- FRCM composite flexural performance can be enhanced with anchorage systems.
- The anchorage systems successfully prohibited the debonding failure mode in the strengthened beams with two PBO sheets and delayed the debonding failure mode in the strengthened beams with four PBO sheets.

- The anchorage systems' effectiveness was based on the FRCM strengthening reinforcement ratio.
- The novel U-wrapped PBO strips increased the ultimate load of the strengthened beam with four PBO sheets by 24% more than the non-anchored strengthened beam with four PBO sheets.
- The U-wrapped PBO strips had superior flexural performance compared to the glass spikes due to their confinement and higher tensile properties.

3.3. RECOMMENDATIONS

Based on the conclusions stated in this research, the following recommendations for future research were developed:

- Investigate the effect of PBO fabric orientations and shear span ratio on the PBO-FRCM composite shear performance.
- Further investigate on the effect of absence the internal transverse reinforcement on the PBO-FRCM composite shear performance.
- Investigate the effect of internal longitudinal reinforcement ratio on the flexural performance of externally bonded FRCM composite.
- Further investigate on the anchorage systems that can be applicable with FRCM composite.

REFERENCES

Abegaz, A. Z. (2014). "Advanced fiber reinforced composites as confining cystems for RC columns." Construction and Building Materials, 73, 332-338.

AC 434, (2013). "Acceptance criteria for masonry and concrete strengthening using fabric-reinforced cementitious matrix (FRCM) composite systems." ICC-Evaluation Service, Whittier, CA.

ACI (American Concrete Institute). (2013). "Guide to design and construction of externally bonded fabric-reinforced cementitious matrix (FRCM) systems for repair and strengthening concrete and masonry structures." ACI 549, Farmington Hills, MI.

Al-Salloum, Y.A., Elsanadedy, H. M., Alsayed, S.H., and Iqbal, R. A., (2012). "Experimental and numerical study for the shear strengthening of reinforced concrete beams using textile-reinforced mortar." Journal of composites for Construction ,10.1061/(ASCE)CC.1943-5614.0000239, 16(1),74-90.

Anania, L., Badalá, A., & D'Agata, G. (2016). "Numerical simulation of tests for the evaluation of the performance of the reinforced concrete slabs strengthening by FRCM." Curved and Layered Structures, 3(1).

Arboleda, D., Loreto, G., De Luca, A., and Nanni, A. (2012). "Material characterization of fiber reinforced cementitious matrix (FRCM) composite laminates." Proc, 10th International Symposium on Ferrocement and Thin Reinforced Cement Composites, Havana, Cuba, 29-37.

Arboleda, D., Babaeidarabad, S., Hays, C. D., and Nanni, A. (2014). "Durability of fabric reinforced cementitious matrix (FRCM) composites.'' The 7th International Conference on FRP Composites in Civil Engineering International Institute for FRP in Construction, Canada, August 20-22.

Arboleda, D., Carozzi, F. G., Nanni, A., and Poggi, C. (2015). "Testing procedures for the uniaxial tensile characterization of fabric-reinforced cementitious matrix composites." Journal of Composites for Construction, 20(3), 04015063.

Azam, R., and Soudki, K. (2014). "FRCM strengthening of shear-critical RC beams." Journal of Composites for Construction, 18(5), 04014012.

Babaeidarabad, S., Caso, F. D., and Nanni, A. (2013). "Out-of-plane behavior of URM walls strengthened with fabric-reinforced cementitious matrix composite." Journal of Composites for Construction, 18(4), 04013057.

Babaeidarabad, S. Loret, G. and Nanni, A. (2014). "Flexural strengthening of RC beams with an externally bonded fabric-reinforced cementitious matrix." Journal of Composites for Construction, 10.1061/(ASCE)CC.1943-5614.0000473, 18(5), 04014009-1.

Babaeidarabad, S., Arboleda, D., Loreto, G., and Nanni, A. (2014). "Shear strengthening of un-reinforced concrete masonry walls with fabric-reinforced-cementitious-matrix." Construction and Building Materials, 65, 243-253.

Bae, S. W., and Belarbi, A. (2012). "Behavior of various anchorage systems used for shear strengthening of concrete structures with externally bonded FRP sheets." Journal of Bridge Engineering, 18(9), 837-847.

Baggio, D., Soudki, K. and Noël, M. (2014). "Strengthening of shear critical RC beams with various FRP systems." Construction and Building Materials, 66, 634–64.

Berardi, F.; Focacci, F.; Mantegazza, G.; and Miceli, G. (2011) "Rinforzo di un Viadotto Ferroviario con PBO-FRCM." Proceedings, 1° Convegno Nazionale Assocompositi, Milan, Italy, May 25-26. (in Italian).

Bisby, L., Stratford, T., Hart, C., and Farren, S. (2013). "Fire performance of well-anchored TRM, FRCM, and FRP flexural strengthening systems." In book: Advanced Composites in Construction, Publisher: Network Group for Composites in Construction.

Butler, M., Mechtcherine, V., and Hempel, S. (2010). "Durability of textile reinforced concrete made with AR glass fiber: effect of the matrix composition." Materials and structures, 43(10), 1351-1368.

Carloni, C., Sneed, L., and D'Antino, T. (2013). "Interfacial bond characteristics of fiber reinforced cementitious matrix for external strengthening of reinforced concrete members." Proceedings of the 8th International Conference on Fracture Mechanics of Concrete and Concrete Structures, Elsevier B.V.

Contamine, R., Si Larbi, A., Hamelin, P. (2011). "Contribution to direct tensile testing of textile reinforced concrete (TRC) composites." Material science and engineering: A, 528(29), 8589-8598.

Colajanni, P., De Domenico, F., Recupero, A., and Spinella, N. (2014). "Concrete columns confined with fibre reinforced cementitious mortars: experimentation and modelling." Construction and Building Materials, 52, 375-384.

D'Ambrisi, A., and Focacci, F. (2011)."Flexural strengthening of RC beams with cement-based composites." Journal of Composites for Construction, 15(5), 707-720.

D'Ambrisi, A., Feo, L., and Focacci, F. (2012). "Bond-slip relations for PBO-FRCM materials externally bonded to concrete." Composites Part B: Engineering, 43(8), 2938-2949.

D'Ambrisi, A., Feo, L., and Focacci, F. (2013). "Experimental analysis on bond between PBO-FRCM strengthening materials and concrete." Composites Part B: Engineering, 44(1), 524-532.

D'Ambrisi, A., Feo, L., and Focacci, F. (2013). "Experimental and analytical investigation on bond between Carbon-FRCM materials and masonry." Composites Part B: Engineering, 46, 15-20.

D'Antino, T., Carloni, C., Sneed, L. H. and Pellegrino, C. (2014). "Matrix–fiber bond behavior in PBO FRCM composites: A fracture mechanics approach." Engineering Fracture Mechanics 117, 94-111.

D'Antino, T., Sneed, L. H., Carloni, C., and Pellegrino, C. (2015). "Influence of the substrate characteristics on the bond behavior of PBO FRCM-concrete joints." Construction and Building Materials, 101, 838-850.

D'Antino, T., Gonzalez, J., Pellegrino, C., Carloni, C., & Sneed, L. H. (2016). "Experimental investigation of glass and carbon FRCM composite materials applied onto concrete supports." In Applied Mechanics and Materials (Vol. 847, pp. 60-67). Trans Tech Publications.

D'Antino, T., Carloni, C., Sneed, L. H., and Pellegrino, C. (2015). "Fatigue and post-fatigue behavior of PBO FRCM-concrete joints." International Journal of Fatigue, 81, 91-104.

De Santis, S., & de Felice, G. (2015). "Tensile behavior of mortar-based composites for externally bonded reinforcement systems." Composites Part B: Engineering, 68, 401-413.

Donnini, J., Corinaldesi, V., & Nanni, A. (2016). "Mechanical properties of FRCM using carbon fabrics with different coating treatments." Composites Part B: Engineering, 88, 220-228.

Ekenel, M., Rizzo, A., Myers, J., and Nanni, A. (2006). "Flexural fatigue behavior of reinforced concrete beams strengthened with FRP Fabric and precured laminate systems." Journal of Composite for Construction, 10, 443-442.

Ekenel M. and Myers J.J. (2009).''Fatigue Performance of CFRP Strengthened RC Beams under Environmental Conditioning and Sustained Load,'' Journal of Composites for Construction,13(2), 93-102.

Grelle, S. V., and Sneed, L. H. (2013). "Review of anchorage systems for externally bonded FRP laminates." International Journal of Concrete Structures and Materials, 7(1), 17-33.

Hartig, F., Jesse, F., Schicktanz, K., Haubler-Combe, U. (2012). "Influence of experimental setups on the apparent uniaxial tensile load-bearing capacity of textile reinforced concrete specimens." Materials and structures, 45, 433-446.

Huang, X., and Chen, G. (2005). "Bonding and anchoring characterization between FRP sheets, concrete, and viscoelastic layers under static and dynamic loading." In Proceedings of the International Symposium on Bond Behavior of FRP in Structures (Vol. 79).

Jung, K., Hong, K., Han, S., Park, J., and Kim, J. (2015). "Prediction of Flexural Capacity of RC Beams Strengthened in Flexure with FRP Fabric and Cementitious Matrix." International Journal of Polymer Science.

Kalfat, R., Al-Mahaidi, R., and Smith, S. T. (2011). "Anchorage devices used to improve the performance of reinforced concrete beams retrofitted with FRP composites: State-of-the-art review." Journal of Composites for Construction, 17(1), 14-33.

Khalifa, A., Alkhrdaji, T., Nanni, A., & Lansburg, S. (1999). "Anchorage of surface mounted FRP reinforcement." Concrete International, 21(10), 49-54.

Kim, Y. J., and Heffernan, P. J. (2008). "Fatigue behavior of externally strengthened concrete beams with fiber-reinforced polymers: state of the art." Journal of Composites for Construction, 12(3), 246-256.

Kim, Y. J., Wight, R. G., & Green, M. F. (2008). "Flexural strengthening of RC beams with prestressed CFRP sheets: Development of nonmetallic anchor systems." Journal of Composites for Construction, 12(1), 35-43.

Loreto, G., Leardini, L., Arboleda, D. and Nanni, A. (2013). "Performance of RC slab-type elements strengthened with fabric-reinforced cementitious-matrix composites." Journal of Composites for Construction, 10.1061/ (ASCE) CC.1943-5614.0000415, 18(3), A4013003-1.

Loreto, G., Leardini, L., Arboleda, D. and Nanni, A. (2014). "Performance of RC slab-type elements strengthened with fabric-reinforced cementitious-matrix composites." Journal of Composites for Construction, 10.1061/ (ASCE) CC.1943-5614.0000415, A4013003-1.

Masoud, S., Soudki, K., and Topper, T. (2001). "CFRP-strengthened and corroded RC beams under monotonic and fatigue loads." Journal of Composites for Construction, 4, 228-236.

Michels, J., Zwicky, D., Scherer, J., Harmanci, Y. E., and Motavalli, M. (2014). "Structural strengthening of concrete with fiber reinforced cementitious matrix (FRCM) at ambient and elevated temperature—recent investigations in Switzerland." Advances in Structural Engineering, 17(12), 1785-1799.

Nanni, A., (2012), "A New tool in the concrete and masonry repair." Concrete International, V. 34, No. 4, Apr., pp. 43-49.

Ombres, L. (2011). "Flexural analysis of reinforced concrete beams strengthened with cement based high strength composite material." Composite Structures 94(1), 143-155.

Ombres, L. (2012). "Debonding analysis of reinforced concrete beams strengthened with fiber reinforced cementitious mortar." Engineering Fracture Mechanics, 81, 94-109.

Ombres, L. (2012). "Shear capacity of concrete beams strengthened with cement based composite materials." In Proceedings of the 6th International Conference on FRP Composites in Civil Engineering, Roma, Italy.

Ombres, L.(2015). "Analysis of the bond between fabric reinforced cementitious mortar (FRCM) strengthening systems and concrete." Composites Part B: Engineering, 69, 418-426.

Olivito, R. S., Codispoti, R., and Cevallos, O. A. (2016). "Bond behavior of Flax-FRCM and PBO-FRCM composites applied on clay bricks: Experimental and theoretical study." Composite Structures, 146, 221-231.

Orlowsky, J., and Raupach, M. (2008). "Durability model for AR-glass fibers in textile reinforced concrete." Materials and Structures, 41(7), 1225-1233.

Orton, S. L., Jirsa, J. O., and Bayrak, O. (2008). "Design considerations of carbon fiber anchors." Journal of Composites for Construction, 12(6), 608-616.

Senthilnath, P., Belarbi, A., & Myers, J. J. (2001). "Performance of CFRP strengthened reinforced concrete (RC) beams in the presence of delamination and lap splices under fatigue loading." In Proceeding of the International Conference in Construction (pp. 323-328).

Smith, S. T., Hu, S., Kim, S. J., and Seracino, R. (2011). "FRP-strengthened RC slabs anchored with FRP anchors." Engineering Structures, 33(4), 1075-1087.

Sneed, L. H., D'Antino, T. Carloni, C., and Pellegrino, C., (2015). "A Comparison of the bond behavior of PBO-FRCM composites determined by double-lap and single-lap shear tests." Cement and Concrete Composites Cement and Concrete Composites 64 (2015) 37- 48.

Pellegrino, C., and D'Antino, T. (2013). "Experimental behavior of existing precast prestressed reinforced concrete elements strengthened with cementitious composites." Composites Part B: Engineering, 55, 31-40.

Piyong, Y., Silva, P. F., and Nanni, A. (2003). "Flexural strengthening of concrete slabs by a three-stage prestressing FRP system enhanced with the presence of GFRP anchor spikes." In Proceedings of the International Conference Composites in Construction (CCC2003) (Vol. 239244).

Tetta, Z. C., Koutas, L. N., & Bournas, D. A. (2015). "Textile-reinforced mortar (TRM) versus fiber-reinforced polymers (FRP) in shear strengthening of concrete beams." Composites Part B: Engineering, 77, 338-348.

Trapko, T., Urbańska, D., and Kamiński, M. (2015). "Shear strengthening of reinforced concrete beams with PBO-FRCM composites." Composites Part B: Engineering, 80, 63-72.

Triantafillou, T. C., and Papanicolaou, C. G. (2006). "Shear strengthening of reinforced concrete members with textile reinforced mortar (TRM) jackets." Materials and structures, 39(1), 93-103.

Toutanji H, Zhao L, and Zhang Y. (2006). "Flexural behavior of reinforced concrete beams externally strengthened with CFRP sheets bonded with an inorganic matrix." Eng Struct, Elsevier; 28:557–66.

Toutanji H, and Deng Y. (2007). "Comparison between organic and inorganic matrices for RC beams strengthened with carbon fiber sheets." J Compos Constr, ASCE; 11(5):507–13.

Tommaso, D.A., Focacci, F., and Mantegazza, G. (2008). "PBO-FRCM composites to strengthen RC beams: mechanics of adhesion and efficiency." In Proceedings of the international conference on FRP composites in civil engineering (CICE), Zurich, Switzerland.

TOYOBO CO., LTD. (2005). ZYLON (PBO fiber) Technical Information.

Wang, Y. C., Lee, M. G., and Chen, B. C. (2007). "Experimental study of FRP-strengthened RC bridge girders subjected to fatigue loading." Composite structures, 81(4), 491-498.

Wu, Y. F., and Huang, Y. (2008). "Hybrid bonding of FRP to reinforced concrete structures." Journal of Composites for Construction, 12(3), 266-273.

You, Y. C., Choi, K. S., and Kim, J. (2012). “An experimental investigation on flexural behavior of RC beams strengthened with prestressed CFRP strips using a durable anchorage system.” Composites Part B: Engineering, 43(8), 3026-3036.

Zhu, D., Peled, A., and Mobasher, B. (2011). “Dynamic tensile testing of fabric–cement composites.” Construction and Building Materials, 25(1), 385-395.